

Synthesis and stereocomplexation of polylactide-*b*- poly(ethylene glycol)-*b*-
polylactide triblock copolymers for potential use as bioplastic films

Supasin Pasee

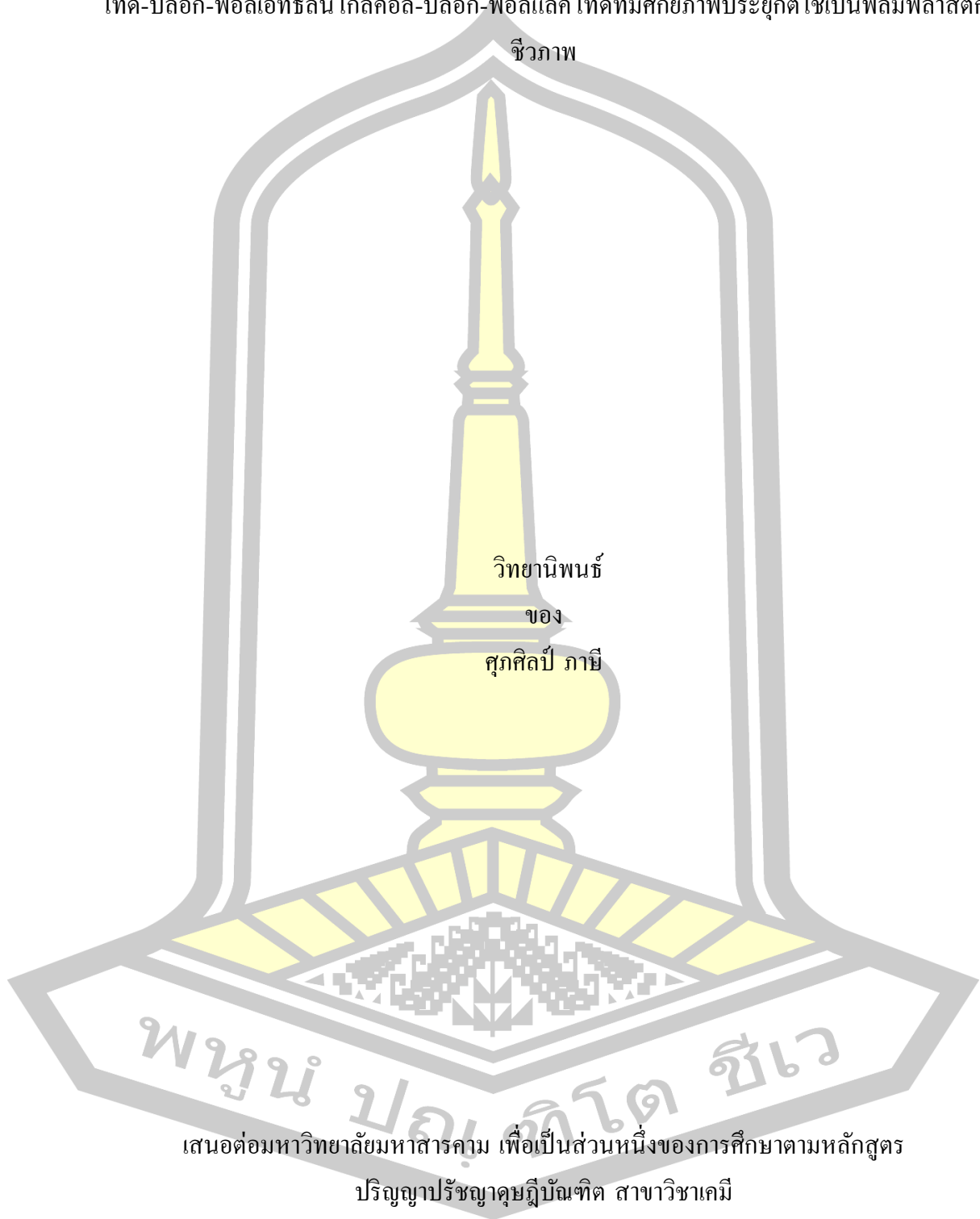
A Thesis Submitted in Partial Fulfillment of Requirements for
degree of Doctor of Philosophy in Chemistry

June 2019

Copyright of Maharakham University

การสังเคราะห์และการเกิดสเตอริโอคอมเพล็กซ์ของพอลิเมอร์ร่วมแบบโคโรลลิกของพอลิแลค
ไทด์-บล็อก-พอลิเอทรีนไกลคอล-บล็อก-พอลิแลคไทด์ที่มีศักยภาพประยุกต์ใช้เป็นฟิล์มพลาสติก

ชีวภาพ



พูนุ ปองกิตโต ซิว

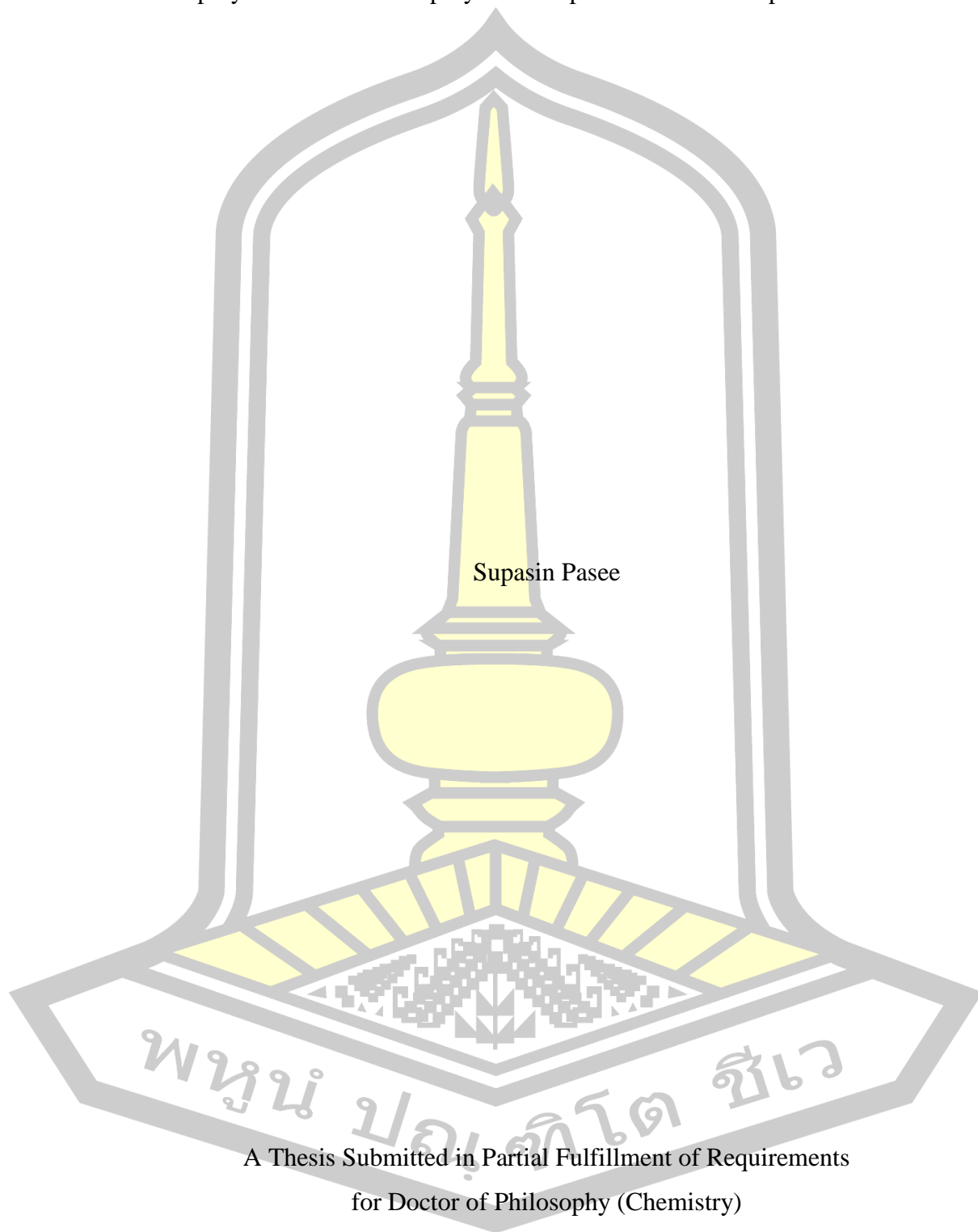
เสนอต่อมหาวิทยาลัยมหาสารคาม เพื่อเป็นส่วนหนึ่งของการศึกษาตามหลักสูตร

ปริญญาปรัชญาดุษฎีบัณฑิต สาขาวิชาเคมี

มิถุนายน 2562

สงวนลิขสิทธิ์เป็นของมหาวิทยาลัยมหาสารคาม

Synthesis and stereocomplexation of polylactide-*b*- poly(ethylene glycol)-*b*-
polylactide triblock copolymers for potential use as bioplastic films



Supasin Pasee

A Thesis Submitted in Partial Fulfillment of Requirements
for Doctor of Philosophy (Chemistry)

June 2019

Copyright of Mahasarakham University



The examining committee has unanimously approved this Thesis, submitted by Mr. Supasin Pasee , as a partial fulfillment of the requirements for the Doctor of Philosophy Chemistry at Mahasarakham University

Examining Committee

Chairman

(Assoc. Prof. Sittipong
Amnuaypanich , Ph.D.)

Advisor

(Assoc. Prof. Yodthong Baimark ,
Ph.D.)

Committee

(Assoc. Prof. Prasong Seehanam ,
Ph.D.)

Committee

(Asst. Prof. Kansiri Pakkethati ,
Ph.D.)

Committee

(Asst. Prof. Onanong Cheerarot ,
Ph.D.)

Mahasarakham University has granted approval to accept this Thesis as a partial fulfillment of the requirements for the Doctor of Philosophy Chemistry

(Prof. Pairoit Pramual , Ph.D.)
Dean of The Faculty of Science

(Asst. Prof. Krit Chaimoon , Ph.D.)
Dean of Graduate School

มหาวิทยาลัยราชภัฏรำไพพรรณี

TITLE	Synthesis and stereocomplexation of polylactide- <i>b</i> - poly(ethylene glycol)- <i>b</i> -polylactide triblock copolymers for potential use as bioplastic films		
AUTHOR	Supasin Pasee		
ADVISORS	Associate Professor Yodthong Baimark , Ph.D.		
DEGREE	Doctor of Philosophy	MAJOR	Chemistry
UNIVERSITY	Maharakham University	YEAR	2019

ABSTRACT

Poly(L-lactide)-*b*-poly(ethylene glycol)-*b*-poly(L-lactide) triblock copolymer, poly(D-lactide) homopolymer and poly(D-lactide)-*b*-poly(ethylene glycol)-*b*-poly(D-lactide) triblock copolymer, designed as PLLA-PEG-PLLA, PDLA and PDLA-PEG-PDLA, respectively, were synthesized via ring-opening polymerization in bulk using stannous octoate as a catalyst. PEG with molecular weight of 20,000 g/mol and 1-dodecanol were used as initiators for synthesizing the triblock copolymers and PDLA, respectively. These polymers were characterized by a combination of analytical techniques: molecular weight methods (dilute-solution viscometry and GPC), spectroscopic method (¹H-NMR), thermal analysis methods (DSC and TGA). The molecular weights of the homo- and copolymers were controlled by the initiator content. The chemical structures were confirmed from the ¹H-NMR spectra. From the DSC results, the triblock copolymers and PDLA were semi-crystalline. PLLA-PEG-PLLA/PDLA and PLLA-PEG-PLLA/PDLA-PEG-PDLA blends without and with chain extension were prepared by melt blending method using an internal mixer. The blend films were prepared using a compression molding machine. The degrees of crystallinity of stereocomplex crystallites of both the blend series increased with the PDLA and PDLA-PEG-PDLA ratios as demonstrated by XRD results. However strain at break of the blend films decreased as increasing the PDLA and PDLA-PEG-PDLA ratio except the non-chain-extended PLLA-PEG-PLLA/PDLA-PEG-PDLA blend film series. Heat resistance of the blend films were better than the PLLA-PEG-PLLA film and increased with the PDLA and PDLA-PEG-PDLA ratios. The PLLA-PEG-PLLA/PDLA blend films exhibited lower strain at break but better heat resistance than that of the PLLA-PEG-PLLA/PDLA-PEG-PDLA blend films. The chain extension significantly improved the tensile properties of the films. In conclusion, the blend films produced in this work show potential for use as flexible and high heat-resistant bioplastic films.

Keyword : Polylactide Block copolymers Stereocomplex Chain extension Heat resistance Bioplastic

ACKNOWLEDGEMENTS

This thesis was gratefully acknowledge the Science Achievement Scholarship of Thailand, (SAST). I am grateful to the Department of Chemistry, Faculty of Science, Maharakham University, for providing chemicals, instrumental support and all other facilities.

I wish to express my deepest and sincere gratitude to my advisor, Assoc. Prof. Dr. Yodthong Baimark, who gave me valuable instructions, excellent suggestions and kindness which are more than I can describe here, that have enable me to pass through this course successfully.

The thesis would not have been accomplished if without the help from several people. First of all, I would like to thank Assoc. Prof. Dr. Sittipong Amnuaypanich, Asst. Prof. Dr. Onanong Cheerarot, Asst. Prof. Dr. Kansiri Pakkethati and Assoc. Prof. Dr. Prasong Srihanam for their valuable suggestions and comments.

I was very fortunate to have many friends both within and outside the Faculty of science during my doctoral life. I thank them all for their being very supportive.

I wish to express my sincere appreciation to Miss Yaowalak Srisuwan, Miss Suchadee Sribenja and all of my friends for their excellent assistance, encouragement, sincerity and impression friendship. Everything will always be in my mind.

Most of all, I wish to express my heartfelt gratitude here to my Pasee family; my beloved parents for their tender love, care, sacrifice, inculcation and encouragement that found me to be a fortitude person.

Supasin Pasee

พหุบัณฑิต ชีวะ

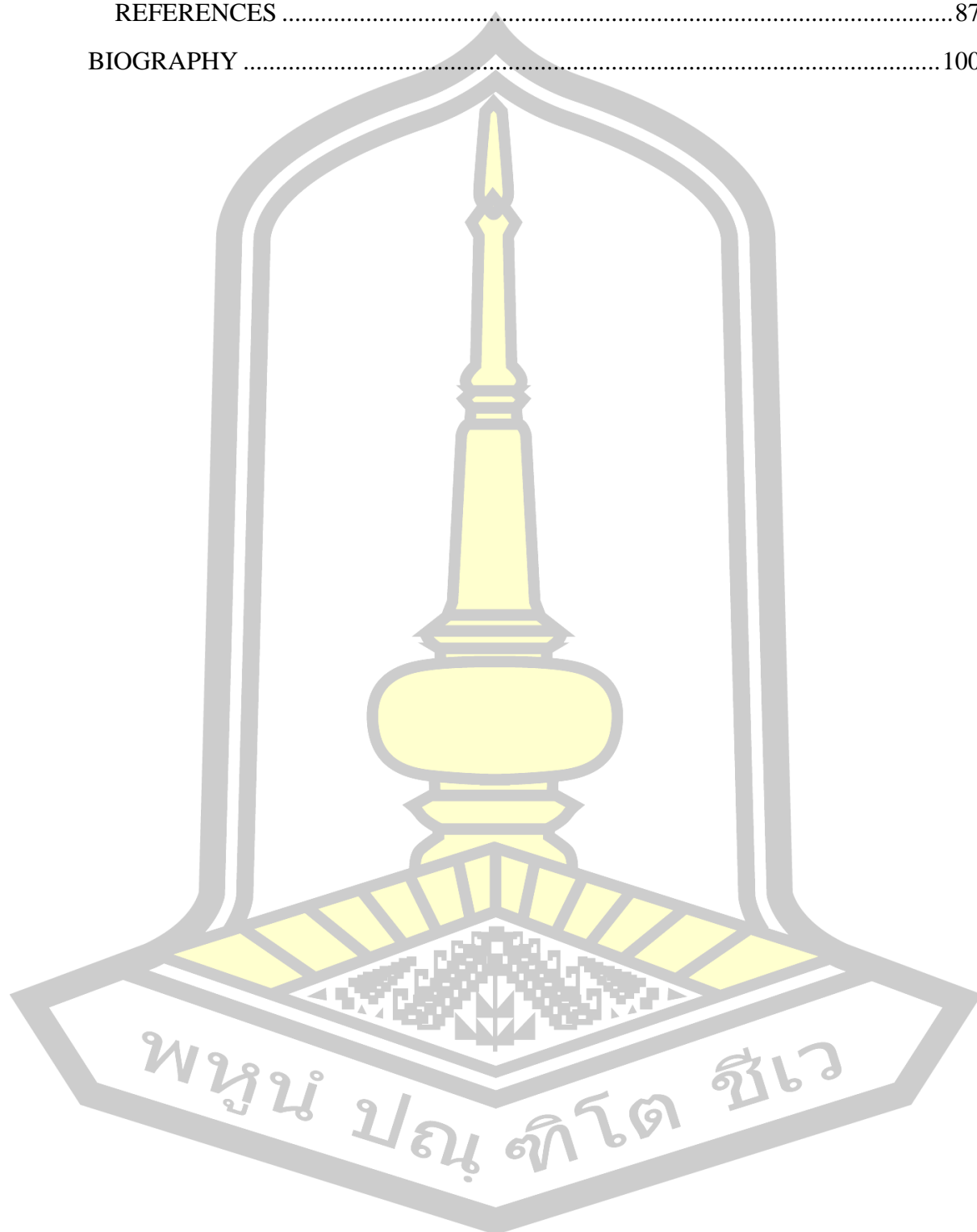
TABLE OF CONTENTS

	Page
ABSTRACT.....	D
ACKNOWLEDGEMENTS.....	E
TABLE OF CONTENTS.....	F
LIST OF TABLES.....	J
LIST OF FIGURES.....	K
CHAPTER I.....	1
INTRODUCTION.....	1
1.1. Biodegradable polymers.....	1
1.2. Classification of biodegradable polymers.....	1
1.3. Poly(lactic acid).....	2
1.4. Stereocomplex polylactides.....	4
1.5. Research objectives.....	6
1.6. Expected results obtained from the research.....	6
1.7. Scopes of research.....	7
1.8. Research Place.....	7
CHAPTER II.....	8
LITERATURE REVIEW.....	8
2.1. Block copolymers of poly(ethylene glycol) and polylactide.....	8
2.2. Stereocomplexation of PLLA/PDLA blends.....	12
2.2.1 Effect of PLLA/PDLA blend ratio on stereocomplexation.....	13
2.2.2 Effect of M.W. of PLLA and PDLA on stereocomplexation.....	14
2.2.3 Effect of stereocomplexation on mechanical properties.....	15
2.2.4 Effect of stereocomplex on thermal stability.....	16
2.3. Stereocomplexation of PLLA/PDLA-PEG-PDLA blends.....	16
2.3.1. Effect of PLLA/PDLA-PEG-PDLA blend ratio on stereocomplexation.....	16

2.3.2. Effect of PEG block length on stereocomplexation	21
2.3.3. Effect of PDLA block length on stereocomplexation	22
2.4. Stereocomplexation of PLLA-PEG-PLLA/PDLA-PEG-PDLA blends	25
CHAPTER III	29
RESEARCH METHODOLOGY	29
3.1 Chemicals and instruments	29
3.1.1 Chemicals	29
3.1.2 Instruments	30
3.2 Monomer preparation and characterization	30
3.3 Synthesis of polylactides	33
3.3.1 Synthesis of triblock copolymers	33
3.3.2 Synthesis of triblock copolymers	34
3.4 Characterization of polylactides	35
3.4.1 Optical rotation property	35
3.4.2 Diluted-solution viscometry	36
3.4.3 Gel permeation chromatography (GPC).....	36
3.4.4 Thermogravimetric analysis (TGA)	37
3.4.5 Differential scanning calorimetry (DSC)	37
3.4.6 ¹ H-NMR spectrometry	37
3.5 Preparation of stereocomplex polylactides	37
3.5.1 PLLA-PEG-PLLA/PDLA blends	37
3.5.2 PLLA-PEG-PLLA/PDLA-PEG-PDLA blends	38
3.6 Characterization of scPLA	39
3.6.1 Differential scanning calorimetry (DSC)	39
3.6.2 X-ray diffractometry.....	40
3.6.3 Tensile testing.....	40
3.6.4 Thermo-mechanical properties	41
3.6.5 Dimensional stability to heat	41
3.7 Data analysis	41

CHAPTER IV	42
RESULTS AND DISCUSSION	42
4.1 Characterization of lactides	42
4.1.1 Optical rotation property	42
4.1.2 Thermal decomposition	42
4.2 Characterization of PLLA-PEG-PLLA, PDLA-PEG-PDLA and PDLA	44
4.2.1 Optical rotation property	44
4.2.2 Measurement of intrinsic viscosity	44
4.2.3 Molecular weight characteristics	45
4.2.4 Thermal decomposition	47
4.2.5 Thermal transition properties	49
4.2.6. Chemical structures	50
4.3 Characterization of PLLA-PEG-PLLA/PDLA blends	53
4.3.1. Thermal transition properties	53
4.3.2. Crystalline structures	58
4.3.3. Tensile properties	61
4.3.4 Thermo-mechanical properties	64
4.3.5 Dimensional stability to heat	66
4.4. Characterization of PLLA-PEG-PLLA/PDLA-PEG-PDLA blends	68
4.4.1. Thermal transition properties	68
4.4.2. Crystalline structures	72
4.4.3. Tensile properties	74
4.4.4. Thermo-mechanical properties	78
4.4.5. Dimensional stability to heat	80
CHAPTER V	82
CONCLUSIONS	82
5.1 Synthesis and characterization of polymers	82
5.2 Preparation and characterization of polymer blends	83
SUGGESTIONS FOR FURTHER WORK	85

REFERENCES86
REFERENCES87
BIOGRAPHY100



LIST OF TABLES

	Page
Table 1 Effect of PEG blend ratio on the T_g of the PLLA (Hu et al., 2003).	9
Table 2. Properties of triblock copolymers of PEG and PLLA (Hu and Liu, 1994). ..	11
Table 3. Information of PDLA-PEG-PDLA copolymers using PEG M.W. of 10,000 g/mol (Liu et al., 2014).	17
Table 4. Molecular characteristics of PLLA-PEG-PLLA and PDLA-PEG-PDLA triblock copolymers (Han et al., 2016).	25
Table 5. Chemicals used in this research.	29
Table 6. Instruments used in this research.	30
Table 7. Formulations of PLLA-PEG-PLLA/PDLA blends.....	38
Table 8. Formulations of PLLA-PEG-PLLA/PDLA-PEG-PDLA blends.	39
Table 9. Optical rotation properties of D-lactide and L-lactide in chloroform at 25 °C.	42
Table 10. $T_{d,max}$ from DTG curves of LLA and DLA monomers.	43
Table 11. Optical rotation property of PLLA-PEG-PLLA, PDLA-PEG-PDLA and PDLA.	44
Table 12. $[\eta]$ and M_v of PDLA and triblock copolymers.	45
Table 13. Molecular weight characteristics from GPC of PDLA and triblock copolymers.	47
Table 14. $T_{d,max}$ of PLLA-PEG-PLLA, PDLA-PEG-PDLA and PDLA.	49
Table 15. Summary of thermal transition properties of PLLA-PEG-PLLA, PDLA-PEG-PDLA and PDLA.	50
Table 16. DSC results of PLLA-PEG-PLLA/PDLA blends from Figure 4.11.	56
Table 17. XRD results of PLLA-PEG-PLLA/PDLA blend films.	60
Table 18. Thermal transition properties of PLLA-PEG-PLLA/PDLA-PEG-PDLA blends.	70
Table 19. XRD results of PLLA-PEG-PLLA/PDLA-PEG-PDLA blend films.....	74

LIST OF FIGURES

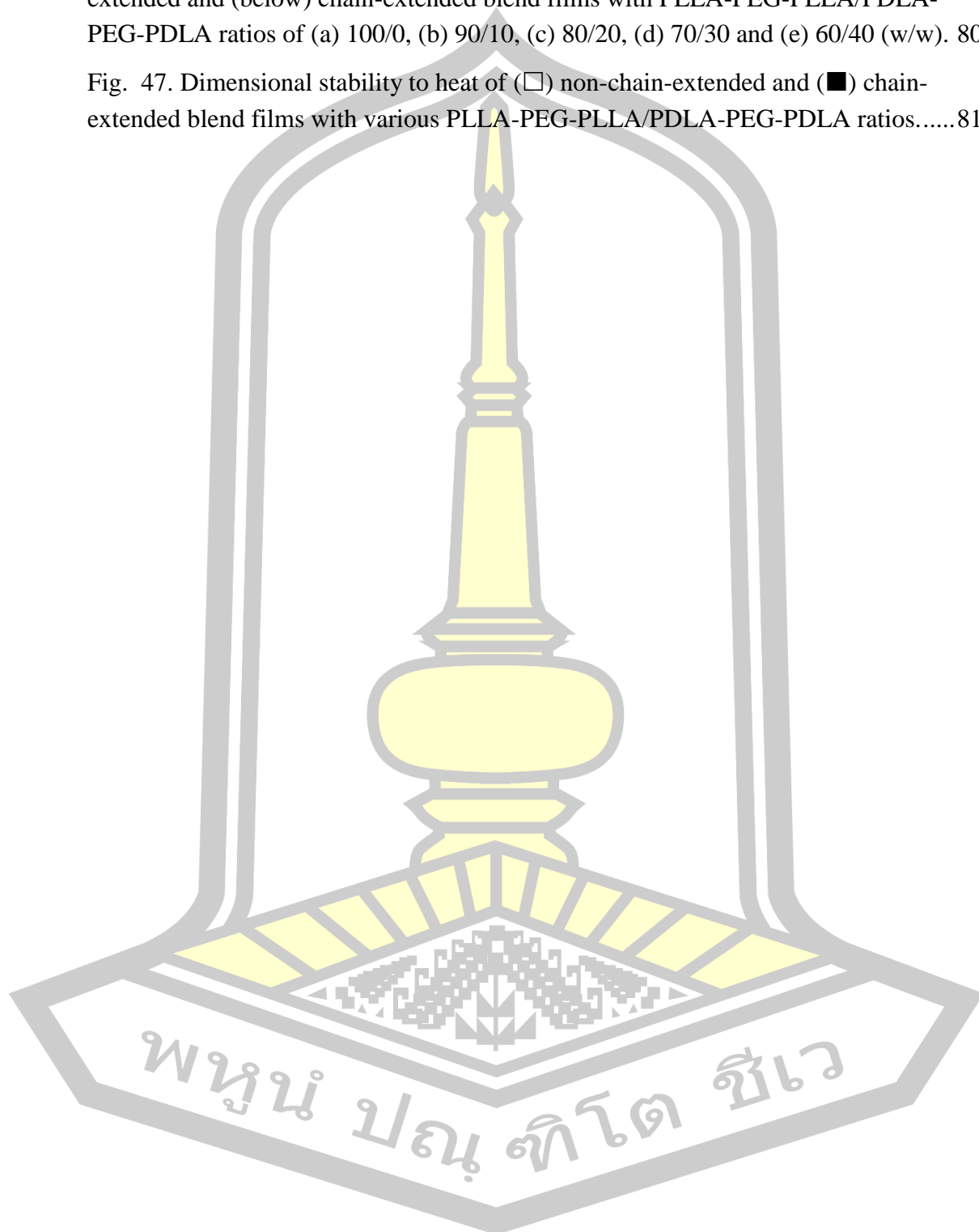
	Page
Fig. 1. Classification of the main biodegradable polymers (Avérous & Pollet, 2012).	2
Fig. 2. Synthesis methods for preparing the high-molecular-weight PLA (Garlotta, 2002).	3
Fig. 3. Synthesis methods for obtaining high molecular weight PLLA and PDLA. (Avérous & Pollet, 2012)	5
Fig. 4. Tensile stress-strain behavior of quenched PLLA and PLLA/PEG blends at ambient temperature (Hu et al., 2003).	10
Fig. 5. Effect of aging under ambient conditions (23°C, about 50% RH) on the tensile stress-strain behavior of the PLLA/PEG 70/30 blend (Hu et al., 2003).	10
Fig. 6. Stereocomplex formation of PLLA/PDLA blends.	13
Fig. 7. DSC thermograms of PLLA, PDLA and PLLA/PDLA blends (M.W. of PLLA and PDLA = 60,000 g/mol) (Tsuji et al., 1991).	13
Fig. 8. DSC thermograms of 50/50 PLLA/PDLA blends prepared with different M.W. of PDLA and PLLA (Tsuji et al., 1991).	14
Fig. 9. DSC thermograms of 50/50 PLLA/PDLA blends prepared with different M.W. of PLLA (M.W. of PDLA = 5,000 g/mol) (Tsuji et al., 1991).	15
Fig. 10. Tensile properties of PLLA, PDLA and scPLA (Tsuji & Ikada, 1993).	15
Fig. 11. TG thermograms of PLLA, PDLA and scPLA in isothermal mode at 250 °C and 260 °C (Tsuji & Fukui, 2003).	16
Fig. 12. WAXD profiles of (a) PLLA/EG2D3 and (b) PDLA/EG1D3 with different weight ratios (Liu et al., 2014).	18
Fig. 13. Heating (a) and cooling (b) curves of PLLA/PDLA-PEG-PDLA blends with different weight ratios (Liu et al., 2014).	19
Fig. 14. Mechanical properties of PLLA/PDLA-PEG-PDLA blends of various compositions (Liu et al., 2014).	21
Fig. 15. DSC scans of PLLA and its blends after quenched from 230°C and then heated at a rate of 20°C/min (Song et al., 2015).	22
Fig. 16. DSC thermograms of PLLA/copolymer blended-films prepared from blending PLLA with (a) PDLA ₅₃ -PEG ₁₈₂ -PDLA ₅₃ , (b) PDLA ₈₁ -PEG ₁₈₂ -PDLA ₈₁ , (c)	

PDLA ₁₂₆ -PEG ₁₈₂ -PDLA ₁₂₆ and (d) PDLA ₂₁₃ -PEG ₁₈₂ -PDLA ₂₁₃ in various compositions; (e) the second heating run thermograms of the copolymers (Tacha et al., 2015)	24
Fig. 17. DSC curves of PLLA-PEG-PLLA/PDLA-PEG-PDLA and PLLA/PDLA blends: (A) cooling scans from the melt state (250 °C); (B) subsequent heating scans after cooling. Both the cooling and heating rates are 10 °C/min (Han et al., 2016)....	26
Fig. 18. Tensile stress vs strain curves for solution-cast films of (A) PLLA-PEG-PLLAs and (B) PLLA-PEG-PLLA/PDLA-PEG-PDLA blends (Han et al., 2016).....	28
Fig. 19. Apparatus used in the two-step preparation of lactide: (a) direct polycondensation of lactic acid and (b) thermal decomposition of low M.W. PLA. ...	32
Fig. 20. Polymerization reaction of PDLA.	34
Fig. 21. Polymerization reaction of triblock copolymers.	35
Fig. 22. TG and DTG curves of (above) LLA and (below) DLA monomers.....	43
Fig. 23. GPC curve of PDLA.....	45
Fig. 24. GPC curve of PLLA-PEG-PLLA.....	46
Fig. 25. GPC curve of PDLA-PEG-PDLA.....	46
Fig. 26. TG and DTG curves of PDLA.....	48
Fig. 27. TG and DTG curves of PLLA-PEG-PLLA.....	48
Fig. 28. TG and DTG curves of PDLA-PEG-PDLA.....	49
Fig. 29. DSC second heating thermograms of PLLA-PEG-PLLA, PDLA-PEG-PDLA and PDLA.	50
Fig. 30. (a) Ring-opening polymerization reaction of PDLA and (b) ¹ H-NMR spectrum of PDLA in CDCl ₃ (peak assignments as shown).....	51
Fig. 31. (a) Ring-opening polymerization reaction of PLA-PEG-PLA, (b) ¹ H-NMR spectrum of PLLA-PEG-PLLA and (c) ¹ H-NMR spectrum of PDLA-PEG-PDLA in CDCl ₃ (peak assignments as shown).	52
Fig. 32. DSC second heating thermograms of (above) non-chain-extended and (below) chain-extended blends with PLLA-PEG-PLLA/PDLA ratios of (a) 100/0, (b) 90/10, (c) 80/20, (d) 70/30 and (e) 60/40 (w/w).	55
Fig. 33. DSC cooling thermograms of (above) non-chain-extended and (below) chain-extended blends with PLLA-PEG-PLLA/PDLA ratios of (a) 100/0, (b) 90/10, (c) 80/20, (d) 70/30 and (d) 60/40 (w/w) (T _c peak and ΔH _c as shown).	57

- Fig. 34. XRD patterns of (above) non-chain-extended and (below) chain-extended blend films with PLLA-PEG-PLLA/PDLA ratios of (a) 100/0, (b) 90/10, (c) 80/20, (d) 70/30 and (e) 60/40 (w/w).....59
- Fig. 35. Tensile curves of (above) non-chain-extended and (below) chain-extended blend films with PLLA-PEG-PLLA/PDLA ratios of (□) 100/0, (◇) 90/10, (Δ) 80/20, (×) 70/30 and (○) 60/40 (w/w).....62
- Fig. 36. Tensile properties of (□) non-chain-extended and (■) chain-extended blend films with various PLLA-PEG-PLLA/PDLA ratios (* = could not determine).63
- Fig. 37. Storage modulus from DMA of (above) non-chain-extended and (below) chain-extended films with various PLLA-PEG-PLLA/PDLA ratios.65
- Fig. 38. Photographs of dimensional stability to heat at 80°C of (above) non-chain-extended and (below) chain-extended blend films with PLLA-PEG-PLLA/PDLA ratios of (a) 100/0, (b) 90/10, (c) 80/20, (d) 70/30 and (e) 60/40 (w/w) (* = could not determine).66
- Fig. 39. Dimensional stability to heat of (□) non-chain-extended and (■) chain-extended blend films with various PLLA-PEG-PLLA/PDLA ratios (* = could not determine).67
- Fig. 40. DSC second heating thermograms of (above) non-chain-extended and (below) chain-extended blends with PLLA-PEG-PLLA/PDLA-PEG-PDLA ratios of (a) 100/0, (b) 90/10, (c) 80/20, (d) 70/30 and (d) 60/40 (w/w).....69
- Fig. 41. DSC cooling thermograms of (above) non-chain-extended and (below) chain-extended blends with PLLA-PEG-PLLA/PDLA-PEG-PDLA ratios of (a) 100/0, (b) 90/10, (c) 80/20, (d) 70/30 and (d) 60/40 (w/w) (T_c peak and ΔH_c as shown).71
- Fig. 42. XRD patterns of (above) non-chain-extended and (below) chain-extended blend films with PLLA-PEG-PLLA/PDLA-PEG-PDLA ratios of (a) 100/0, (b) 90/10, (c) 80/20, (d) 70/30 and (e) 60/40 (w/w).73
- Fig. 43. Tensile curves of (above) non-chain-extended and (below) chain-extended blend films with PLLA-PEG-PLLA/PDLA-PEG-PDLA ratios of (□) 100/0, (◇) 90/10, (Δ) 80/20, (×) 70/30 and (○) 60/40 (w/w).76
- Fig. 44. Tensile properties of (□) non-chain-extended and (■) chain-extended blend films with various PLLA-PEG-PLLA/PDLA-PEG-PDLA ratios.77
- Fig. 45. Storage modulus from DMA of (above) non-chain-extended and (below) chain-extended films with various PLLA-PEG-PLLA/PDLA-PEG-PDLA ratios.....79

Fig. 46. Photographs of dimensional stability to heat at 80°C of (above) non-chain-extended and (below) chain-extended blend films with PLLA-PEG-PLLA/PDLA-PEG-PDLA ratios of (a) 100/0, (b) 90/10, (c) 80/20, (d) 70/30 and (e) 60/40 (w/w). 80

Fig. 47. Dimensional stability to heat of (□) non-chain-extended and (■) chain-extended blend films with various PLLA-PEG-PLLA/PDLA-PEG-PDLA ratios.....81



CHAPTER I

INTRODUCTION

1.1. Biodegradable polymers

Nowadays, the petroleum-based polymeric wastes have become a serious environmental problem in all over the world. Recently, biodegradable polymers are being intensively studied and developed by as an alternative to petroleum-based polymers in order to reduce their impact on the environment (Danner & Braun, 1999; Gross & Kalra, 2002; Ikada & Tsuji, 2000; Yu *et. al.*, 2006).

“Biodegradable” means “capable of undergoing decomposition into carbon dioxide, methane, water, inorganic compounds, and biomass” according to ASTM standard D-5488-94d and European norm EN 13432. The predominant biodegradation mechanism is the enzymatic action of microorganisms such as bacteria and fungi etc., which can be determined by standard tests over a specific period of time, reflecting available disposal conditions. There are different media (liquid, inert, or compost medium) to analyze biodegradability. Biodegradation is the degradation of an organic material caused by biological activity, mainly microorganisms’ enzymatic action. The biodegraded products are CO₂ and water (in the presence of oxygen, i.e. aerobic conditions) or methane (in the absence of oxygen, i.e., anaerobic conditions), as defined in the European Standard EN 13432:2000 (Avérous & Pollet, 2012).

1.2. Classification of biodegradable polymers

Biodegradable polymers are formed in natural environment during the growth cycles of organisms (e.g. starch, cellulose, chitin, chitosan, silk and polyhydroxyalkanoates etc.) or are synthesized (e.g. polylactide, polycaprolactone and polyglycolide etc.). Some microorganisms and enzymes capable of degrading such polymers have been identified (Velde & Kiekens, 2001). Four classifications of biodegradable polymers have been proposed as shown in Fig.1.: (i) agro-polymers from agro-resources (e.g. starch or cellulose), (ii) biopolyesters obtained by microbial production such as the polyhydroxyalkanoates (PHAs), (iii) biopolyesters

conventionally and chemically synthesized from monomers obtained from agro-resources, e.g. the poly(lactic acid) (PLA), and (iv) polymers obtained from fossil resources. Only the first three categories (i–iii) are obtained from renewable resources. We can further classify these biodegradable polymers into two main categories: the agro-polymers (category i) and the biodegradable polyesters or biopolyesters (categories ii–iv).

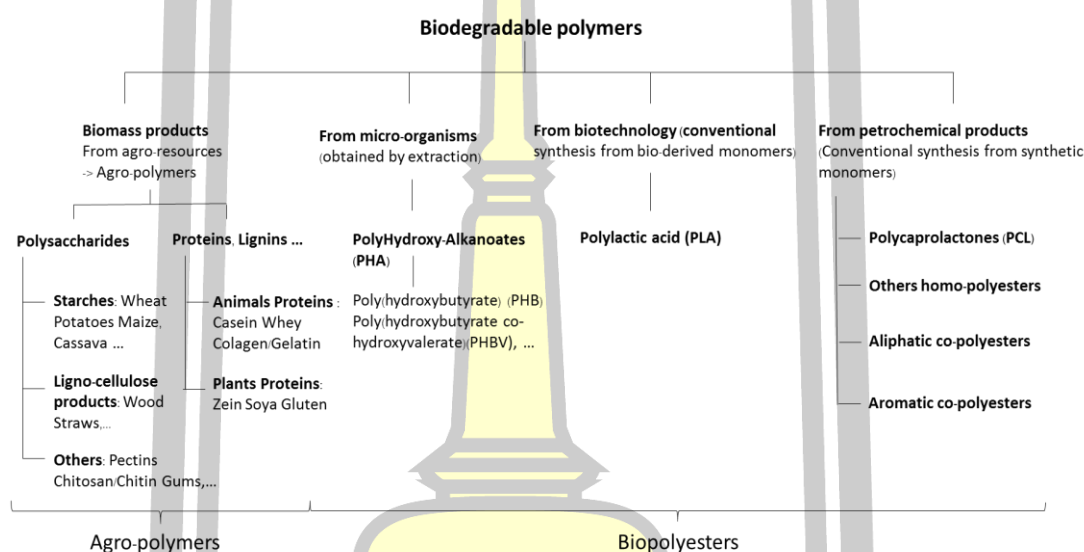


Fig. 1. Classification of the main biodegradable polymers (Avérous & Pollet, 2012).

The biodegradable and biorenewable polyesters (category iii) have widely interested because of they can be prepared from renewable resources and processed using conventional processing machines such as injection molding, melt spinning and blow film techniques.

1.3. Poly(lactic acid)

Lactic acid (LA) is a chiral molecule existing as two stereoisomers, L-lactic acid(LLA) and D-lactic acid (DLA) as below.

However, the resulted PLA is a low molecular weight (<10,000 g/mol) with low mechanical properties. This due to hydrolysis of water by-product had occurred. High molecular weight PLA can be obtained by ring-opening polymerization of lactide monomers due to water by-product did not form. The lactide was synthesized through direct polycondensation of lactic acid followed with thermal decomposition of low molecular weight of PLA. The polyester obtained from lactide was then called as polylactide (PLA). Poly(L-lactide) (PLLA) and Poly(D-lactide) (PDLA) were prepared by ring-opening polymerization of L-lactide (LLA) and D-lactide (DLA), respectively.

Main disadvantages of the PLA are brittleness and low heat resistance. The high glass transition temperature (T_g) of the PLA ($\sim 60^\circ\text{C}$) induced high brittleness. Plasticization effects can reduce the PLA brittleness by decreasing the T_g of PLA (Martin & Averous, 2001). Moreover the PLA showed very slow crystallization rate after melt processing. The low crystallinity PLA gave low heat resistant properties. The crystallinity of PLA has been improved by addition of nucleating agents and stereocomplex formation (PLLA/PDLA blending) (Saeidlou *et al.*, 2012)

1.4. Stereocomplex poly lactides

The PLA is considerate as an environment-friendly polymer due to its biorenewability, biodegradability and biocompatibility (Fortunati *et al.*, 2010; Pan *et al.*, 2011). The PLA and modified PLA are possible to use instead of petroleum-based plastics because of its good processability and mechanical strength etc. (Wei *et al.*, 2014). The PLA has two optical isomers: the PLLA and PDLA. Repeating units of the PLLA and PDLA homopolymer synthesized from L-lactide and D-lactide monomer, respectively are shown in Fig. 3. Stereocomplex PLA (scPLA), which has a melting temperature around 230°C higher than both the PLLA and PDLA ($\sim 170^\circ\text{C}$) that is prepared by blending PLLA with PDLA (He *et al.*, 2008; Tsuji & Ikada, 1999). The scPLA showed thermal resistant property higher than both the PLLA and PDLA (Sun *et al.*, 2011).

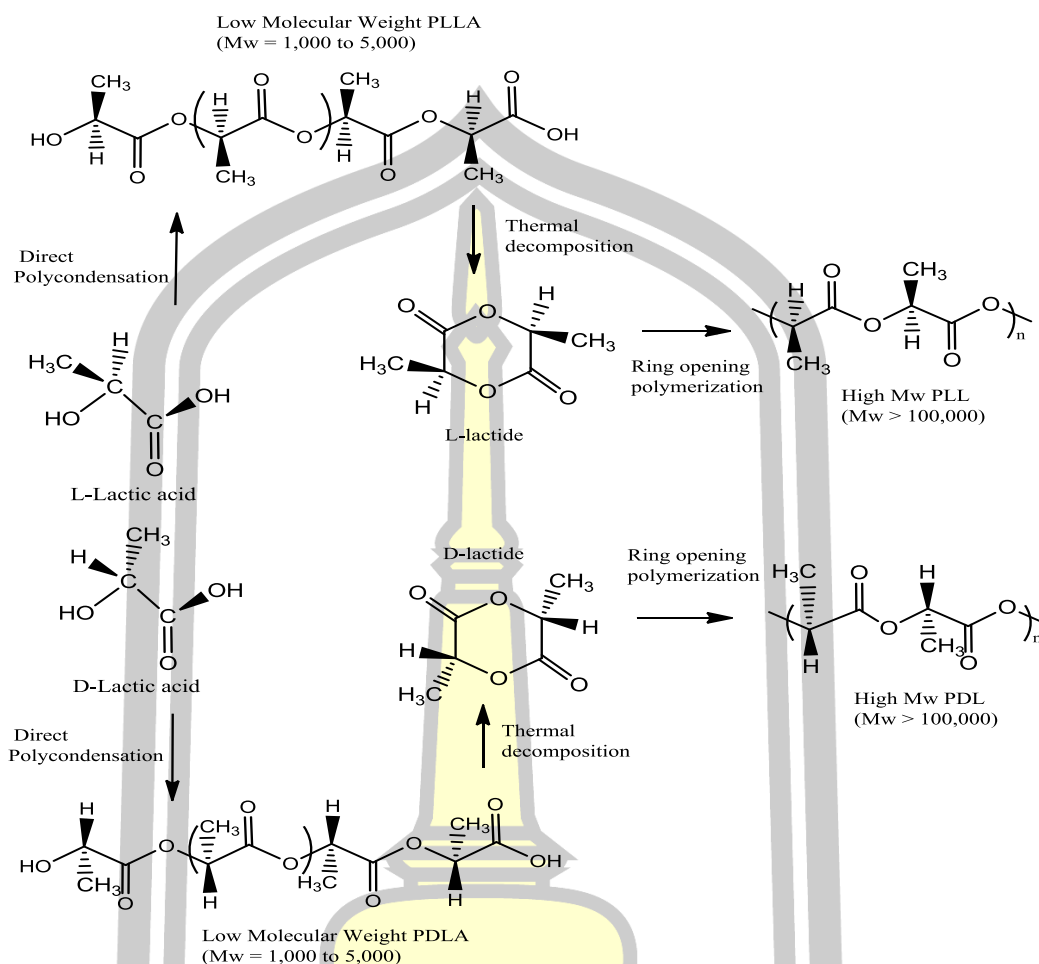


Fig. 3. Synthesis methods for obtaining high molecular weight PLLA and PDLA. (Avérous & Pollet, 2012)

The stereocomplex crystallites of PLA is stabilized by stronger van der Waals interactions between opposite configuration of the PLLA and PDLA chains. As results, thermal stability of stereocomplex was much improved (Brizzolara *et al.*, 1996; Okihara *et al.*, 1991). Stereocomplexation between the PLLA and PDLA can occur in solution, in melt blend, during polymerization or hydrolytic degradation, provided that L-lactic acid and D-lactic acid chains coexist in a polymer system (Ikada & Tsuji, 2000). Stereocomplex crystallites predominantly formed from the equimolar solutions of the PLLA and PDLA, as long as either PDLA or PLLA has a low molecular weight (M.W.) (Quynh *et al.*, 2007; Tsuji *et al.*, 1991). At high processing temperatures (>230 °C), the scPLA can also develop from melt blend of the PLLA and PDLA, however PLA homopolymers might be significant degraded. The tensile properties of PL stereocomplex films obtained from melt blends of high M.W. PLLA and PDLA slightly

reduced though their heat stability significantly improved (Quynh *et al.*, 2007). This may be due to the thermal decomposition of PLA homopolymers at high temperature (Fan *et al.*, 2004).

The use of low M.W. PLLA and PDLA for stereocomplexation can significantly reduce the processing temperature and increase their crystallinity. On the other hand, the stereocomplex films and fibers prepared from the low M.W. homopolymers are reported to be very brittle and weak (Tsuji & Ikada, 1999). The stereocomplexation of low M.W. PLLA and high M.W. PDLA not only reduce the processing temperature but also can produce the samples with tensile strength and heat stability higher than that of both PLLA and PDLA homopolymers, met the practical requirements for specific applications. However, the scPLA based materials are still brittle. Therefore, their applications still limited (Celli & Scandola, 1992; Garlotta, 2002; Slager & Domb, 2003).

1.5. Research objectives

Flexible poly(ethylene glycol) (PEG) blocks were attached to the PLLA and PDLA blocks formed as PLLA-*b*-PEG-*b*-PLLA and PDLA-*b*-PEG-*b*-PDLA by ring-opening polymerization of LLA and DLA monomers, respectively. Stereocomplex PLA-*b*-PEG-*b*-PLA triblock copolymers of PLLA-*b*-PEG-*b*-PLLA/PDLA and PLLA-*b*-PEG-*b*-PLLA/ PDLA-*b*-PEG-*b*-PDLA were prepared by melt blending. Effects of blend ratio and chain extension on stereocomplexation, thermal properties, mechanical properties and heat resistance were investigated.

1.6. Expected results obtained from the research

To synthesize triblock copolymers of PLLA-*b*-PEG-*b*-PLLA and PDLA-*b*-PEG-*b*-PDLA with controllable molecular weight.

To synthesize PDLA homopolymer with controllable molecular weight.

To know the effects of blend ratio and chain extension on stereocomplex formation, thermal properties, mechanical properties and heat resistance of the stereocomplex triblock copolymers.

1.7. Scopes of research

1.7.1 The PDLA homopolymer with molecular weight of 5,000 g/mol was synthesized using 1-dodecanol as an initiator and stannous octoate as a catalyst.

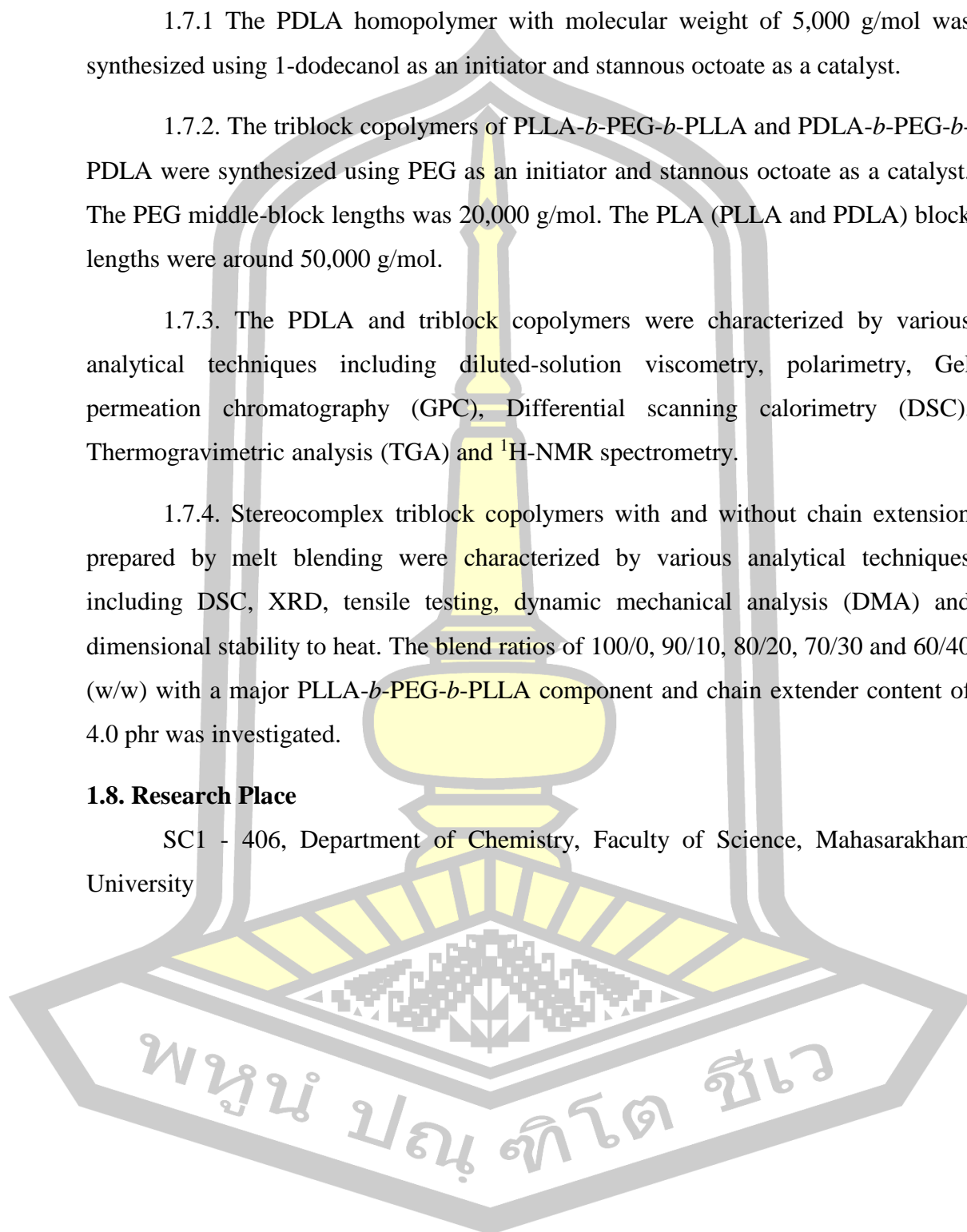
1.7.2. The triblock copolymers of PLLA-*b*-PEG-*b*-PLLA and PDLA-*b*-PEG-*b*-PDLA were synthesized using PEG as an initiator and stannous octoate as a catalyst. The PEG middle-block lengths was 20,000 g/mol. The PLA (PLLA and PDLA) block lengths were around 50,000 g/mol.

1.7.3. The PDLA and triblock copolymers were characterized by various analytical techniques including diluted-solution viscometry, polarimetry, Gel permeation chromatography (GPC), Differential scanning calorimetry (DSC), Thermogravimetric analysis (TGA) and ¹H-NMR spectrometry.

1.7.4. Stereocomplex triblock copolymers with and without chain extension prepared by melt blending were characterized by various analytical techniques including DSC, XRD, tensile testing, dynamic mechanical analysis (DMA) and dimensional stability to heat. The blend ratios of 100/0, 90/10, 80/20, 70/30 and 60/40 (w/w) with a major PLLA-*b*-PEG-*b*-PLLA component and chain extender content of 4.0 phr was investigated.

1.8. Research Place

SC1 - 406, Department of Chemistry, Faculty of Science, Mahasarakham University



CHAPTER II

LITERATURE REVIEW

2.1. Block copolymers of poly(ethylene glycol) and polylactide

The universal use of non-biodegradable plastic products has caused serious environmental pollution. One of the most effective ways to solve the problem is the development of biodegradable polymers. Among these biodegradable polymers, poly(L-lactide) (PLLA) is one of the most important polyesters that are derived from renewable biomass such as corn and sugar beets. It is known for its biocompatibility, low toxicity and immunogenicity and resorbability through natural pathway (*Ren et al.*, 2005) and it has a variety of application in many fields such as drug delivery (*Lee et al.*, 2007; *Prabaharan et al.*, 2009) tissue engineering (*He et al.*, 2011), food packaging (*Martínez-Abad et al.*, 2014; *Plackett et al.*, 2006). For a widely commodity applications, a good material must has good mechanical and processability. However, the disadvantages of poor mechanical properties and slow crystallization rate of PLLA limit its wide application. The PLLA is a rather brittle and rigid polymer. While PLLA has a glass transition temperature well above room temperature and was amorphous at room temperature, the elongation ratio is only about 5%. Crystallinity, if developed, increases the elastic modulus and further enhance the brittleness (*Pan et al.*, 2011; *Perego et al.*, 1996). Considerable efforts have been made to improve the mechanical properties of PLLA, such as blending, copolymerization and plasticization (*Li & Shimizu*, 2009; *Zhang et al.*, 2011).

Plasticizers are widely used in the plastics industry to improve processability, flexibility and ductility of glassy polymers ((*Sears et al.*, 1982)). The PLLA was plasticized with various plasticizers and their efficiency was evaluated in two aspects: one is the shift of glass transition temperature (T_g), the other is the improvement mechanical properties (*Martin & Averous*, 2001). Poly(propylene glycol) (PPG) and poly(ethylene glycol) (PEG) were found to be efficient plasticizers for PLLA (*Piorkowska et al.*, 2006). The elongation at break of PLLA was greatly increased. The PLLA has melt-blended with an ethylene glycol/propylene glycol random copolymer poly(ethyleneglycol-*co*-propylene glycol) (PEPG)(*He et al.*, 2008). With 5~20% PEPG additive, the toughness increased. The PLLA was plasticized with triphenyl phosphate

(TPP) and the results showed that the crystallinity of plasticized PLLA markedly increased when compared with neat PLLA (Xiao *et al.*, 2011). Oligomeric lactic acid (OLA), glycerol, epoxidized palm oil, and partial fatty acid esters also have been used as plasticizers for PLLA (Giita Silverajah *et al.*, 2012; Martin & Averous, 2001).

Table 1. shows effect of PEG blend ratio on the T_g of PLLA. Molecular weights of the PLLA and PEG were 200,000 and 8,000 g/mol, respectively (Hu *et al.*, 2003). It can be seen that the T_g values decreased steadily as the PEG ratio increased. The elongation at break of the PLLA blend films also increased with the PEG blend ratio as shown in Fig. 4. Aging PLLA/PEG 70/30 films under ambient conditions (23°C, about 50%RH) produced the changes in tensile properties seen in Fig. 5. With time, the films changed from low modulus elastomer-like materials to higher modulus thermoplastic-like materials. After aging for 500 h the modulus increased almost two orders of magnitude and the fracture strain decreased from 500 to 250%. This suggests that migration of PEG on PLLA/PEG blends had occurred during aging to decrease plasticization effect.

Table 1 Effect of PEG blend ratio on the T_g of the PLLA (Hu *et al.*, 2003).

PLLA/PEG blend ratio (w/w)	T_g of PLLA (°C)
100/0	58
90/10	36
85/15	30
80/20	21
70/30	9

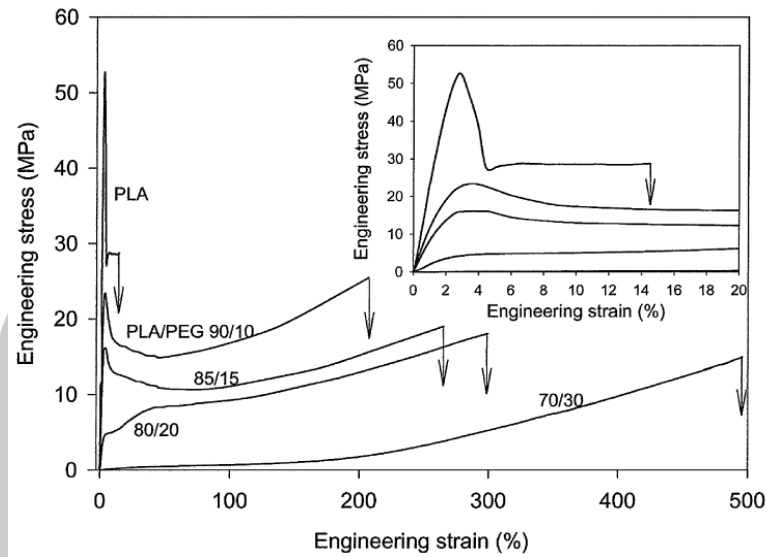


Fig. 4. Tensile stress-strain behavior of quenched PLLA and PLLA/PEG blends at ambient temperature (Hu *et al.*, 2003).

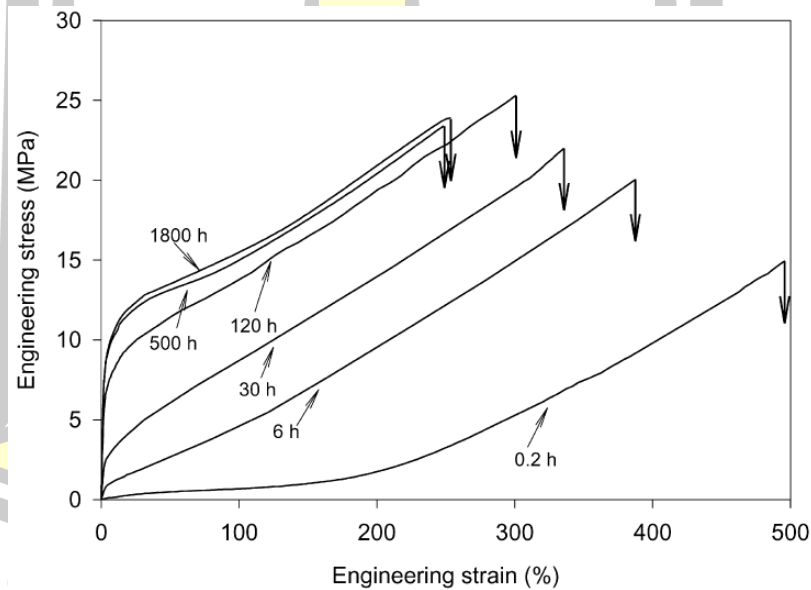


Fig. 5. Effect of aging under ambient conditions (23°C, about 50% RH) on the tensile stress-strain behavior of the PLLA/PEG 70/30 blend (Hu *et al.*, 2003).

PEG was considered a good plasticizer for PLLA, the hydrophilicity, crystallization behavior, melting behavior and its application in drug release of PLLA-PEG diblock or triblock copolymers were always been investigated in most works.

Triblock copolymers of PEG and PLLA were synthesized by ring-opening polymerization of L-lactide monomer using PEG and stannous octoate as initiator and catalyst, respectively. As shown in Table 2., melting temperature (T_m) and glass transition temperature (T_g) of the PLLA blocks decreased as the feed ratio and molecular weight of PEG increased. This indicates the PEG act as plasticizer for PLLA to reduce the T_g of PLLA. The molecular weight of most PLLA-PEG copolymer been investigated in most works are not more than 50,000 g/mol and the molecular weight of PEG are always range from 400-4,000 g/mol. These copolymers can use in drug delivery applications but did not in packaging applications. High molecular weight of the triblock copolymers need to prepared for this purpose.

Table 2. Properties of triblock copolymers of PEG and PLLA (Hu and Liu, 1994).

PEG feed ratio (%wt.)	M.W. of PEG (g/mol)	Final wt% PEG ratio (NMR)	T_m (°C)	T_g (°C)	M.W. of copolymer (g/mol, GPC)
2	2,000	4.4	161	51	24,100
3	2,000	5.4	156	45	19,812
5	2,000	9.6	150	43	15,783
10	2,000	18.3	134	43	9,801
10	4,000	16.2	131	41	21,035
10	6,000	12.7	117	41	30,760

For further use in food packaging, both the crystallinity and toughness of PLLA need to be further improved. Soft PEG segment was used to accelerate the crystallization rate and improve the toughness of PLLA in this study. To avoid the migration of PEG from the plastic result in lower the mechanical properties of packaging film and the contamination of foods, high molecular weight PLLA-PEG-PLLA triblock copolymers with various lengths of the PLLA segment was synthesized by copolymerization.

The PEG, for its part, is well known for its hydrophilicity, water-solubility, lack of toxicity and excellent biocompatibility (Stefani *et al.*, 2006). The interest of the

association of PLA and PEG is that it combines the mechanical properties of PLLA and the hydrophilicity and flexibility of PEG. The PLLA-*b*-PEG-*b*-PLLA triblock copolymers with various block lengths allow larger range of mechanical properties and degradation rates (Garric *et al.*, 2012). That leads this copolymer an excellent candidate for tissue engineering applications (Tessmar & Göpferich, 2007). Block copolymers based on PEG and poly(α -hydroxyacid) such as poly(D,L-lactide) (PDLLA) and poly(lactide-*co*-glycolide) (PLG) are being studied for drug delivery, owing to their biocompatibility, controlled biodegradability of poly(α -hydroxy acid) (Discher & Ahmed, 2006). It is reported that folate conjugation can increase the stability of FA-copolymer micelle compared to copolymer (PLA-MPEG) only, which was in part due to the lower micelle concentration (Zhu *et al.*, 2011). In the latter case, feasibility of controlled release of insulin from a poly(D,L-lactide-*co*-glycolide)-*b*-poly(ethylene glycol)-*b*-poly(D,L-lactide-*co*-glycolide) (PDLLAG-*b*-PEG-*b*-PDLLAG) sol-gel has been established (Zhang *et al.*, 2011).

2.2. Stereocomplexation of PLLA/PDLA blends

The scPLAs were first prepared by solution blending of low molecular weight PLLA and PDLA before solvent evaporation (Ikeda *et al.*, 2011). After that, many researchers have investigated full stereocomplex formation. Heat resistant property of melt blended scPLA did not significant increase for the co-existence of homocrystallites and stereocomplex crystallites. Thus the melt mixing process of PLLA and PDLA became a challenge because it was valuable in the industrial scale. Stereocomplex formation of PLLA/PDLA blends is shown in Fig. 6.

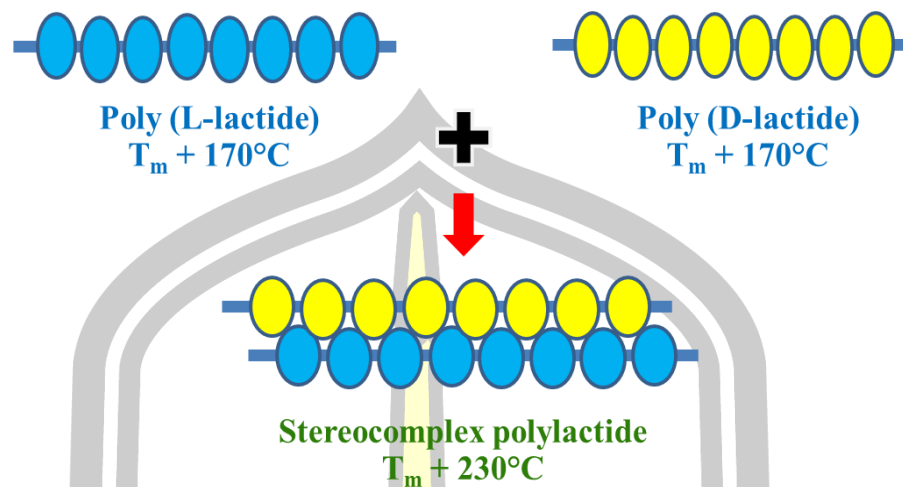


Fig. 6. Stereocomplex formation of PLLA/PDLA blends.

2.2.1 Effect of PLLA/PDLA blend ratio on stereocomplexation

The scPLA showed T_m around 230°C that was higher than the T_m of both PLLA and PDLA ($\sim 170^\circ\text{C}$). Fig. 7 shows effect of PLLA/PDLA blend ratio on stereocomplex formation. The PLLA/PDLA blends show two T_m of homocrystallites and stereocomplex crystallites. Only 50/50 (w/w) PLLA/PDLA blend ratio exhibits complete stereocomplex formation. The T_m of homo-crystallites has disappeared (Tsuji *et al.*, 1991).

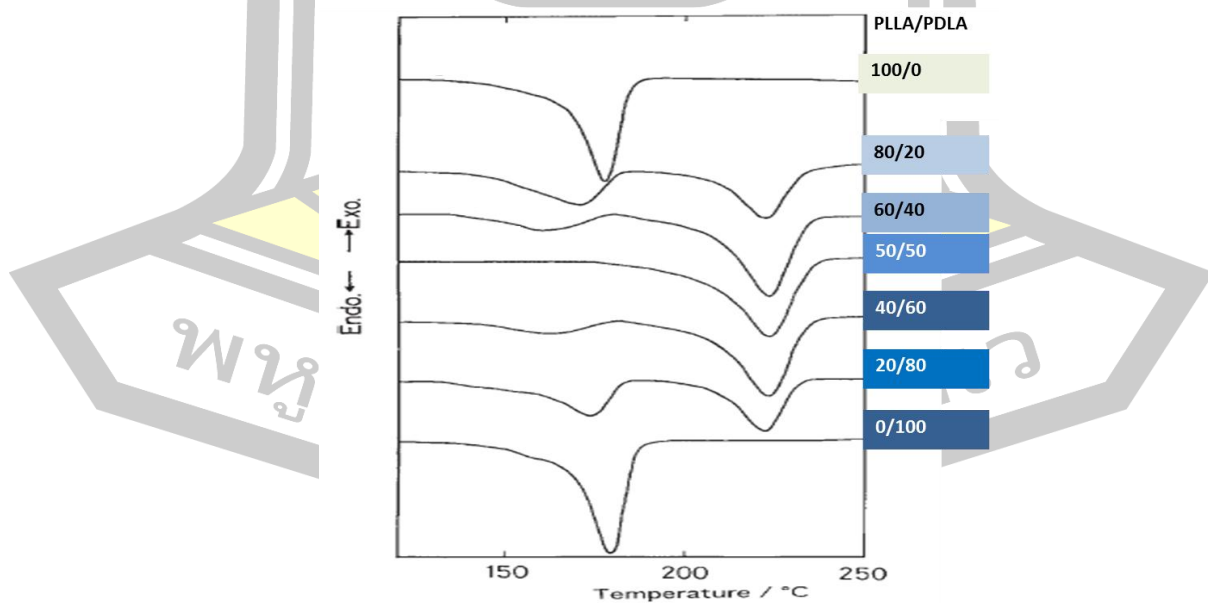


Fig. 7. DSC thermograms of PLLA, PDLA and PLLA/PDLA blends (M.W. of PLLA and PDLA = 60,000 g/mol) (Tsuji *et al.*, 1991).

2.2.2 Effect of M.W. of PLLA and PDLA on stereocomplexation

Influence of M.W. of PLA on stereocomplex formation is shown in Figs. 8 and 9. The blending ratio was kept constant at 50/50 w/w PLLA/PDLA. As shown in Fig. 8, low-low and medium-medium M.W. can induce complete stereocomplexation. In addition, the low M.W. PDLA gave complete stereocomplex formation with low, medium and high M.W. PLLA as shown in Fig. 9 (Tsuji *et al.*, 1991).

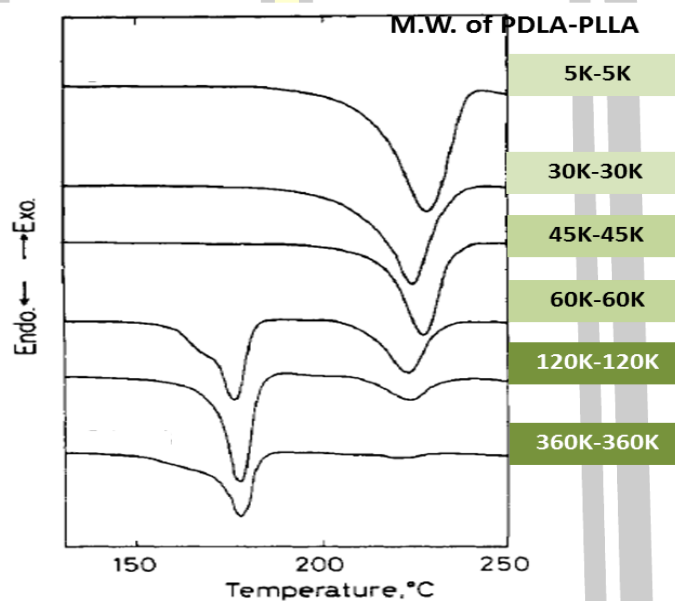


Fig. 8. DSC thermograms of 50/50 PLLA/PDLA blends prepared with different M.W. of PDLA and PLLA (Tsuji *et al.*, 1991).

พหุ ประถมศึกษา

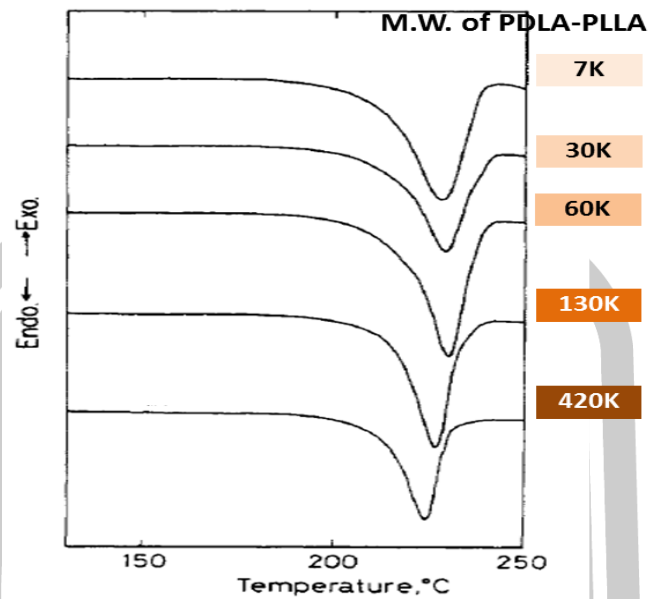


Fig. 9. DSC thermograms of 50/50 PLLA/PDLA blends prepared with different M.W. of PLLA (M.W. of PDLA = 5,000 g/mol) (Tsuji *et al.*, 1991).

2.2.3 Effect of stereocomplexation on mechanical properties

Fig. 10 illustrates influence of M.W. of PLAs on tensile strength and elongation at break of PLLA, PDLA and scPLA. It can be seen that the scPLA exhibited higher tensile strength and elongation at break than both the PLLA and PDLA. In addition, the tensile strength and elongation at break increased as the M.W. of PLAs increased (Tsuji & Ikada, 1993).

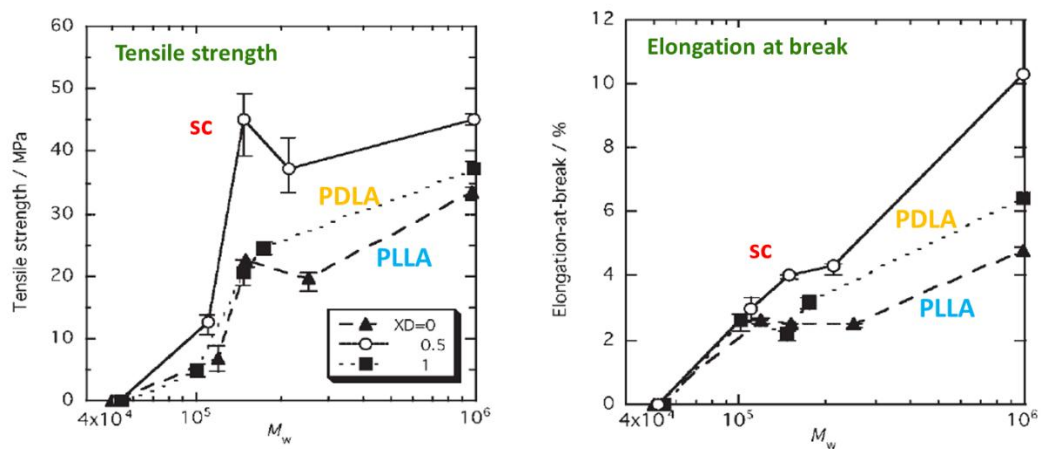


Fig. 10. Tensile properties of PLLA, PDLA and scPLA (Tsuji & Ikada, 1993).

2.2.4 Effect of stereocomplex on thermal stability

Fig. 11 presented thermogravimetric (TG) thermograms of PLLA, PDLA and scPLA in isothermal mode at different temperatures. It can be seen that the scPLA showed higher thermal stability at 250°C and 260°C than both PLLA and PDLA. The stronger van der Waal forces of scPLA enhanced its thermal stability (Tsuji & Fukui, 2003).

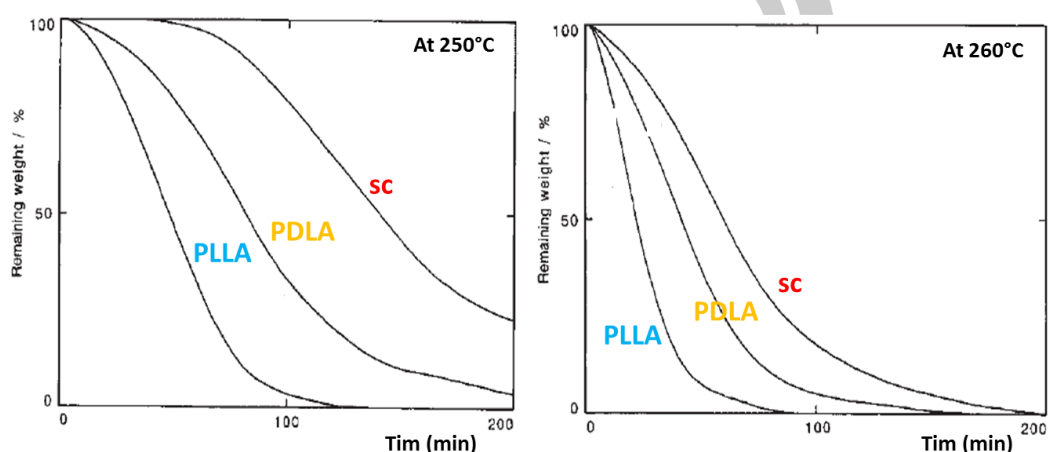


Fig. 11. TG thermograms of PLLA, PDLA and scPLA in isothermal mode at 250 °C and 260 °C (Tsuji & Fukui, 2003).

2.3. Stereocomplexation of PLLA/PDLA-PEG-PDLA blends

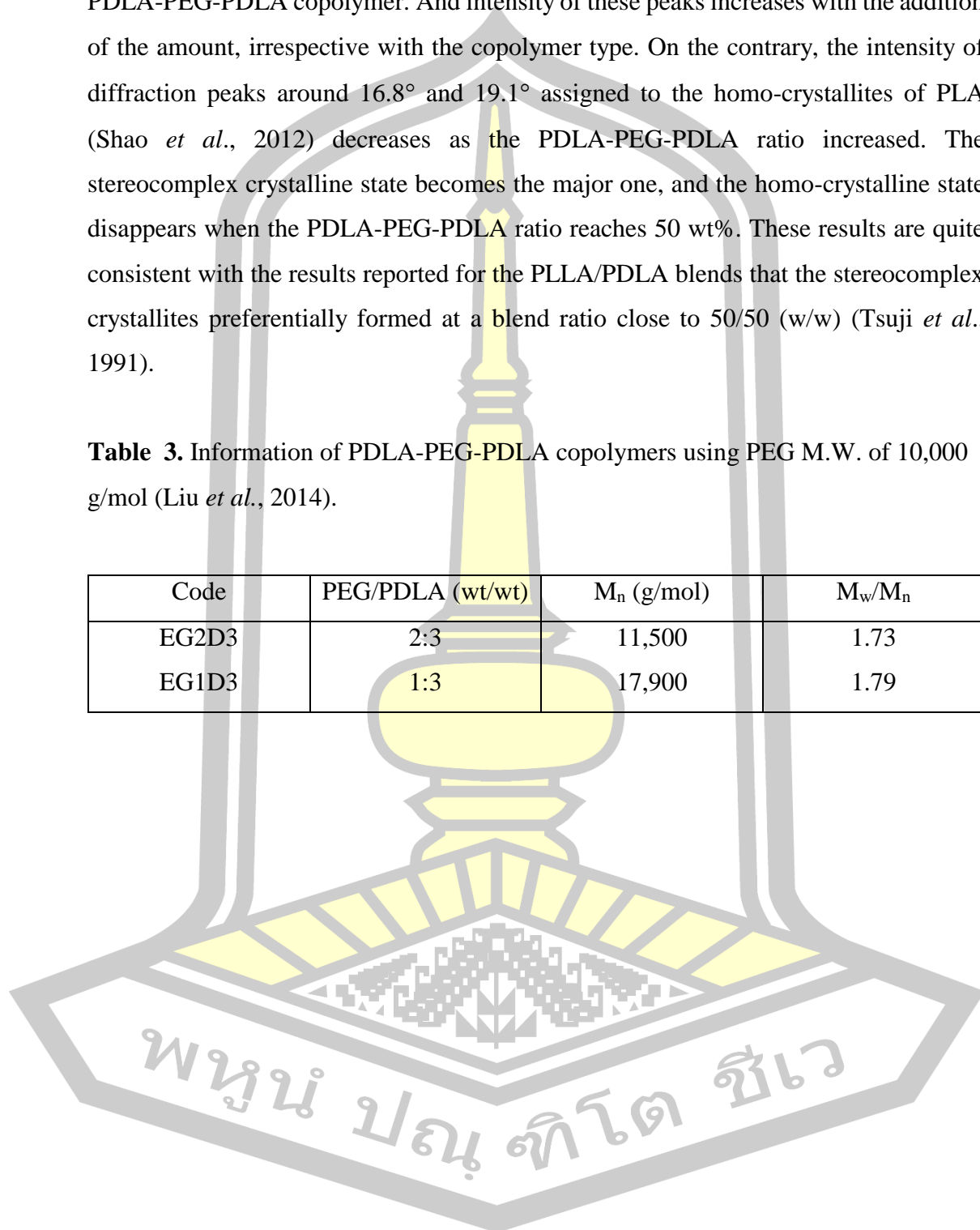
2.3.1. Effect of PLLA/PDLA-PEG-PDLA blend ratio on stereocomplexation

The PDLA-PEG-PDLA triblock copolymers were blended with the PLLA for improve flexibility of the resulted scPLA. (Liu *et al.*, 2014) have synthesized two PDLA-PEG-PDLA copolymers with different PDLA end-block lengths, as presented in Table 3. The PLLA/PDLA-PEG-PDLA blend films were prepared by solution blending. The stereocomplex formed between PLLA and PDLA blocks of PDLA-PEG-PDLA occurred during the solvent evaporation. The wide-angle X-ray diffraction (WAXD) and DSC methods are used to determine the crystalline state of these blend films. Fig. 12 shows WAXD profiles of the blend films prepared with different blend ratios and PDLA end-block lengths. The diffraction peaks around 12°, 21° and 24°

corresponding to stereocomplex crystallites could be observed with the presence of PDLA-PEG-PDLA copolymer. And intensity of these peaks increases with the addition of the amount, irrespective with the copolymer type. On the contrary, the intensity of diffraction peaks around 16.8° and 19.1° assigned to the homo-crystallites of PLA (Shao *et al.*, 2012) decreases as the PDLA-PEG-PDLA ratio increased. The stereocomplex crystalline state becomes the major one, and the homo-crystalline state disappears when the PDLA-PEG-PDLA ratio reaches 50 wt%. These results are quite consistent with the results reported for the PLLA/PDLA blends that the stereocomplex crystallites preferentially formed at a blend ratio close to 50/50 (w/w) (Tsuji *et al.*, 1991).

Table 3. Information of PDLA-PEG-PDLA copolymers using PEG M.W. of 10,000 g/mol (Liu *et al.*, 2014).

Code	PEG/PDLA (wt/wt)	M_n (g/mol)	M_w/M_n
EG2D3	2:3	11,500	1.73
EG1D3	1:3	17,900	1.79



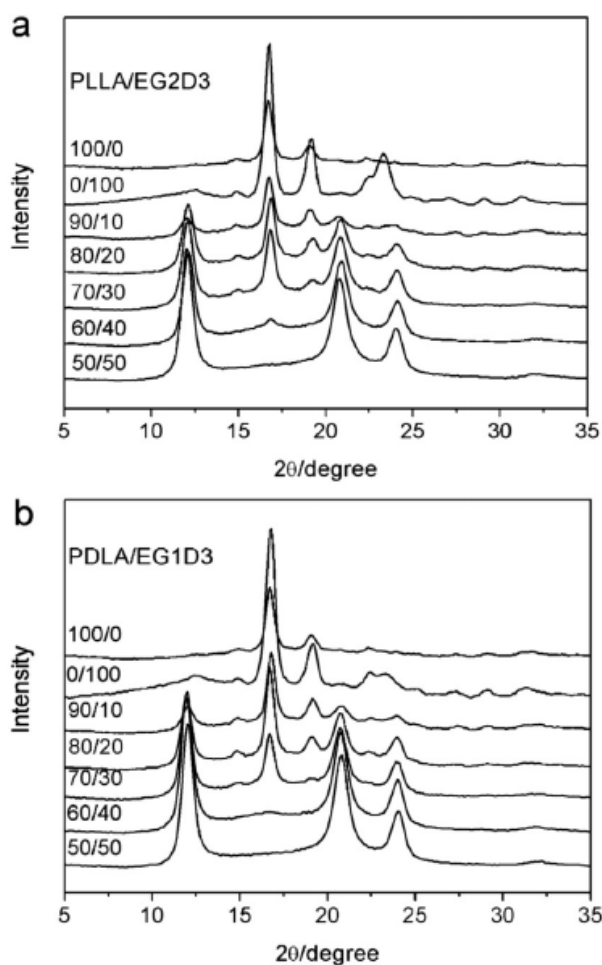


Fig. 12. WAXD profiles of (a) PLLA/EG2D3 and (b) PDLA/EG1D3 with different weight ratios (Liu *et al.*, 2014).

In Figs. 13(a), the heating curves of PLLA/EG2D3 and PDLA/EG1D3 are presented. The T_m of neat PLLA was detected at 178°C corresponding to homo-crystallites. The neat PDLA-PEG-PDLA copolymer, the T_m values of PEG and PDLA blocks were found at 39°C and 154°C, respectively. The homo-crystalline of PLLA and PDLA blocks were suppressed when the PDLA-PEG-PDLA was blended and its blend ratio was increased, which is consistent with the WAXD results. The stereocomplexation efficiency between the PLLA and PDLA chains is enhanced by the presence of PEG part of the copolymers. The full stereocomplex could be obtained when the amount of copolymer reaches 40 wt% (the actual amount of PDLA is less than 40 wt%), while the general opinion is that the full stereocomplex could be formed at PDLA to PLLA ratio from 40/60 to 60/40 (Kakuta *et al.*, 2009).

The homo-crystallization temperature (T_c) of neat PLL ($\sim 110^\circ\text{C}$) increased with the PDLA-PEG-PDLA ratio owing to the nucleation effect caused by stereocomplexation during the cooling process [Figs. 13(b)], and it disappears when the PDLA-PEG-PDLA ratio exceeds 40 wt%. Whereas the T_c of stereocomplex crystallization also increases with the PDLA-PEG-PDLA ratio.

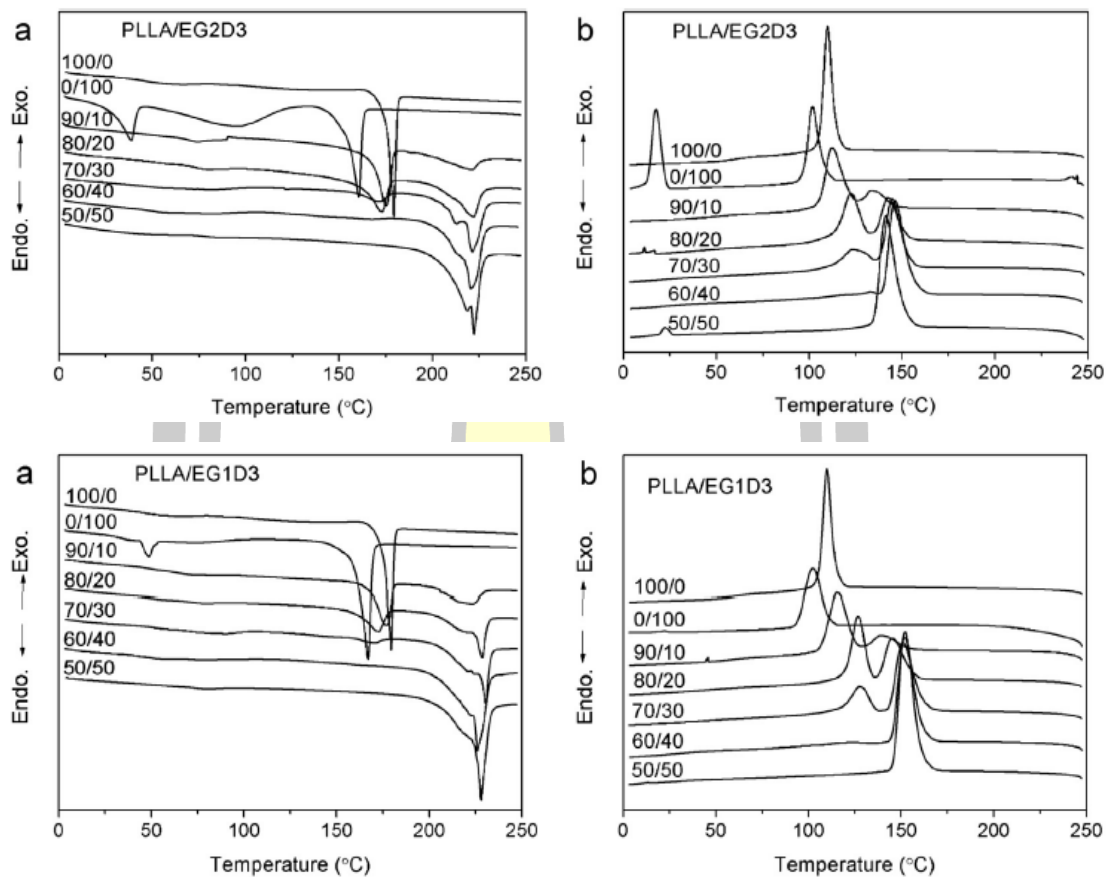


Fig. 13. Heating (a) and cooling (b) curves of PLLA/PDLA-PEG-PDLA blends with different weight ratios (Liu *et al.*, 2014).

Fig. 14 shows tensile results of the blend films. The tensile strength of the blend films slightly increased with increase in the content of PDLA-PEG-PDA ratio. The maximum values of tensile strength was obtained with 30 wt% PDLA-PEG-PDLA ratio, then the decreased of tensile can be observed. These tensile behaviors can be seen as the synergistic effect of stereocomplexation and molecular weight. The PLLA/PDLA

stereocomplexation give higher tensile strength (Tsuji & Ikada, 1999), but the M.W. of PDLA-PEG-PDLA copolymer is much lower than PLLA in this case, so the tensile strength is governed by the M.W. of PDLA-PEG-PDLA copolymers after a critical amount.

The elongations at break were no obvious increase when 10 wt% and 20 wt% PDLA-PEG-PDLA were blended, but enormous increase of elongation at break can be found with 30 wt% and 40 wt% PDLA-PEG-PDLA ratio. However the elongation at break decreases to around 50%, when 50 wt% copolymers are added, which might be caused by physical crosslinking effect of stereocomplex that limits the mobility of molecular chains, or by the M.W. of copolymers thjat lower than the critical value.

The relative content of PEG/PDLA has significant effect on mechanical properties of blends, as can be seen in Figs. 14(c) and (d). The PLLA/PDLA stereocomplexation increases the tensile strength with the PDLA content less than 25 wt%, whereas the copolymer with higher PDLA content (EG1D3) has greater contribution on tensile strength [Fig. 14(c)]. On the contrary, the copolymer with higher PEG content (EG2D3) has greater effect on elongation at break as can be seen in Fig. 14(d).

The toughening effect of the addition of PDLA-PEG-PDLA into PLLA could be explained by the synergistic effect of stereocomplexation between PLLA and PDLA blocks of PDLA-PEG-PDLA copolymer and plasticization effect from PEG blocks of PDLA-PEG-PDLA copolymer for short. The stereocomplexation could form a 3D crosslinking structure that increase the tensile strength whereas the existence of sufficient PEG promotes the slippery of crystallites, thus increasing the elongation at break of the samples. The balanced mechanical properties with good tensile and toughness could be achieved when 30 wt% PDLA-PEG-PDLA copolymer are added.

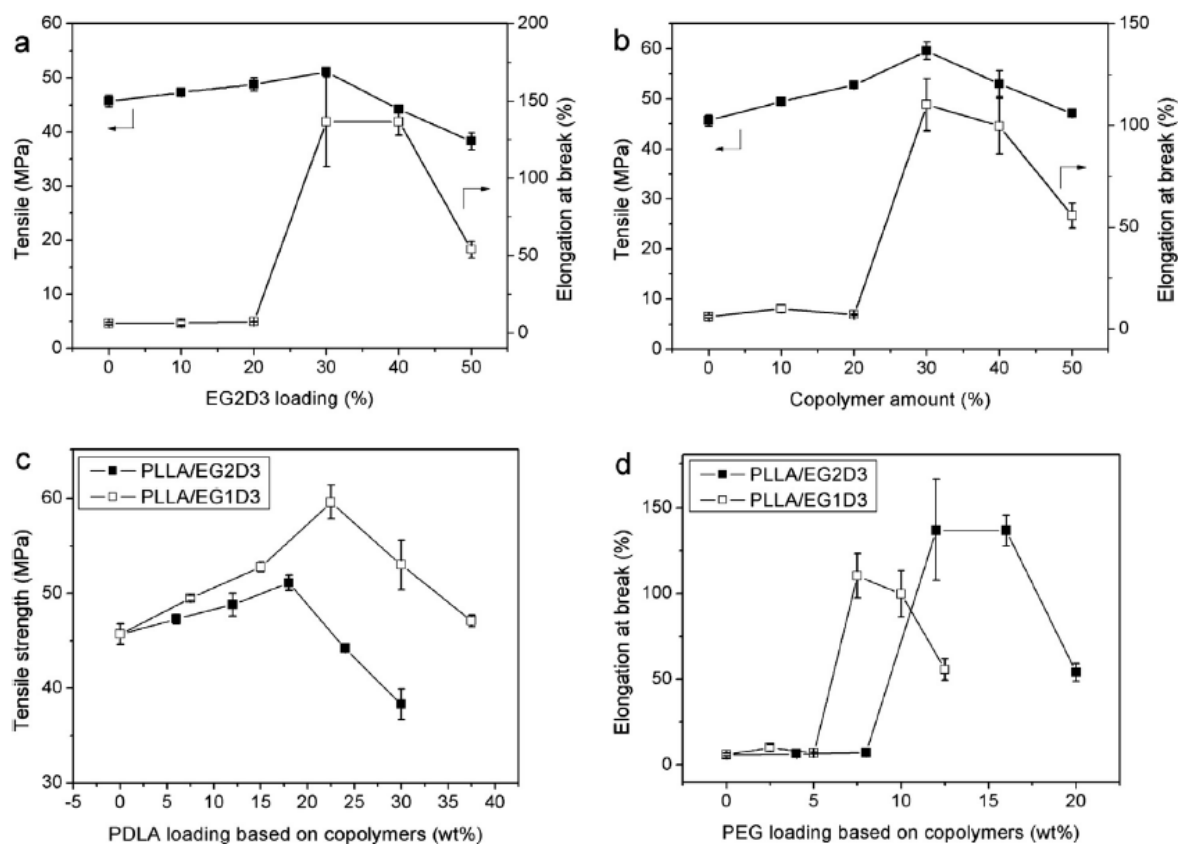


Fig. 14. Mechanical properties of PLLA/PDLA-PEG-PDLA blends of various compositions (Liu *et al.*, 2014).

2.3.2. Effect of PEG block length on stereocomplexation

The effect of PEG block length of PDLA-PEG-PDLA on stereocomplexation was investigated by using PLLA with M.W. of 45,000 (45k) g/mol. The PDLA block length of PDLA-PEG-PDLA was kept constant at 2,000 (2k) g/mol. The various PEG block lengths (0.4k, 1k and 2k g/mol) were used to synthesize the PDLA-PEG-PDLA copolymers (Song *et al.*, 2015). The PLLA/PDLA-PEG-PLLA blend films were prepared by solution blending before film casting.

Fig. 15 shows the heating scans of blend films after quenched from the melt. The T_g of neat PLLA is 62°C. For PLLA/PDLA, it decreases to 56°C with low molecular weight of PDLA acting as a plasticizer. For the blends of PLLA/PDLA-PEG-PDLA, the T_g of the blend with the longer PEG block is lower than that of the blend with a shorter PEG block. These results indicate that both the low molecular weight PDLA

and PEG blocks could act as a plasticizer to reduce the T_g of PLLA after blending due to the higher chain mobility of PDLA and the flexibility of PEG chains.

Moreover, upon heating, both neat PLLA and the PLLA/PDLA blend show only one crystallization peak (the peak temperature was marked with T_{c1}), whereas PLLA/PDLA-PEG-PDLA blends show two crystallization peaks (T_{c1} and T_{c2}). Also, with the increasing length of PEG, these crystallization peaks become sharper and the T_{c1} and T_{c2} shift to lower temperatures. This result indicates that the longer PEG block is more conducive for improving the crystallization rate of the blends.

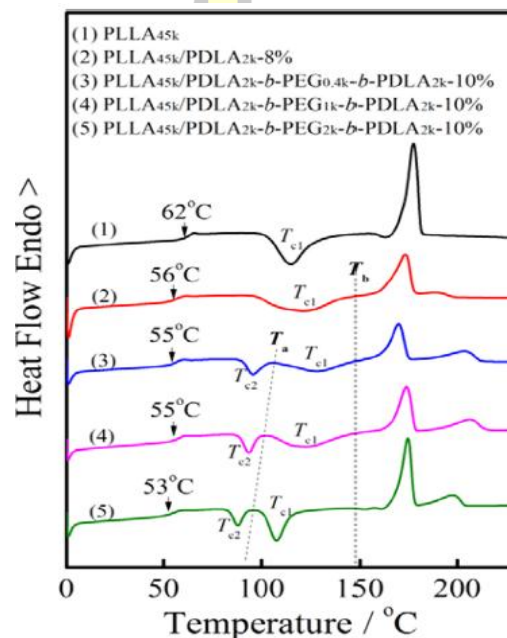


Fig. 15. DSC scans of PLLA and its blends after quenched from 230°C and then heated at a rate of 20°C/min (Song *et al.*, 2015).

2.3.3. Effect of PDLA block length on stereocomplexation

The effect of PDLA block length of PDLA-PEG-PDLA on stereocomplexation was investigated by using PLL with M.W. of 160,000 g/mol. The PEG block length of PDLA-PEG-PDLA was kept constant at 8,000 g/mol (PEG₁₈₂). The various PDLA repeating units (53, 81, 126 and 213 units) were prepared (Tacha *et al.*, 2015). The PLLA/PDLA-PEG-PLLA blend films were prepared by solution blending before film casting.

The DSC thermograms of the films prepared from blending PLLA with PDLA₅₃-PEG₁₈₂-PDLA₅₃, PDLA₈₁-PEG₁₈₂-PDLA₈₁, PDLA₁₂₆-PEG₁₈₂-PDLA₁₂₆ and PDLA₂₁₃-PEG₁₈₂-PDLA₂₁₃ are shown in Figs. 16 (a) - (d), respectively. All T_m at about 150°C corresponding to homo-crystalline melting temperatures were clearly observed in both the neat PLLA film and the blend films with added copolymer up to 30 wt%. Unlike PLLA/PDLA blend films, the addition of, at least, 40 wt% copolymer brought the complete stereocomplexation of the two PLA enantiomers, i.e. PLLA and PDLA, in all blend films as can be seen from a single melting peak observed at about 200°C, corresponding to a characteristic melting temperature of stereocomplex crystallites (Tsuji & Ikada, 1999; Tsuji et al., 1991). The stereocomplex crystallinity (% X_{sc}) was, in addition, increased with increasing the copolymer composition in the blend films. It should be noted that all the PLLA/copolymer blend films, with the addition of copolymers higher than 20 wt%, demonstrated the amount of % X_{sc} more than PLLA/PDLA blend films. These relative high values of % X_{sc} were resulted from the plasticization effect of PEG in the copolymers that facilitated the mobility of the polymer chains and, thus, substantial alignment of the PLLA and PDLA blocks (Kulinski & Piorkowska, 2005). The mobility of the polymer chains, however, was restricted by the increase of PDLA blocks in the copolymers. The longer PDLA blocks led to the progressive decrease of % X_{sc} of the films for the same blend ratios.

Also, it should be noted that the melting peaks of PEG block in the copolymer was decreased in its intensity when the PDLA block increased from 53 (in PDLA₅₃-PEG₁₈₂-PDLA₅₃) to 81 (in PDLA₈₁-PEG₁₈₂-PDLA₈₁), respectively shown in Figs. 16(a) to (b) bottom thermograms, and the PEG melting peak was completely disappeared when the PDLA block further increased, i.e. from 126 (in PDLA₁₂₆-PEG₁₈₂-PDLA₁₂₆) to 213 (in PDLA₂₁₃-PEG₁₈₂-PDLA₂₁₃) as respectively observed in Figs. 16(c) to (d) bottom thermograms. The effect was clearly exemplified in Fig. 16(e), showing the thermograms in second heating scan where the thermal history of the copolymers was erased. The gradual decline and eventual disappearance of PEG melting peak with increasing PDLA block length in the copolymers clearly suggested that the crystallization of PEG was restricted by the addition of PLA. This effect was also emphasized when blending PLLA with the copolymers. The thermograms of PLLA/copolymer films mostly exhibited no PEG melting temperature. The

crystallization of PEG, therefore, was interrupted and, thus, prohibited by either adding PDLA or PLLA in the system (Kulinski & Piorkowska, 2005). In addition, the melting temperature of PDLA in the copolymers slightly shifted to higher temperature with increasing PDLA block length.

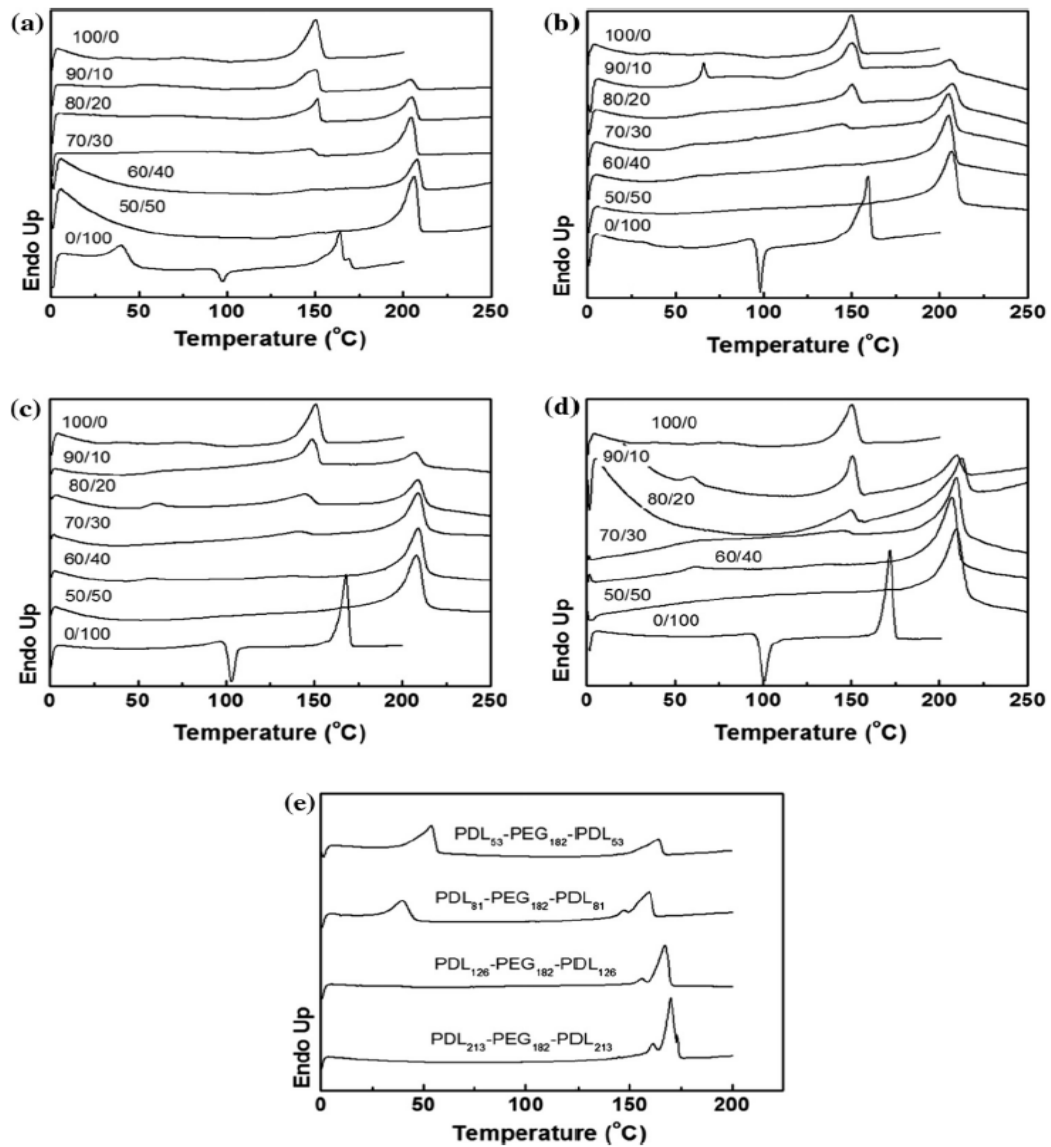


Fig. 16. DSC thermograms of PLLA/copolymer blended-films prepared from blending PLLA with (a) PDLA₅₃-PEG₁₈₂-PDLA₅₃, (b) PDLA₈₁-PEG₁₈₂-PDLA₈₁, (c) PDLA₁₂₆-PEG₁₈₂-PDLA₁₂₆ and (d) PDLA₂₁₃-PEG₁₈₂-PDLA₂₁₃ in various compositions; (e) the second heating run thermograms of the copolymers (Tacha *et al.*, 2015)

2.4. Stereocomplexation of PLLA-PEG-PLLA/PDLA-PEG-PDLA blends

The PLLA-PEG-PLLA (LEL) and PDLA-PEG-PDLA (DED) were synthesized by ring-opening polymerization of L- and D-lactide monomers, respectively using PEG as the initiator. The PLLA-PEG-PLLA/PDLA-PEG-PDLA blend films were prepared by solution blending before solvent evaporation. These copolymers with different PEG, PLLA and PDLA block lengths were synthesized as reported in Table 4 (Han *et al.*, 2016).

Table 4. Molecular characteristics of PLLA-PEG-PLLA and PDLA-PEG-PDLA triblock copolymers (Han *et al.*, 2016).

Sample ^a	$M_{n,th}$ ^b (kDa)	$M_{n,NMR}$ ^c (kDa)	$M_{n,GPC}$ ^d (kDa)	PDI	mPEG ^e (wt%)
LE _{2k} L _{44k}	78.8	89.3	125.9	1.30	2.2
DE _{2k} D _{43k}	77.1	87.4	105.9	1.25	2.3
LE _{6k} L _{44k}	88.9	93.8	94.4	1.32	6.4
DE _{6k} D _{42k}	86.2	89.8	90.8	1.26	6.7
LE _{20k} L _{45k}	104.1	110.2	100.5	1.43	18.1
DE _{20k} D _{45k}	102.4	109.3	99.0	1.25	18.3
LE _{20k} L _{30k}	83.7	79.5	60.3	1.29	25.2
DE _{20k} D _{32k}	84.6	83.4	61.5	1.28	24.0
LE _{20k} L _{22k}	65.7	63.2	45.0	1.27	31.6
DE _{20k} D _{21k}	64.5	62.2	41.6	1.35	32.2

^a PLLA-PEG-PLLA and PDLA-PEG-PDLA are abbreviated as LE_xL_y and DE_xD_y, respectively, where x is the M_n of PEG middle-block and y is the M_n (calculated from ¹H-NMR) of each PLLA or PDLA end-block.

^b M_n calculated theoretically, $M_{n,th} = [M]/[I] \times 144.13 \times \text{yield} + M_{m,PEG}$, where $M_{m,PEG}$ is the M_n of PEG middle-block.

^c M_n determined by ¹H-NMR.

^d M_n measured by GPC.

^e Weight percentage of PEG in triblock copolymer.

Fig. 17 shows the DSC curves of 50/50 (w/w) PLLA-PEG-PLLA/PDLA-PEG-PDLA blends obtained in the cooling and subsequent heating scans. DSC curves of PLLA/PDLA blend with the similar molecular weight are included in Fig. 17 for comparison. Crystallization and melting behavior of enantiomeric blends depend strongly on the lengths of PEG middle-block and PLLA, PDLA end-blocks. For the enantiomeric blends with similar PLLA, PDLA block lengths (i.e., PLLA/PDLA, LE_{20k}L_{44k}/DE_{20k}D_{43k}, LE_{6k}L_{42k}/DE_{6k}D_{42k}, LE_{20k}L_{45k}/DE_{20k}D_{45k}), their ΔH_c , $\Delta H_{m,SC}$, $X_{c,SC}$, and $f_{SC,DSC}$ values increase and the cold crystallization peaks observed in subsequent heating scans gradually diminish as the length of PEG middle-block increases (Fig. 17). This suggests that the presence of flexible PEG middle-block enhances the crystallization rate and stereocomplexation ability of PLLA and PDLA. Similar acceleration effects of PEG on the crystallization of PLLA have been found in the PLLA/PEG blends (Hu *et al.*, 2003; Lai *et al.*, 2004; Wei *et al.*, 2014) Previous reports have demonstrated that PLLA and PEG have good miscibility (Hu *et al.*, 2003; Lai *et al.*, 2004) and the PLLA/PEG block copolymers with a wide M_n range of PLL and PEG blocks are miscible in melt state (Yang *et al.*, 2015; Yang *et al.*, 2012; Zhou *et al.*, 2015). The acceleration effects of PEG on PLLA/PDLA crystallization are attributed to the enhanced chain diffusion and mobility (Wei *et al.*, 2014).

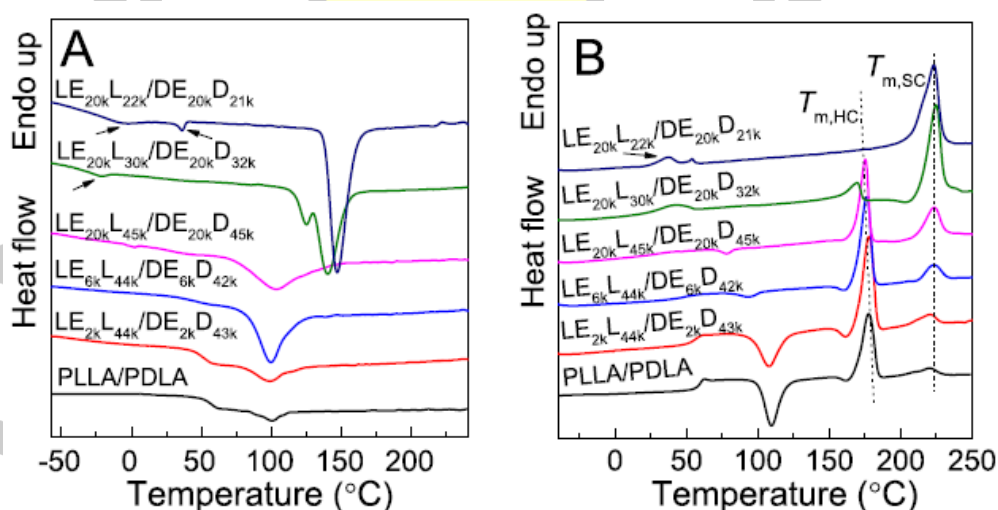


Fig. 17. DSC curves of PLLA-PEG-PLLA/PDLA-PEG-PDLA and PLLA/PDLA blends: (A) cooling scans from the melt state (250 °C); (B) subsequent heating scans after cooling. Both the cooling and heating rates are 10 °C/min (Han *et al.*, 2016).

As shown in Fig. 18. PLLA homopolymer and PLLA/PDLA blend are brittle. The PLLA/PDLA blend has a tensile strength of 53.7 MPa, a modulus of 1.38 GPa, and an elongation-at-break of 11.9%, compared to the 41.5 MPa, 1.35 GPa, and 4.6% of PLLA. As the length of PEG middle-block increases, the tensile strengths and moduli of PLLA-PEG-PLLAs, PLLA-PEG-PLLA/PDLA-PEG-PDLA blends decrease and their elongations-at-break increases, because the flexible PEG segments promote the slippery of PLLA, PDLA crystallites under mechanical deformation (Nijenhuis *et al.*, 1996). Interestingly, the stereocomplexation of PLLA/PDLA blends exerts dual effects on the mechanical properties. It not only enhances the mechanical strength but also improves the ductility and toughness of stereocomplexed materials. The PLLA/PDLA and PLLA-PEG-PLLA/PDLA-PEG-PDLA blends exhibit larger tensile strength and elongation at break than the corresponding PLLA and PLLA-PEG-PLLA. The tensile strength and elongation at break of $LE_{20k}L_{22k}$ increase from 12.3 MPa, 41.1% to 31.6 MPa, 410.4% after stereocomplexation with the same amount of $LE_{20k}L_{21k}$, respectively. The elongation at break of PLLA-PEG-PLLAs having the PEG_{20k} middle-block enhance by 4-10 folds after stereocomplexation with the corresponding PDLA-PEG-PDLAs. The increased strength of enantiomeric blends is stemmed from the higher strength and compact chain packing in SCs; this is consistent with the results of the PLLA/PDLA blend (Tsuji & Ikada, 1999) and stereocomplex thermoplastic elastomers (Chang *et al.*, 2015; Huang *et al.*, 2016; Huang *et al.*, 2014). On the other hand, SC formation is a typical process of intermolecular crystallization, in which the PLLA and PDLA blocks coming from different macromolecules pack together in the same crystal lattice. Accordingly, SCs can serve as the physical crosslinks in the PLLA-PEG-PLLA/PDLA-PEG-PDLA blends (Wei *et al.*, 2014; Yamane *et al.*, 2004). The presence of such physically-crosslinked domains would facilitate the energy absorption and dissipation when the external stress is applied, leading to the increased ductility and toughness for the stereocomplexed materials.

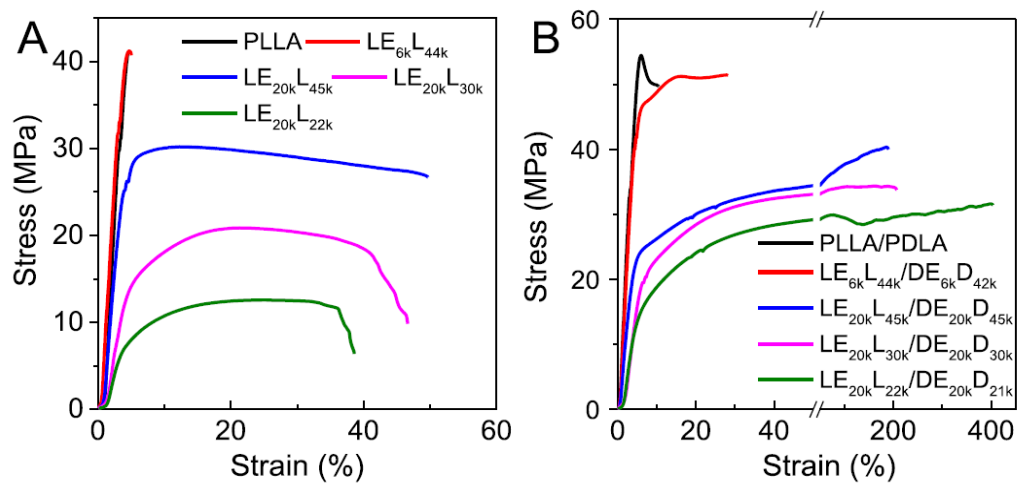


Fig. 18. Tensile stress vs strain curves for solution-cast films of (A) PLLA-PEG-PLLAs and (B) PLLA-PEG-PLLA/PDLA-PEG-PDLA blends (Han *et al.*, 2016).



CHAPTER III

RESEARCH METHODOLOGY

3.1 Chemicals and instruments

3.1.1 Chemicals

The chemicals used in this research were listed in Table 5.

Table 5. Chemicals used in this research.

Chemicals	Usage	Grade	Supplier
D-Lactic acid	Monomer precursor	D-form $\geq 99\%$	Haihang (China)
L-Lactic acid	Monomer precursor	Heat stable grade (L-form $\geq 95\%$)	PURAC (Thailand)
Poly(ethylene glycol) (PEG)	Initiator	Molecular weight of 20,000 g/mol	Sigma-Aldrich
Zinc Oxide	Catalyst	AR	Ajax Finechem
1-Dodecanol	Initiator	98%	Acros Organics
Stannous octoate	Catalyst	95%	Sigma
Ethyl acetate	Solvent	Commercial grade*	Carlo Erba
Chloroform	Solvent	AR	Merck
Joncryl® ADR-4386	Chain extender	ADR 4368	BASF (Thailand)

* Fraction distillation before use.

3.1.2 Instruments

The main items of instruments used in this research were listed in Table 6.

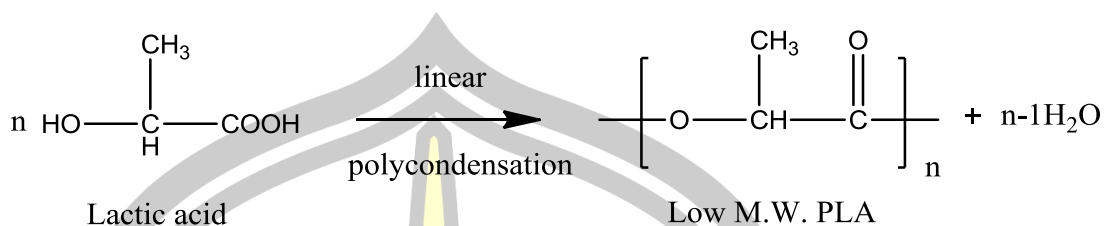
Table 6. Instruments used in this research.

Instruments	Model	Company
X-ray diffractometer	D8 Advance	Bruker
Thermogravimetric analyzer	SDT Q600	TA Instruments
Vacuum oven	Vacucell	MMM Group
Tensile tester	LRX+	Lloyds
High vacuum pump	Rv. 8	Edward
Ubbelohde viscometer	12350	Schott Gerate
Melt flow indexer	MPI200	Tinius Olsen
Internal mixer	Rheomex	Haake
Compression molding machine	Auto CH 25 Ton	Carver, Inc.
¹ H-NMR Spectrometer	DPX 400	Bruker Advance
Dynamic mechanical analysis (DMA)	Q800	TA Instruments

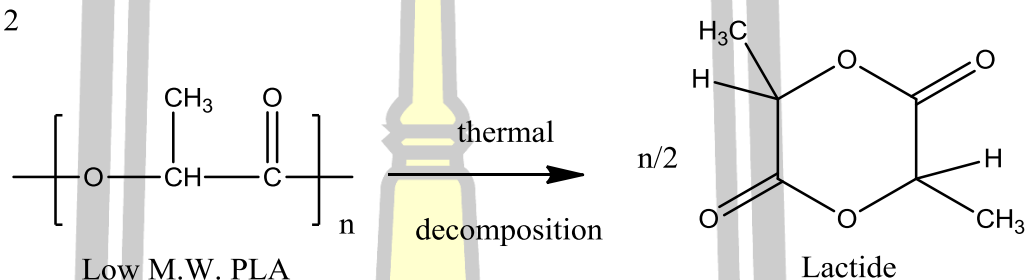
3.2 Monomer preparation and characterization

L-lactide (LLA) and D-lactide (DLA) monomers were synthesized from its cheaper precursors; L-lactic and D-lactic acid, respectively. The synthesis of monomer is a two-step process involving, firstly, the direct polycondensation of lactic acid to low molecular weight poly(lactic acid) (low M.W. PLA) followed, secondly, by thermal decomposition of the low M.W. PLA to yield crude lactide as the primary decomposition product, as shown below.

Step 1



Step 2



In a typical synthesis experiment in this work, approximately 5,000 g lactic acid was added into a 5 L round-bottomed flask which contained about 3 g zing oxide as a catalyst. The flask was then heated at 180°C in a conventional short-path distillation apparatus for 3 h [see Fig. 19 (a)]. The pressure of system was reduced (ca. -25 inch Hg) for 1 h to facilitate further removal of water and to increase the polymer yield. The product at this stage was low M.W. PLA.

The 5 g of Sn(Oct)₂ was added before adjusting to higher vacuum. The temperature was kept constant at 230-240°C under a reduced pressure of -28 inch Hg for 2 h to thermally degrade the low M.W. PLA to yield lactide as the primary product [see Fig. 19 (b)]. Crude lactide began to distill out of the flask as a pale brown crystalline solid in approximately 50-60% yield based on the initial lactic acid.

พหุ ประถมศึกษา

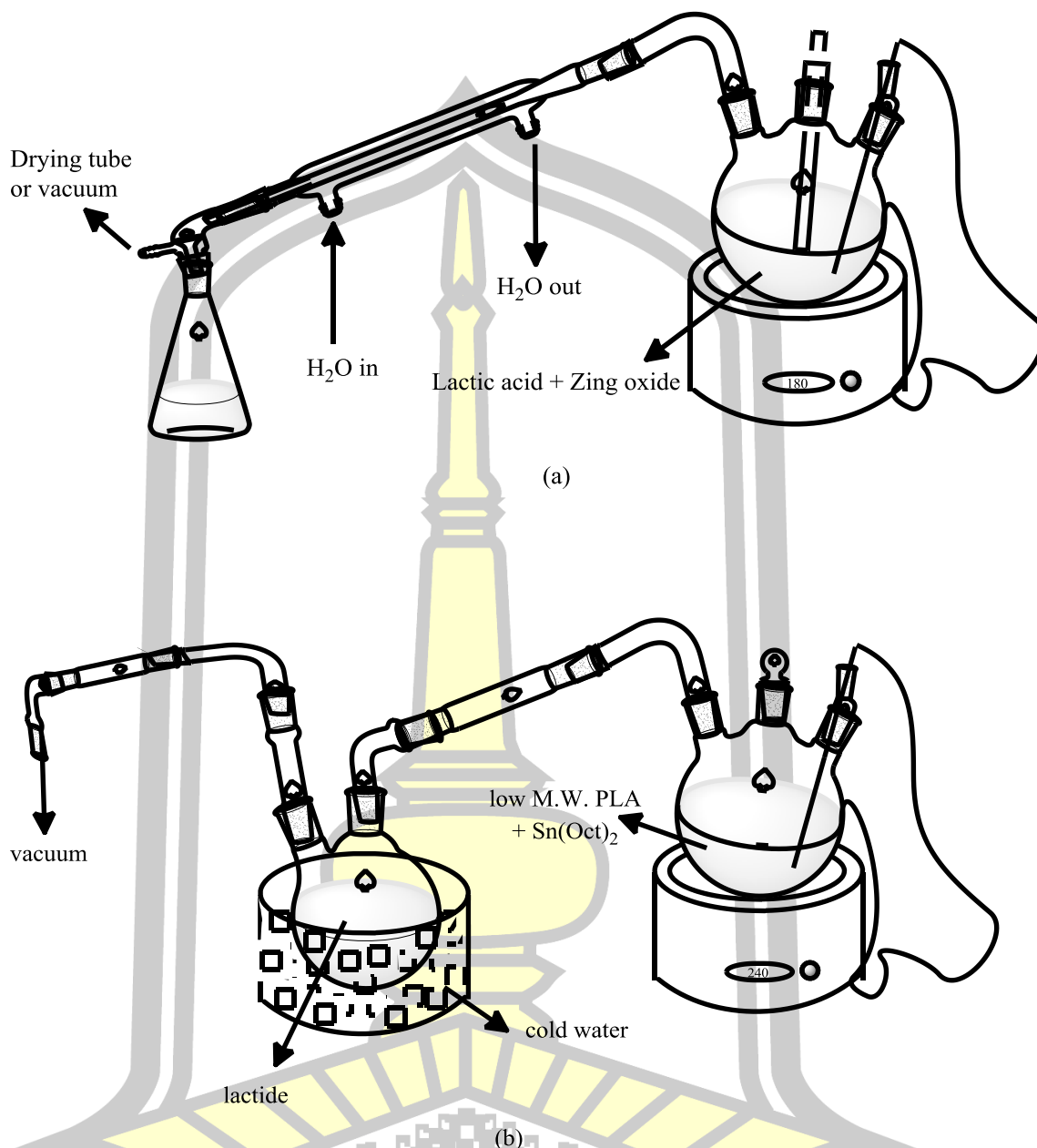


Fig. 19. Apparatus used in the two-step preparation of lactide: (a) direct polycondensation of lactic acid and (b) thermal decomposition of low M.W. PLA.

The crude lactide which had collected in the round bottom flask [Fig. 19(b)] was carefully and quickly removed due to its hygroscopic nature. After that it was purified at least 4 times by re-crystallisation from distilled ethyl acetate. The purified lactide was obtained as a white, needle-like, crystalline solid. It was dried in a vacuum oven at 55°C for at least 48 h before use in polymerization.

Optical rotation property of LLA and DLA monomers were determined by polarimetry. The approximate 0.1 g of sample was dissolved in 10 mL of benzene before determining at 25 °C with sodium D line of 589 nm Degree of optical rotation of lactide unit (α_{lactide}) was calculated from equation (3.1). Specific optical rotation of lactide unit measured at 25 °C with sodium D line of 589 nm ($[\alpha]_{589}^{25}$) was calculated from the α_{lactide} , as shown in equation (3.2). (Feng *et al.*, 2010; Kumar *et al.*, 2016)

$$\alpha_{\text{lactide}} = \alpha/2 \quad (3.1)$$

$$[\alpha]_{589}^{25} = \alpha_{\text{lactide}}/cl \quad (3.2)$$

α = degree of optical rotation of lactide unit (deg)

α_{lactide} = degree of optical rotation of lactide unit (half of lactide unit) (deg)

$[\alpha]_{589}^{25}$ = specific optical rotation of lactide unit (half of lactide unit) (deg · g⁻¹ · ml · dm⁻¹)

c = lactide concentration (g · ml⁻¹)

l = length of sample tube (1 dm)

Fractions of L-lactide unit (X_L) and D-lactyl unit (X_D) were determined from equations (3.3) and (3.4), respectively.

$$X_L (\%) = 100([\alpha]_{589}^{25} - 297)/(-297 - 297) \quad (3.3)$$

$$X_L + X_D = 100 \quad (3.4)$$

X_L = fraction of L-lactide unit

X_D = fraction of D-lactide unit

Where $[\alpha]_{589}^{25}$ of 100% pure L-lactide ($X_L = 100\%$) is -297 deg · g⁻¹ · ml · dm⁻¹ for benzene (Zhang *et al.*, 2005) and $[\alpha]_{589}^{25}$ of 100% pure L-lactide ($X_L = 100\%$) is -287 deg · g⁻¹ · ml · dm⁻¹ for chloroform. (Feng *et al.*, 2010)

Thermal decomposition of LLA and DLA monomers were characterized from TGA. The 5 - 10 mg of sample was heated at the heating rate of 20 °C/min under nitrogen flow.

3.3 Synthesis of polylactides

3.3.1 Synthesis of triblock copolymers

Poly(D-lactide) (PDLA) with feed M.W. of 5,000 g/mol was synthesized by ring-opening polymerization of DLA at 165°C for 2.5 h using Sn(Oct)₂ (0.01 mol%) as a

catalyst and 1-dodecanol (26.92 mol%) as an initiator. The polymerization reaction was presented in Fig. 20. The obtained polymers were granulated before dried in a vacuum oven at 110°C for 2 h to remove some un-reacted DLA.

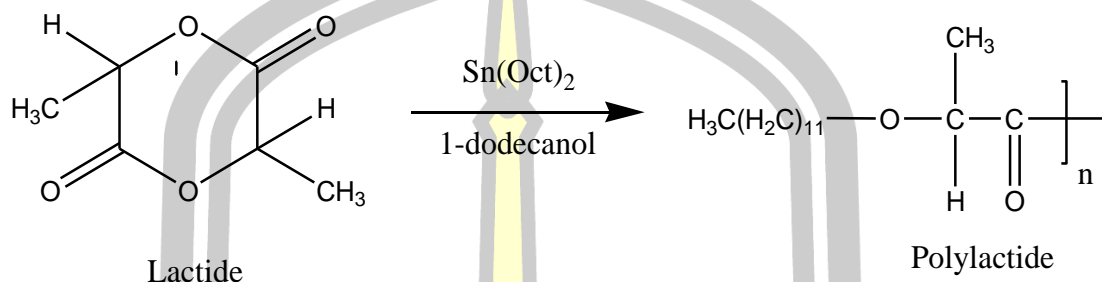


Fig. 20. Polymerization reaction of PDLA.

3.3.2 Synthesis of triblock copolymers

Triblock copolymers of poly(L-lactide)-*b*-poly(ethylene glycol)-*b*-poly(L-lactide) (PLLA-PEG-PLLA) and poly(D-lactide)-*b*-poly(ethylene glycol)-*b*-poly(D-lactide) (PDLA-PEG-PDLA) with feed M.W. of 120,000 g/mol were synthesized by ring-opening polymerization in bulk of LLA and DLA monomers, respectively, under a nitrogen atmosphere at 165°C for 6 h using Sn(Oct)₂ (0.075 mol%) as a catalyst. The PEG with M.W. of 20,000 g/mol were used as an initiator. The polymerization reaction was presented in Fig. 21. The obtained copolymers were granulated before dried in a vacuum oven at 110°C for 2 h to remove some un-reacted lactides.



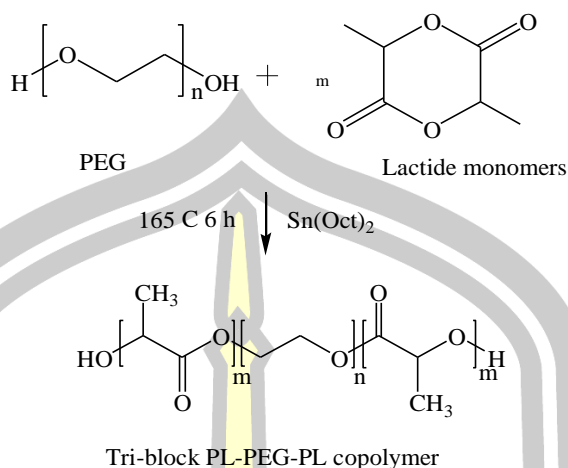


Fig. 21. Polymerization reaction of triblock copolymers.

3.4 Characterization of polylactides

The PDLA, PLLA-PEG-PLLA and PLLA-PEG-PDLA were characterized by the following of instrumental methods:

3.4.1 Optical rotation property

Optical rotation property of polymer sample was studied from polarimetry. The approximate 0.1 g of sample was dissolved in 10 mL of chloroform before determining at 25 °C with sodium D line of 589 nm (Kumar *et al.*, 2016). Degree of optical rotation of lactyl unit (α_{lactyl}) was calculated from equation (3.5). Specific optical rotation of lactyl unit measured at 25 °C with sodium D line of 589 nm ($[\alpha]_{589}^{25}$) was calculated from the α_{lactyl} , as shown in equation (3.6). (Feng *et al.*, 2010; Kumar *et al.*, 2016)

$$\alpha_{\text{lactyl}} = \alpha / 2 \quad (3.5)$$

$$[\alpha]_{589}^{25} = \alpha_{\text{lactyl}} / c l \quad (3.6)$$

α = degree of optical rotation of lactyl unit (deg)

α_{lactyl} = degree of optical rotation of lactyl unit (deg)

$[\alpha]_{589}^{25}$ = specific optical rotation of lactyl unit ($\text{deg} \cdot \text{g}^{-1} \cdot \text{ml} \cdot \text{dm}^{-1}$)

c = lactyl concentration ($\text{g} \cdot \text{ml}^{-1}$)

l = length of sample tube (1 dm)

Fractions of L-lactyl unit (X_L) and D-lactyl unit (X_D) were determined from equations (3.7) and (3.8), respectively.

$$X_L (\%) = 100([\alpha]_{589}^{25} - 157)/(-157 - 157) \quad (3.7)$$

$$X_L + X_D = 100 \quad (3.8)$$

X_L = fraction of L-lactyl unit

X_D = fraction of D-lactyl unit

Where $[\alpha]_{589}^{25}$ of 100% pure L-lactyl ($X_L = 100\%$) is $-157 \text{ deg} \cdot \text{g}^{-1} \cdot \text{ml} \cdot \text{dm}^{-1}$.

(Feng *et al.*, 2010)

3.4.2 Diluted-solution viscometry

Intrinsic viscosity, $[\eta]$, of PDLA and triblock copolymers directly related to its molecular weight was determined by diluted-solution viscometry in chloroform solution at 25°C using an Ubbelohde-type viscometer. Polymer concentration with approximate 0.02 g/dL was used to determine the $[\eta]$ by equation (3.9) (Feng *et al.*, 2013). Viscosity-average molecular weight (M_v) of PDLA was calculated by Mark–Howing–Sakurada equation (3.10). (Garlotta, 2002).

$$[\eta] = \frac{\sqrt{2(\eta_{sp} - \ln\eta_r)}}{c} \quad (3.9)$$

$$[\eta] = 5.45 \times 10^{-4} M_v^{0.73} \quad (3.10)$$

Where: $[\eta]$ is the intrinsic viscosity of samples, dL g^{-1} , $\eta_{sp} = (t-t_0)/t_0$; c is the sample concentration, g dL^{-1} ; t and t_0 are the elution time for the sample solution and the CH_3Cl , s and M_v is a viscosity-averaged molecular weight.

3.4.3 Gel permeation chromatography (GPC)

Number-average molecular weight (M_n) and dispersity index (DI) of PDLA and triblock copolymers were determined by GPC method at 40°C with flow rate of 1.0 mL/min. Tetrahydrofuran was used as a solvent at 40 °C. Polystyrenes with narrow DI value were used as standard for calibration curves.

3.4.4 Thermogravimetric analysis (TGA)

Thermal decomposition behaviors of PDLA and triblock copolymers were determined by thermogravimetric analyzer (TGA). The 5 - 10 mg of sample was heated at the heating rate of 20 °C/min under nitrogen flow.

3.4.5 Differential scanning calorimetry (DSC)

Thermal transition properties of PDLA and triblock copolymers were studied by differential scanning calorimeter (DSC). The 2 - 5 mg of sample was sealed in an aluminum pan that was melted at 200°C for 2 min to eliminate its thermal history before quenching to 0°C and re-heated from 0 to 200°C at the rate of 10 °C/min under nitrogen atmosphere in order to observe their glass transition temperature (T_g), cold crystallization temperature (T_{cc}), enthalpy of cold crystallization (ΔH_{cc}), melting temperature (T_m) and enthalpy of melting (ΔH_m).

3.4.6 $^1\text{H-NMR}$ spectrometry

Chemical functional groups and compositions of PDLA and triblock copolymers were determined by $^1\text{H-NMR}$ spectrometer at room temperature. Deuterated chloroform (CDCl_3) was used as a solvent.

3.5 Preparation of stereocomplex poly lactides

3.5.1 PLLA-PEG-PLLA/PDLA blends

Prior to mixing, all materials were vacuum dried at 55°C overnight. The stereocomplex poly lactides (scPLA) of PLLA-PEG-PLLA/PDLA blends were fabricated by melt blending using an internal mixer at 200°C for 4 min with rotor speed of 100 rpm. The films of scPLA were fabricated by compression molding at 240°C. The films were pre-melted for 1.0 min before being compressed with 5 ton for 1.0 min. Allowed to cool to room temperature with water. The formulations of the scPLA with different PLLA-PEG-PLLA/PDLA weight ratios (100/0, 90/10, 80/20, 70/30 and 60/40) and Joncryl® contents (0.0 and 4.0 phr) were prepared. Table 7 shows formulations of the scPLA.

Table 7. Formulations of PLLA-PEG-PLLA/PDLA blends.

PLLA-PEG-PLLA/PDLA ratio (w/w)	PLLA-PEG-PLLA (g)	PDLA (g)	Joncryl® (g)
100/0	50	-	-
90/10	45	5	-
80/20	40	10	-
70/30	35	15	-
60/40	30	20	-
100/0	50	-	2.0
90/10	45	5	2.0
80/20	40	10	2.0
70/30	35	15	2.0
60/40	30	20	2.0

3.5.2 PLLA-PEG-PLLA/PDLA-PEG-PDLA blends

Prior to mixing, all materials were vacuum dried at 55°C overnight. The stereocomplex poly lactides (scPLA) of PLLA-PEG-PLLA/ PDLA-PEG-PDLA blends were fabricated by melt blending using an internal mixer at 200°C for 4 min with rotor speed of 100 rpm. The films of scPLA were fabricated by compression molding at 240°C. The films were pre-melted 1.0 min before being compressed with 5 ton for 1.0 min. Allowed to cool to room temperature with water. The formulations of the scPLA with different PLLA-PEG-PLLA/ PDLA-PEG-PDLA weight ratios (100/0, 90/10, 80/20, 70/30 and 60/40) and Joncryl® contents (0.0 and 4.0 phr) were prepared. Table 8 shows formulations of the scPLA.

Table 8. Formulations of PLLA-PEG-PLLA/PDLA-PEG-PDLA blends.

PLLA-PEG-PLLA/PDLA-PEG-PDLA ratio (w/w)	PLLA-PEG-PLLA(g)	PDLA-PEG-PDLA(g)	Joncryl® (g)
100/0	50	-	-
90/10	45	5	-
80/20	40	10	-
70/30	35	15	-
60/40	30	20	-
100/0	50	-	2.0
90/10	45	5	2.0
80/20	40	10	2.0
70/30	35	15	2.0
60/40	30	20	2.0

3.6 Characterization of scPLA

3.6.1 Differential scanning calorimetry (DSC)

Thermal transition properties of scPLA pellets were studied by DSC. For heating scan, the 2 - 5 mg of sample was sealed in an aluminum pan that was melted at 250°C for 2 min to eliminate its thermal history before quenching to 0°C and re-heated from 0 to 250°C at the rate of 10 °C/min under nitrogen atmosphere in order to observe their T_g , T_{cc} and T_m of homo-crystallites ($T_{m,hc}$) and stereocomplex crystallites ($T_{m,sc}$).

Degree of crystallinity from DSC (DSC- X_c) of homo-crystallites (DSC- $X_{c,hc}$) and stereocomplex crystallites (DSC- $X_{c,sc}$) were calculated using equations (3.11) and (3.12), respectively.

$$\text{DSC-}X_{c,hc} (\%) = [\Delta H_{m, hc} / (93 \times W_{\text{PLA}})] \times 100 \quad (3.11)$$

$$\text{DSC-}X_{c,sc} (\%) = [\Delta H_{m, sc} / (142 \times W_{\text{PLA}})] \times 100 \quad (3.12)$$

Where $\Delta H_{m,hc}$ and $\Delta H_{m,sc}$ are enthalpies of melting for homo- and stereocomplex crystallites, respectively. The 93 and 142 J/g are theoretical 100% X_c for homocrystallites and stereocomplex crystallites, respectively (Xie *et al.*, 2018). W_{PLA} is weight fraction of PLA that are 1.00 and 0.83 for PDLA and triblock copolymer, respectively (Baimark *et al.*, 2018).

For cooling curves, the sample was melted at 250°C for 2.0 min to remove thermal history before cooling from 250 to 0°C at the rate of 10°C/min to observe crystallization temperature (T_c) and enthalpy of crystallization (ΔH_c).

3.6.2 X-ray diffractometry

The crystalline structure of the film samples was determined by wide-angle X-ray diffractometry (XRD) at 25°C operated at 40 kV and 40 mA CuK α radiation. For XRD, the film samples were recorded in a 2θ range 5° to 30° at a scan rate of 3°/min. The degree of crystallinity from XRD ($XRD-X_c$) for homo-crystallites ($XRD-X_{c,hc}$) [equation (3.13)] and stereocomplex crystallites ($sc-X_{c,XRD}$) [equation (3.14)] of the film samples were calculated. (Pan *et al.*, 2018)

$$XRD-X_{c,hc} (\%) = \frac{S_{hc}}{(S_{hc} + S_{sc} + S_a)} \times 100 \quad (3.13)$$

$$XRD-X_{c,sc} (\%) = \frac{S_{sc}}{(S_{hc} + S_{sc} + S_a)} \times 100 \quad (3.14)$$

Where S_{hc} , S_{sc} and S_a are the integrated intensity peaks for homo-crystallites and stereocomplex crystallites as well as the integrated intensity of the amorphous halo, respectively.

3.6.3 Tensile testing

Tensile properties including stress at break, elongation at break and Young's modulus of the scPLA films were investigated by Universal Testing Machine. The films (10×100 mm) were performed at 25 °C and 65% relative humidity with the speed of 50 mm/min. The gauge length of 50 mm was used. The experimental values for mechanical properties represent averages of measurements from the five replicate films.

3.6.4 Thermo-mechanical properties

The thermo-mechanical properties of the film samples ($5 \times 20 \times 0.2$ mm) were measured by dynamic mechanical analysis (DMA) under a tensile mode with the scan amplitude of $10 \mu\text{m}$ and the scanning frequency of 1 Hz from 40 to 140°C at a heating rate of $2^\circ\text{C}/\text{min}$. The scan amplitude was set to be $10 \mu\text{m}$ and the scanning frequency was 1 Hz.

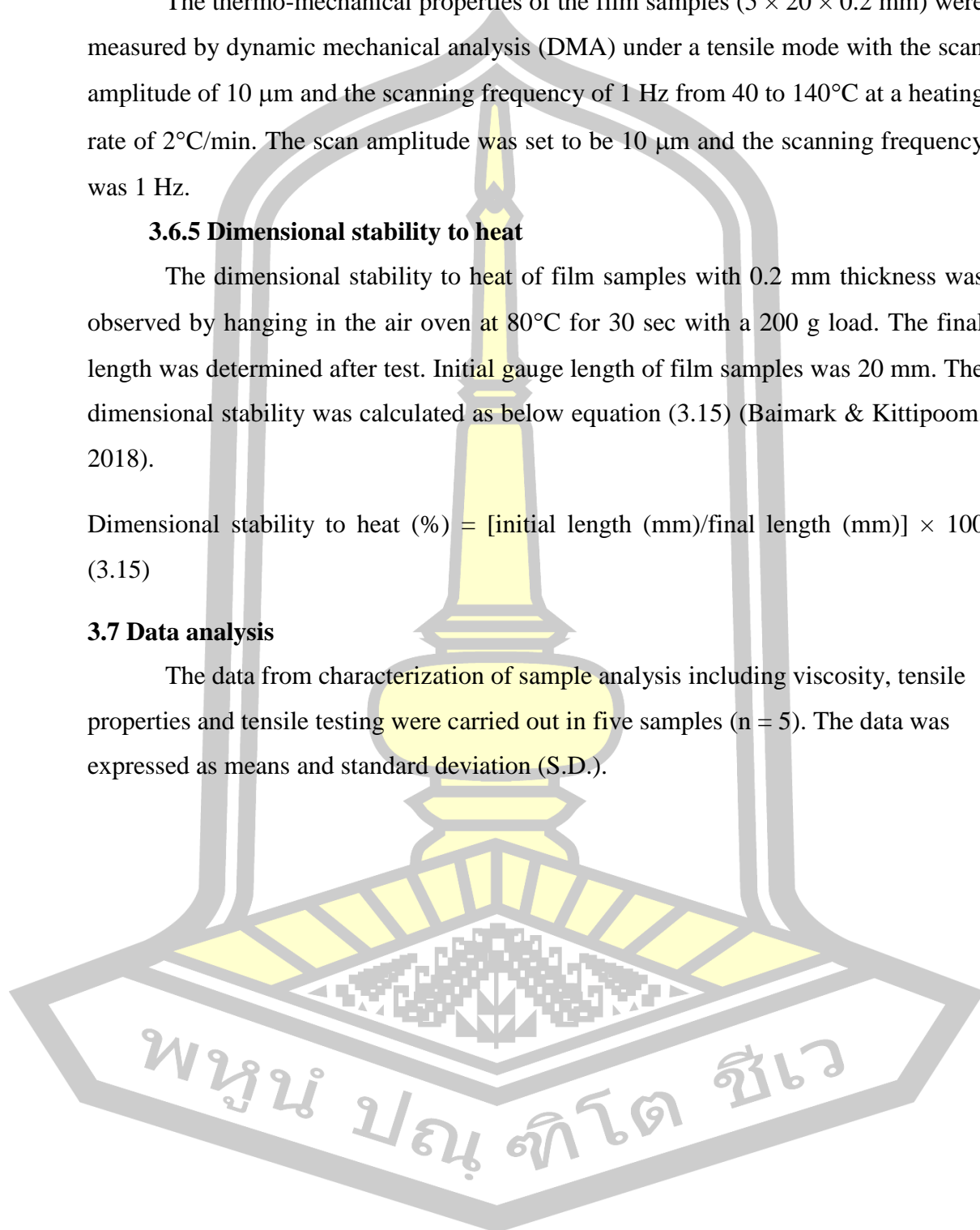
3.6.5 Dimensional stability to heat

The dimensional stability to heat of film samples with 0.2 mm thickness was observed by hanging in the air oven at 80°C for 30 sec with a 200 g load. The final length was determined after test. Initial gauge length of film samples was 20 mm. The dimensional stability was calculated as below equation (3.15) (Baimark & Kittipoom, 2018).

$$\text{Dimensional stability to heat (\%)} = [\text{initial length (mm)}/\text{final length (mm)}] \times 100 \quad (3.15)$$

3.7 Data analysis

The data from characterization of sample analysis including viscosity, tensile properties and tensile testing were carried out in five samples ($n = 5$). The data was expressed as means and standard deviation (S.D.).



CHAPTER IV

RESULTS AND DISCUSSION

4.1 Characterization of lactides

4.1.1 Optical rotation property

Table 9 shows optical purities of LLA and DLA monomers in benzene. The X_L and X_D of LLA and DLA were 99.20% and 96.98%, respectively. These monomers had very high optical purity (> 95%). These monomers can be used to prepare the polylactides with high optical purity.

Table 9. Optical rotation properties of D-lactide and L-lactide in chloroform at 25 °C.

Lactide	$[\alpha]_{589}^{25}$ (deg · g ⁻¹ · ml · dm ⁻¹)	X_L (%)	X_D (%)
LLA	-292.29	99.20	0.79
DLA	279.12	3.01	96.98

4.1.2 Thermal decomposition

The thermal decomposition of LLA and DLA was determined from thermogravimetric (TG) curves as illustrated in Fig. 22. It can be seen that both the LLA and DLA monomers started weight loss at around 100°C. They were completely thermal decomposed at around 160°C. The temperature of maximum decomposition rate ($T_{d,max}$) obtained from DTG curves were summarized in Table 10. The thermal decomposition of LLA and DLA were similar.

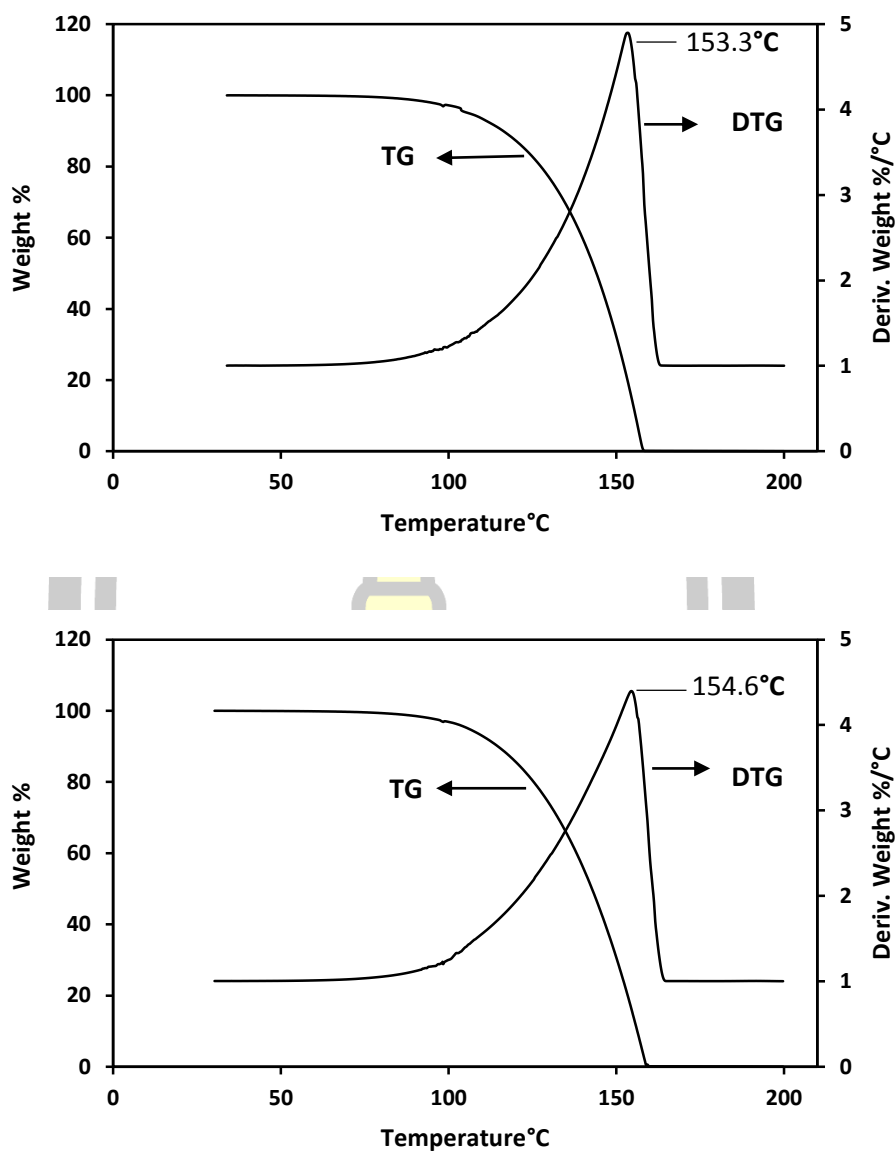


Fig. 22. TG and DTG curves of (above) LLA and (below) DLA monomers.

Table 10. $T_{d,max}$ from DTG curves of LLA and DLA monomers.

Lactide	$T_{d,max}$ (°C)
LLA	153.3
DLA	154.6

4.2 Characterization of PLLA-PEG-PLLA, PDLA-PEG-PDLA and PDLA

In this work, the PLLA-PEG-PLLA, PDLA-PEG-PDLA and PDLA were characterized by the following of instrumental methods.

4.2.1 Optical rotation property

Optical rotation property of polymer sample was studied from polarimetry. The approximate 0.1 g of sample was dissolved in 10 mL of chloroform before being determined at 25 °C with sodium D line of 589 nm. (Kumar *et al.*, 2016) The data of optical rotation property are summarized in Table 11.

Table 11. Optical rotation property of PLLA-PEG-PLLA, PDLA-PEG-PDLA and PDLA.

Sample	$[\alpha]_{589}^{25}$ (deg · g ⁻¹ · ml · dm ⁻¹)	X _L (%)	X _D (%)
PLLA-PEG-PLLA	-122.5	-	-
PDLA-PEG-PDLA	+121.5	-	-
PDLA	+143.1	4.44	95.56

4.2.2 Measurement of intrinsic viscosity

Table 12 reports the $[\eta]$ and M_v of PDLA and triblock copolymers. The $[\eta]$ and M_v of PDLA were 0.28 dL/g and 5,200 g/mol, respectively. The M_v of triblock copolymers could not calculate because of there are no constant values for Mark-Houwling-Sakurada equation. However, the $[\eta]$ of PLLA-PEG-PLLA and PDLA-PEG-PDLA were similar.

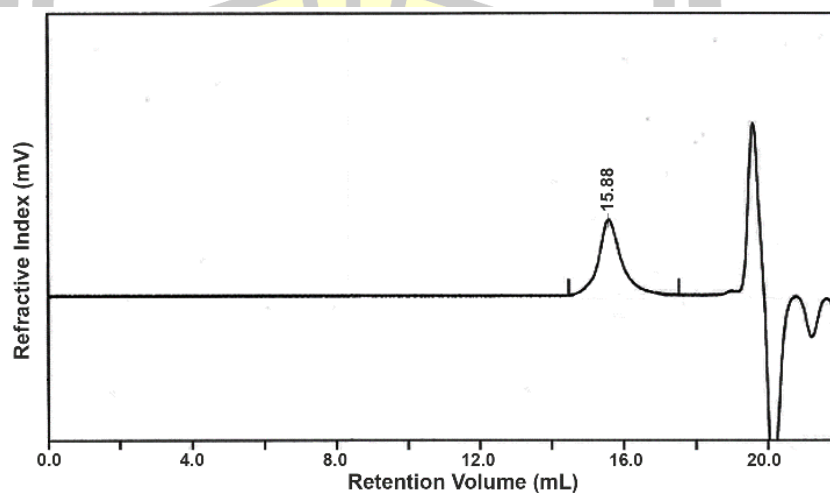
Table 12. $[\eta]$ and M_v of PDLA and triblock copolymers.

Polylactide	$[\eta]$ (dL/g)	M_v (g/mol)
PLLA-PEG-PLLA	1.20	*
PDLA-PEG-PDLA	1.21	*
PDLA	0.28	5,200

* The M_v of triblock copolymers could not calculate.

4.2.3 Molecular weight characteristics

Figs. 23, 24 and 25 show GPC curves of PDLA, PLLA-PEG-PLLA and PDLA-PEG-PDLA, respectively. GPC traces of these sample are unimodal. The GPC results are summarized in Table 13. The M_n of PDLA was nearly value with the feed M_n (5,000 g/mol) suggested that the 1-dodecanol initiator can control molecular weight of the PDLA. However, the M_n of triblock copolymers were lower than the feed M_n (120,000 g/mol). This may be due to thermal decomposition and transesterification may occur during polymerization. The dispersity (\mathcal{D}) of molecular weights of these polymers were in range 1.9-2.8.

**Fig. 23.** GPC curve of PDLA.

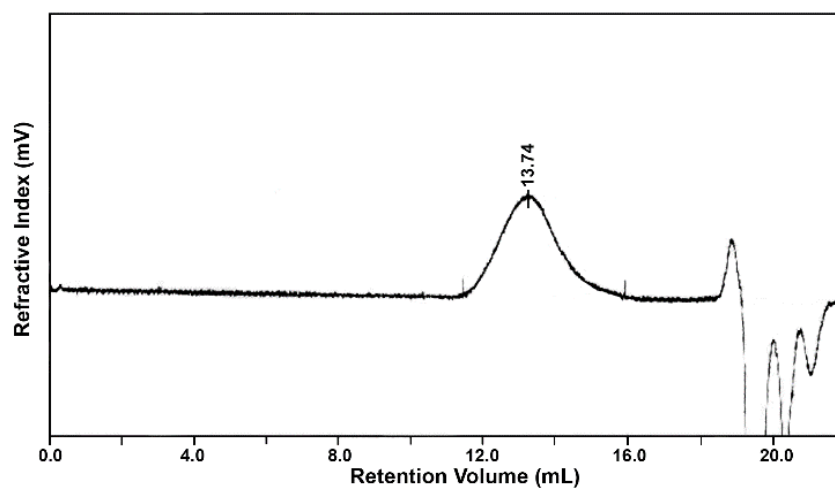


Fig. 24. GPC curve of PLLA-PEG-PLLA.

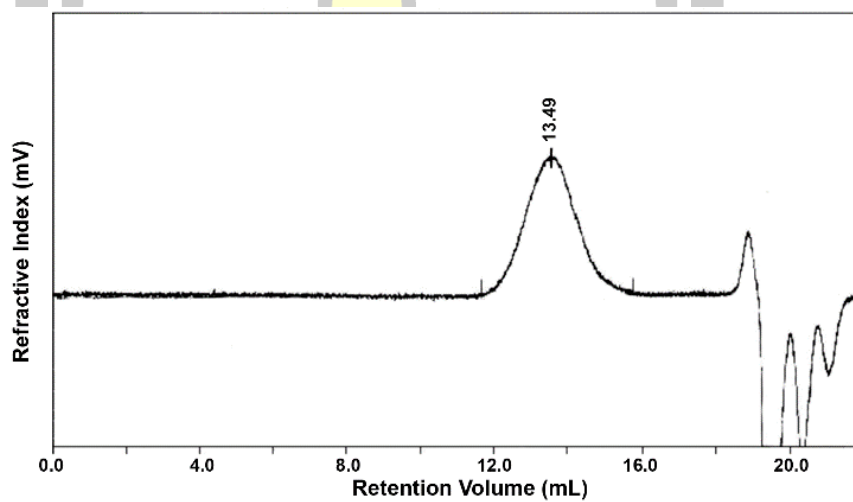


Fig. 25. GPC curve of PDLA-PEG-PDLA.

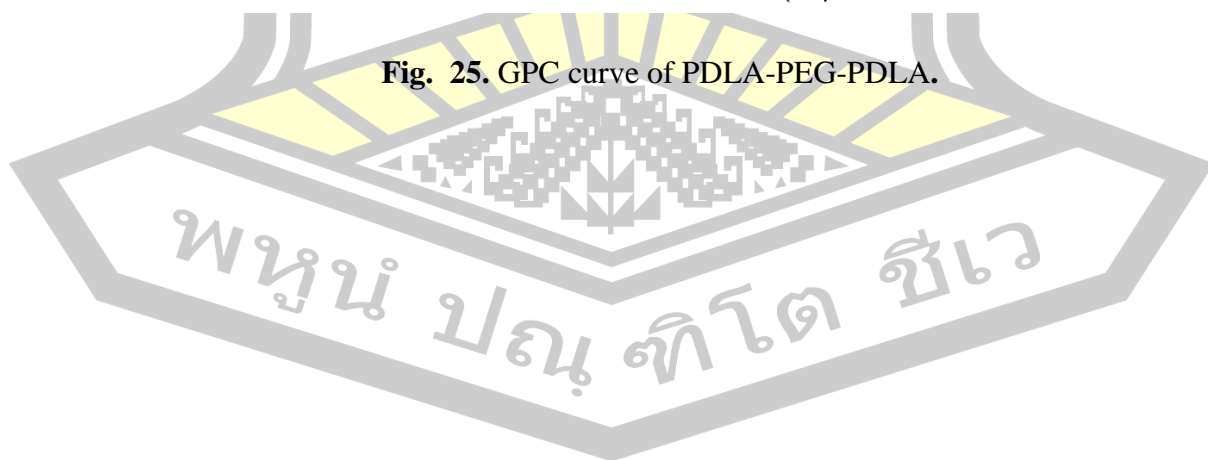
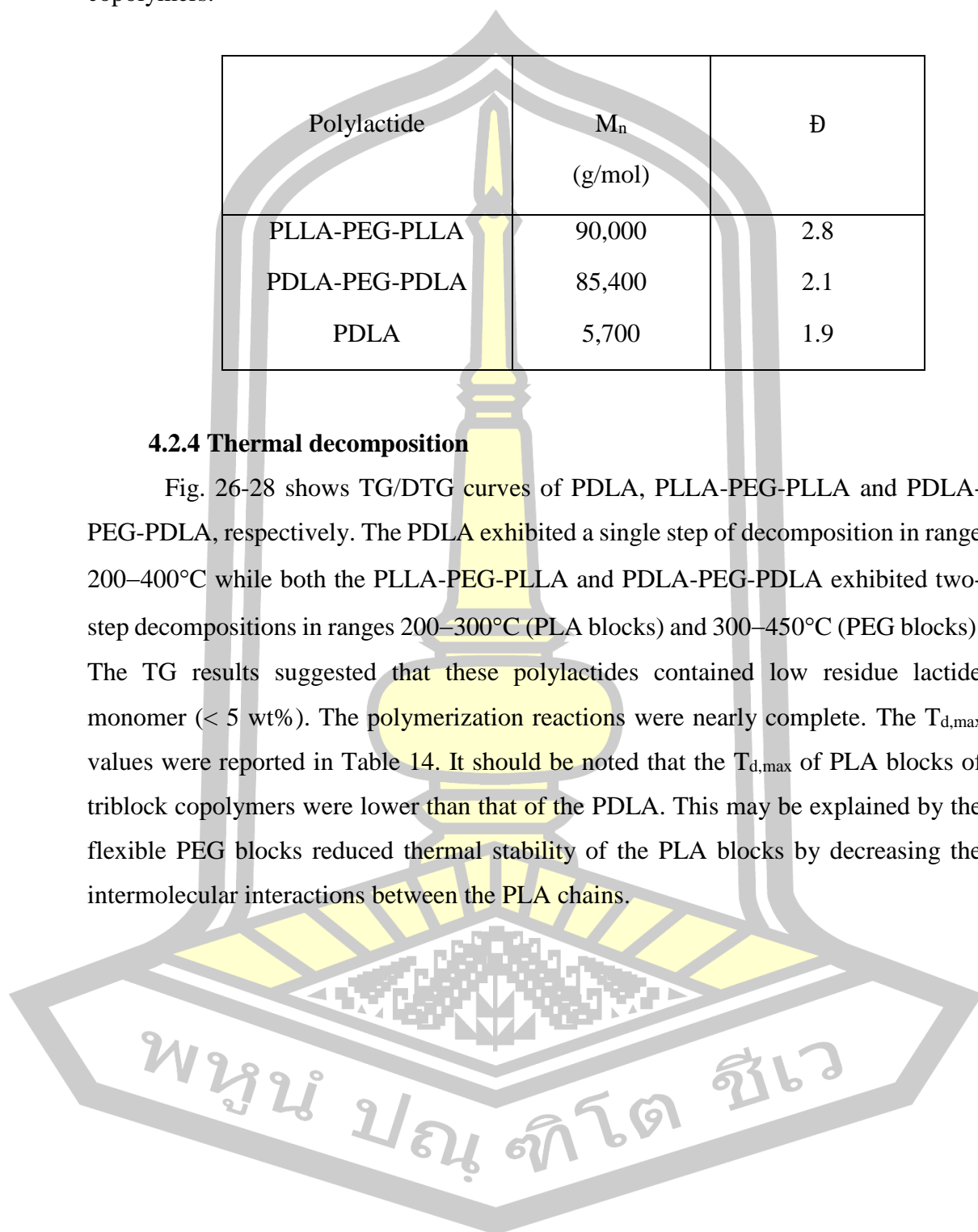


Table 13. Molecular weight characteristics from GPC of PDLA and triblock copolymers.

Poly lactide	M_n (g/mol)	\bar{D}
PLLA-PEG-PLLA	90,000	2.8
PDLA-PEG-PDLA	85,400	2.1
PDLA	5,700	1.9

4.2.4 Thermal decomposition

Fig. 26-28 shows TG/DTG curves of PDLA, PLLA-PEG-PLLA and PDLA-PEG-PDLA, respectively. The PDLA exhibited a single step of decomposition in range 200–400°C while both the PLLA-PEG-PLLA and PDLA-PEG-PDLA exhibited two-step decompositions in ranges 200–300°C (PLA blocks) and 300–450°C (PEG blocks). The TG results suggested that these polylactides contained low residue lactide monomer (< 5 wt%). The polymerization reactions were nearly complete. The $T_{d,max}$ values were reported in Table 14. It should be noted that the $T_{d,max}$ of PLA blocks of triblock copolymers were lower than that of the PDLA. This may be explained by the flexible PEG blocks reduced thermal stability of the PLA blocks by decreasing the intermolecular interactions between the PLA chains.



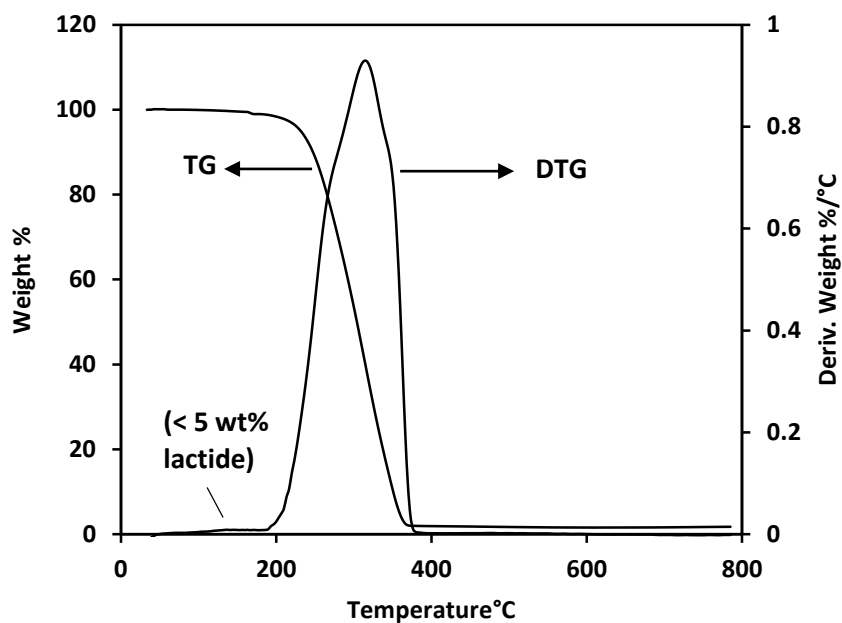


Fig. 26. TG and DTG curves of PDLA.

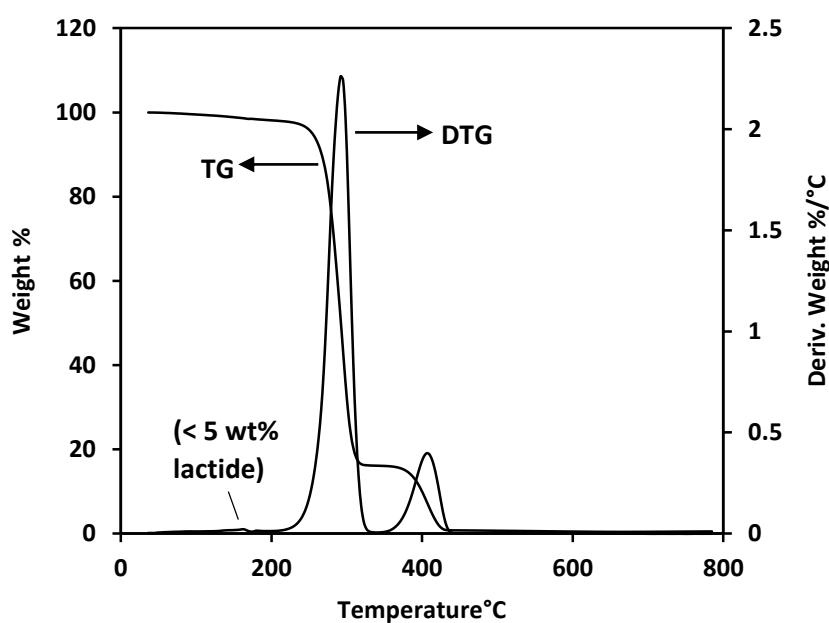


Fig. 27. TG and DTG curves of PLLA-PEG-PLLA.

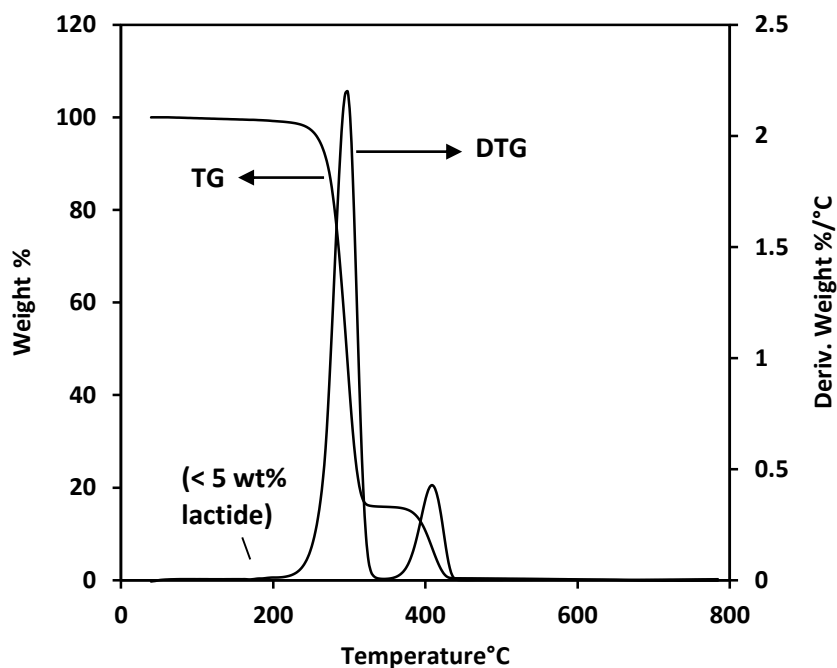


Fig. 28. TG and DTG curves of PDLA-PEG-PDLA.

Table 14. $T_{d,max}$ of PLLA-PEG-PLLA, PDLA-PEG-PDLA and PDLA.

Poly lactide	$T_{d,max}$ of PLLA block (°C)	$T_{d,max}$ of PEG block (°C)
PDLA	316	-
PLLA-PEG-PLLA	292	406
PDLA-PEG-PDLA	298	409

4.2.5 Thermal transition properties

Fig. 29 shows DSC heating curves of PLLA-PEG-PLLA, PDLA-PEG-PDLA and PDLA. Both the triblock copolymers had lower T_g and T_{cc} than the PDLA. This is due to the PEG middle blocks acting as plasticizers to enhance chain mobility of the PLA blocks. There are no T_m of PEG (60°C). The PEG middle-blocks were connected with the PLA end-blocks. Therefore, the PEG chains could not crystallize.

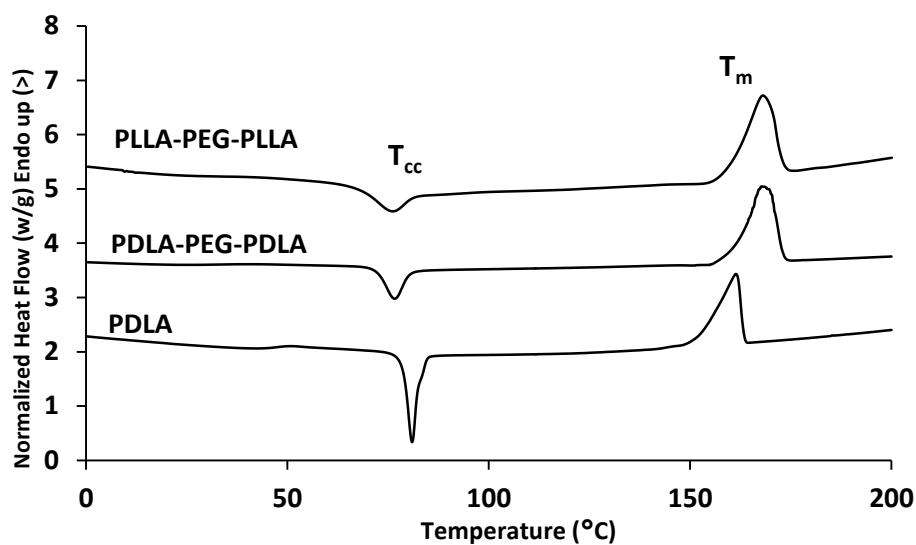


Fig. 29. DSC second heating thermograms of PLLA-PEG-PLLA, PDLA-PEG-PDLA and PDLA.

Table 15. Summary of thermal transition properties of PLLA-PEG-PLLA, PDLA-PEG-PDLA and PDLA.

Sample	T_g ($^{\circ}\text{C}$)	T_{cc} ($^{\circ}\text{C}$)	ΔH_{cc} (J/g)	T_m ($^{\circ}\text{C}$)	ΔH_m (J/g)
PLLA-PEG-PLLA	34	75	75.9	170	37.7
PDLA-PEG-PDLA	33	76	76.5	170	41.3
PDLA	47	81	81.0	161	50.1

4.2.6. Chemical structures

Chemical functional groups of PLDA and triblock copolymers were determined by $^1\text{H-NMR}$ spectrometry. Fig. 30 shows polymerization reaction and $^1\text{H-NMR}$ spectrum of PDLA. The peaks of methyl (peak a) and methine (peak b) protons of DLA units were detected. Figs. 31(a), 31(b) and 31(c) show polymerization reaction of PLA-PEG-PLA, $^1\text{H-NMR}$ spectrum of PLLA-PEG-PLLA and $^1\text{H-NMR}$ spectrum of PDLA-PEG-PDLA, respectively. The peaks of methyl (peak a) and methine (peak d) protons of lactide units and methylene protons (peak b) of ethylene oxide (EO) units (repeating

units of PEG blocks) were observed. The last methylene protons of EO units (peak f) are shown in the inset spectra in Figs. 31(b) and 31(c), indicating that the reaction between PEG and LLA had successfully occurred (Tacha *et al.*, 2015).

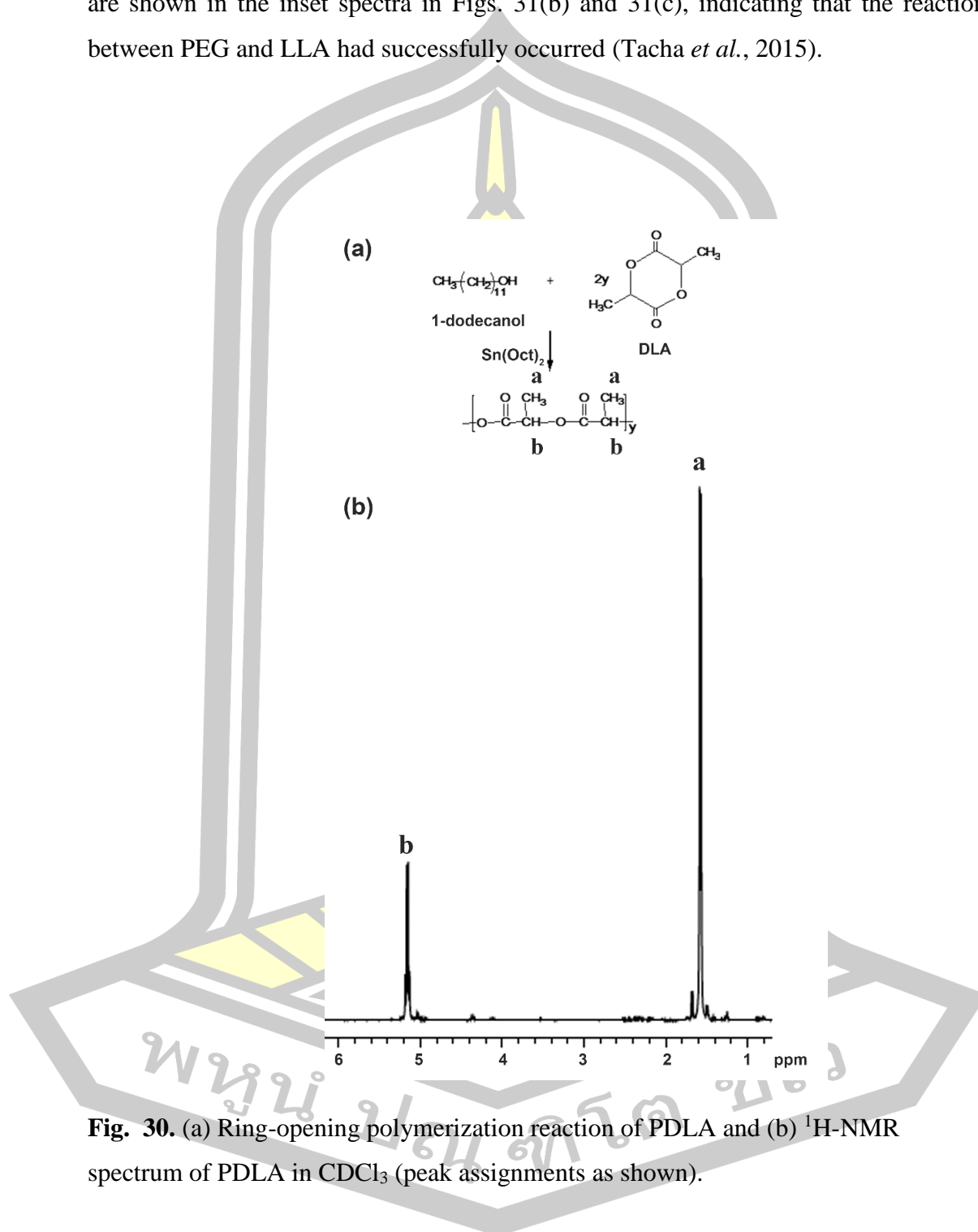


Fig. 30. (a) Ring-opening polymerization reaction of PDLA and (b) ^1H -NMR spectrum of PDLA in CDCl_3 (peak assignments as shown).

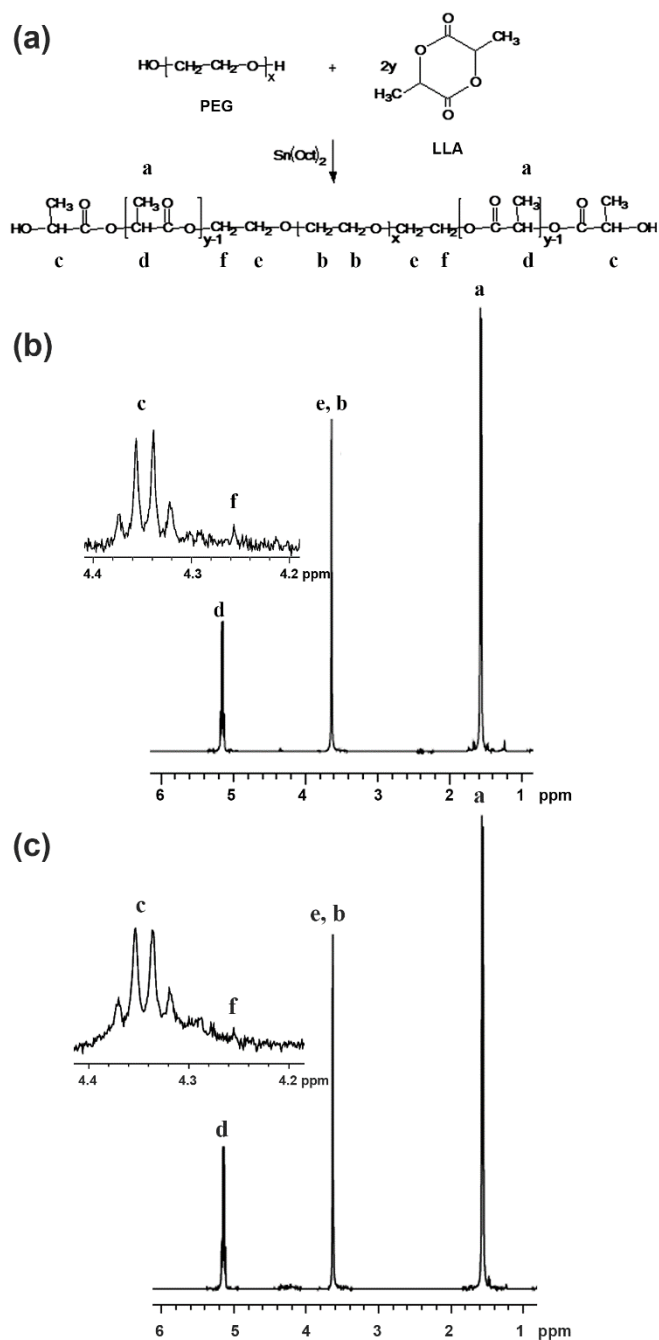


Fig. 31. (a) Ring-opening polymerization reaction of PLA-PEG-PLA, (b) $^1\text{H-NMR}$ spectrum of PLLA-PEG-PLLA and (c) $^1\text{H-NMR}$ spectrum of PDLA-PEG-PDLA in CDCl_3 (peak assignments as shown).

4.3 Characterization of PLLA-PEG-PLLA/PDLA blends

4.3.1. Thermal transition properties

Fig. 32 shows DSC heating curves of PLLA-PEG-PLLA and blends. The corresponding DSC data are reported in Table 16. The T_g of PLLA-PEG-PLLA and blends were in range 30–35°C was lower than those of the PLLA (approximately 60°C). This can be explained by flexible PEG middle-blocks act as plasticizers to decreasing T_g of PLLA end-blocks. The T_m of homo-crystallites ($T_{m,hc}$) decreased and that of the stereocomplex crystallites ($T_{m,sc}$) slightly increased as the PDLA ratio increased. This indicating that PLA crystallization with higher PDLA ratio improves the integrity of the stereocomplex crystallites and their lamella thickness.

It was also found that the $T_{m,hc}$ peaks of blends disappeared for 30 wt% and 40 wt% PDLA for both the blend series with and without chain extender. This indicated that the stereocomplexation of PLLA end-blocks was complete with 30 wt% PDLA or higher. This low M.W. PDLA acted as a good stereocomplex enhancer after complete melting because its highly chain-diffusion (Shao *et al.*, 2015; Srisuwan & Baimark, 2018). For degree of crystallinity from DSC, the DSC- $X_{c,hc}$ significantly decreased and DSC- $X_{c,sc}$ steadily increased as the PDLA ratio increased.

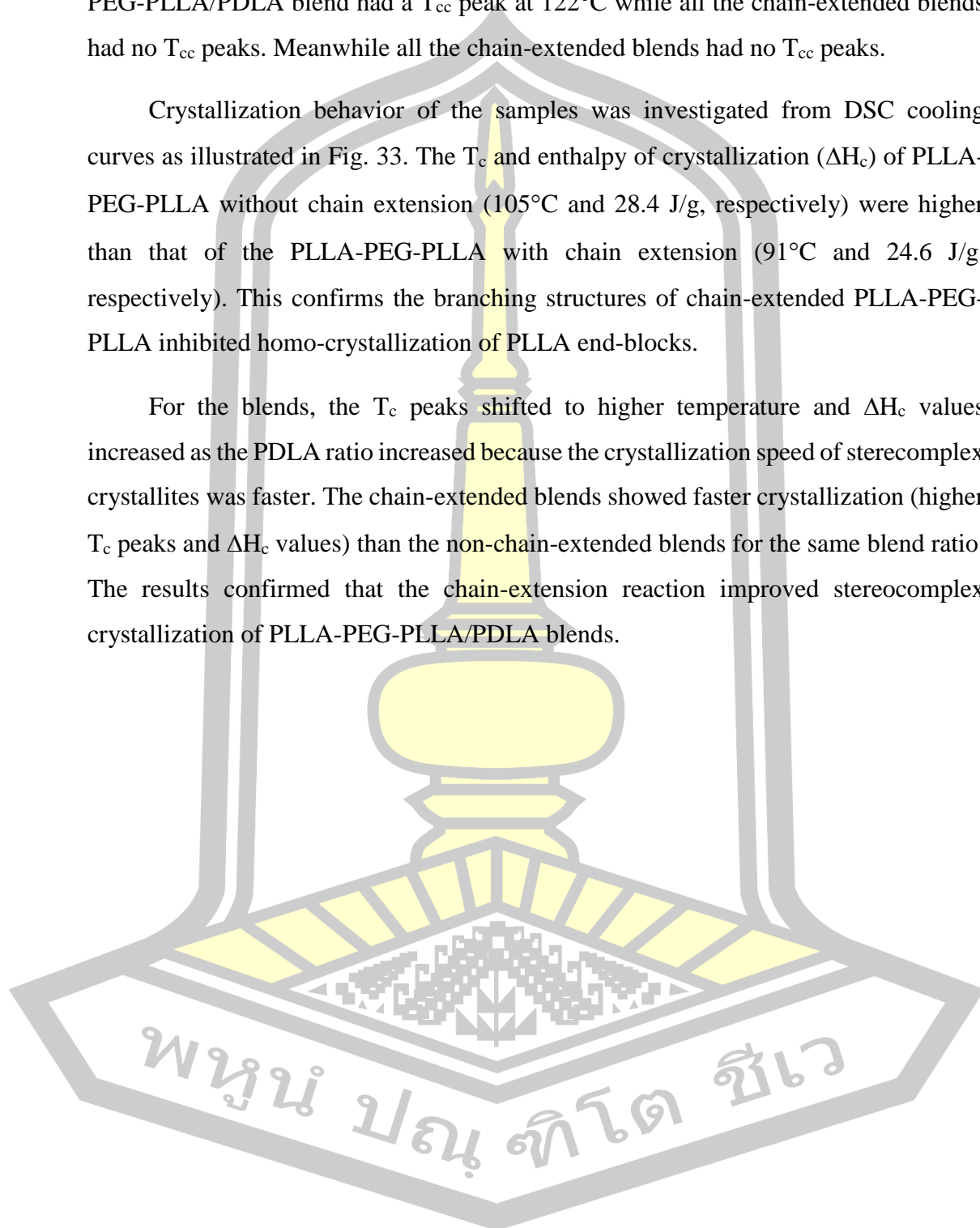
The chain-extended blends had lower DSC- $X_{c,hc}$ than the non-chain-extended blends for the same blend ratio. It has been reported that the branched structures of PLLA inhibited its homo-crystallization (Baimark & Kittipoom, 2018) However, it is surprising that the DSC- $X_{c,sc}$ of chain-extended blends was slightly larger than the non-chain-extended blends. This can be explained by more free-volume of branching structures of chain-extended PLLA-PEG-PLLA blends enhanced chain mobility of flexible PEG middle-blocks. (Baimark *et al.*, 2018) This improved stereocomplexation between PLLA and PDLA chains because interactions between PLLA and PDLA were stronger than between PLLA and PLLA. (Lee *et al.*, 2018).

The non-chain-extended PLLA-PEG-PLLA had no peak of cold-crystallization temperature (T_{cc}) as shown in Fig. 32 (above, a). The good chain-mobility of PLLA-PEG-PLLA due to flexible PEG middle-blocks enhancing crystallization of PLLA end-blocks. However, the chain-extended PLLA-PEG-PLLA showed a T_{cc} peak at 74°C

[Fig. 32 (below, a)]. For the non-chain-extended blend series, only the 90/10 PLLA-PEG-PLLA/PDLA blend had a T_{cc} peak at 122°C while all the chain-extended blends had no T_{cc} peaks. Meanwhile all the chain-extended blends had no T_{cc} peaks.

Crystallization behavior of the samples was investigated from DSC cooling curves as illustrated in Fig. 33. The T_c and enthalpy of crystallization (ΔH_c) of PLLA-PEG-PLLA without chain extension (105°C and 28.4 J/g, respectively) were higher than that of the PLLA-PEG-PLLA with chain extension (91°C and 24.6 J/g, respectively). This confirms the branching structures of chain-extended PLLA-PEG-PLLA inhibited homo-crystallization of PLLA end-blocks.

For the blends, the T_c peaks shifted to higher temperature and ΔH_c values increased as the PDLA ratio increased because the crystallization speed of stereocomplex crystallites was faster. The chain-extended blends showed faster crystallization (higher T_c peaks and ΔH_c values) than the non-chain-extended blends for the same blend ratio. The results confirmed that the chain-extension reaction improved stereocomplex crystallization of PLLA-PEG-PLLA/PDLA blends.



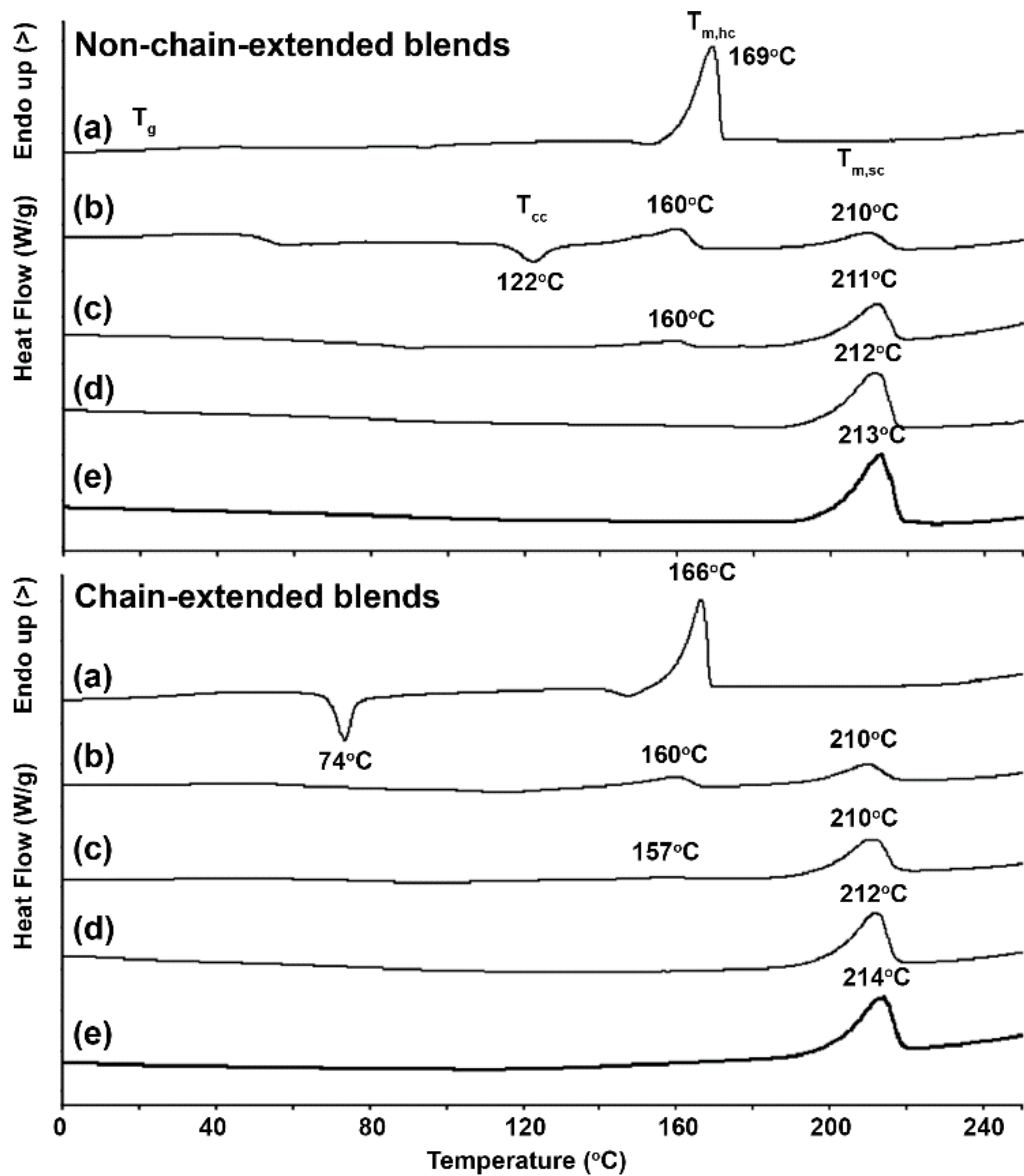
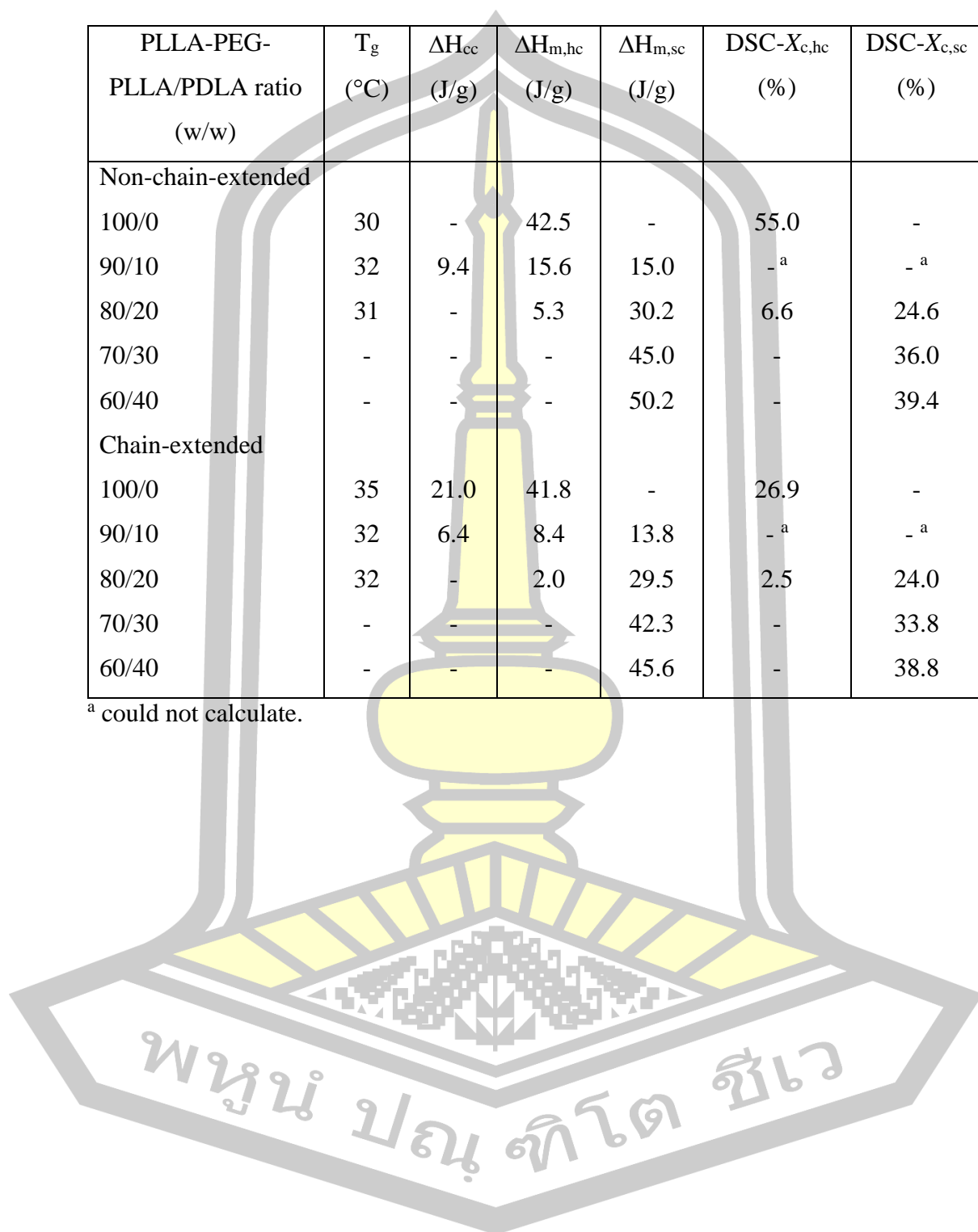


Fig. 32. DSC second heating thermograms of (above) non-chain-extended and (below) chain-extended blends with PLLA-PEG-PLLA/PDLA ratios of (a) 100/0, (b) 90/10, (c) 80/20, (d) 70/30 and (e) 60/40 (w/w).

Table 16. DSC results of PLLA-PEG-PLLA/PDLA blends from Figure 4.11.

PLLA-PEG- PLLA/PDLA ratio (w/w)	T _g (°C)	ΔH _{cc} (J/g)	ΔH _{m,hc} (J/g)	ΔH _{m,sc} (J/g)	DSC-X _{c,hc} (%)	DSC-X _{c,sc} (%)
Non-chain-extended						
100/0	30	-	42.5	-	55.0	-
90/10	32	9.4	15.6	15.0	- ^a	- ^a
80/20	31	-	5.3	30.2	6.6	24.6
70/30	-	-	-	45.0	-	36.0
60/40	-	-	-	50.2	-	39.4
Chain-extended						
100/0	35	21.0	41.8	-	26.9	-
90/10	32	6.4	8.4	13.8	- ^a	- ^a
80/20	32	-	2.0	29.5	2.5	24.0
70/30	-	-	-	42.3	-	33.8
60/40	-	-	-	45.6	-	38.8

^a could not calculate.



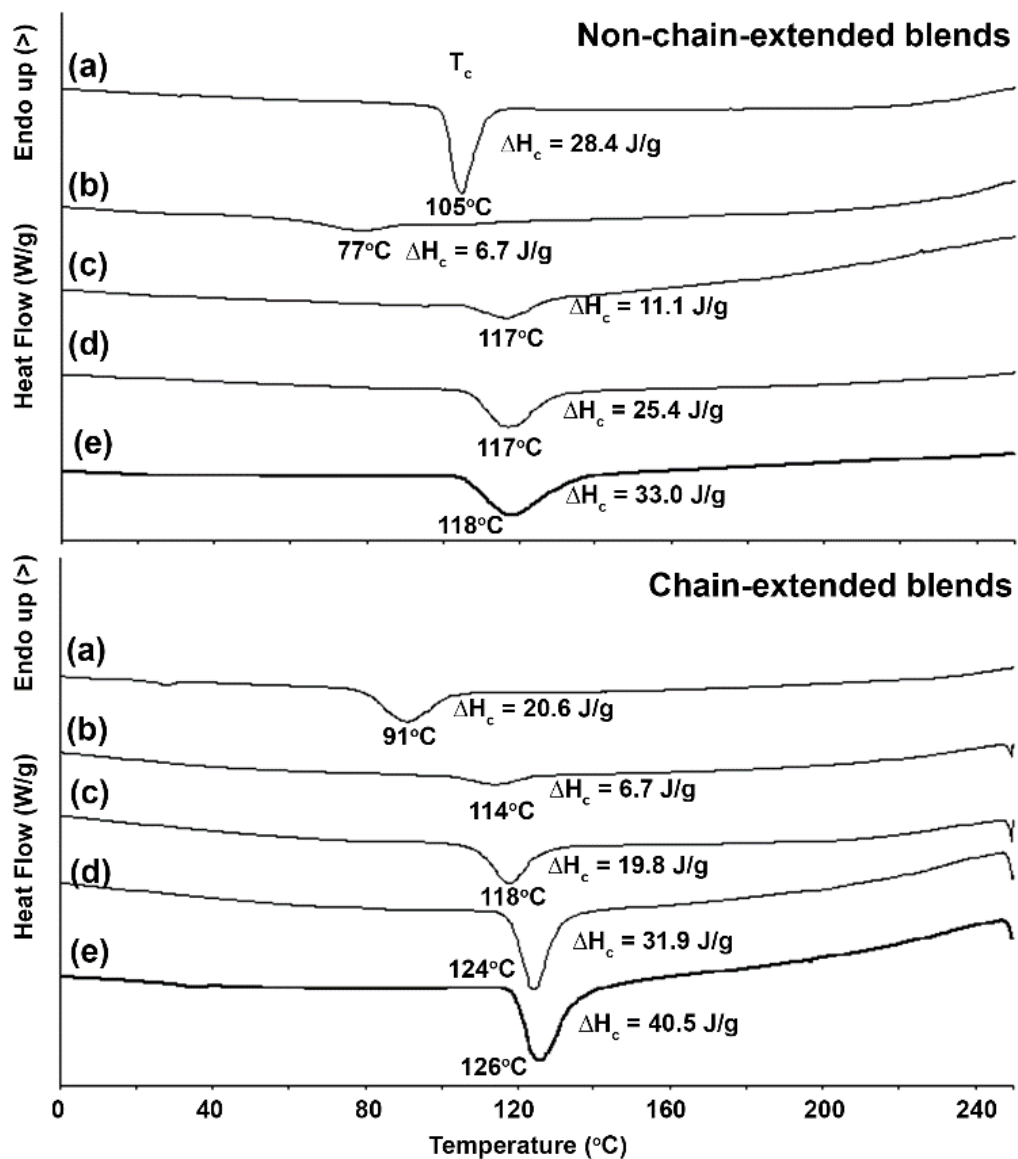


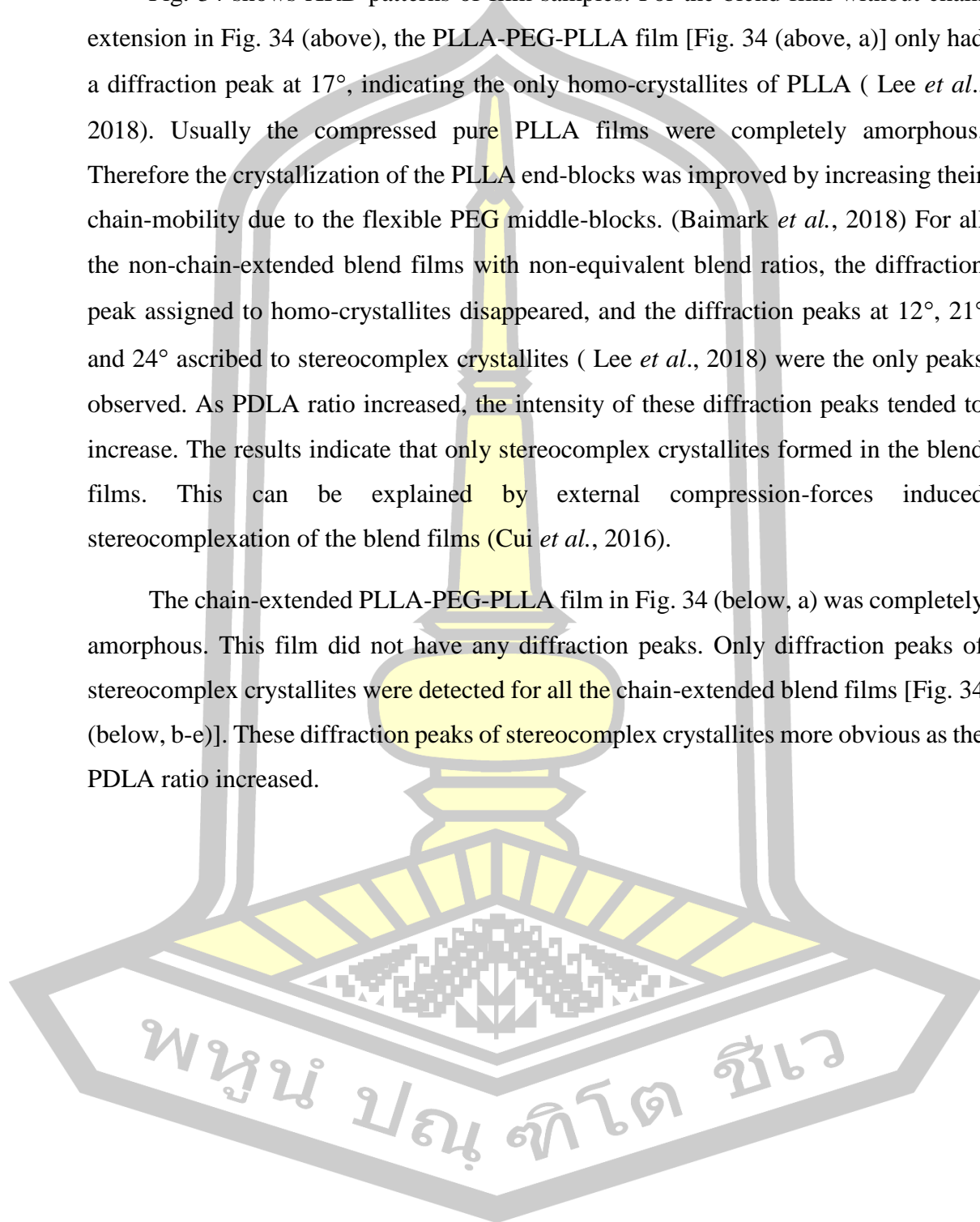
Fig. 33. DSC cooling thermograms of (above) non-chain-extended and (below) chain-extended blends with PLLA-PEG-PLLA/PDLA ratios of (a) 100/0, (b) 90/10, (c) 80/20, (d) 70/30 and (e) 60/40 (w/w) (T_c peak and ΔH_c as shown).

พหุ ประถมศึกษา

4.3.2. Crystalline structures

Fig. 34 shows XRD patterns of film samples. For the blend film without chain extension in Fig. 34 (above), the PLLA-PEG-PLLA film [Fig. 34 (above, a)] only had a diffraction peak at 17° , indicating the only homo-crystallites of PLLA (Lee *et al.*, 2018). Usually the compressed pure PLLA films were completely amorphous. Therefore the crystallization of the PLLA end-blocks was improved by increasing their chain-mobility due to the flexible PEG middle-blocks. (Baimark *et al.*, 2018) For all the non-chain-extended blend films with non-equivalent blend ratios, the diffraction peak assigned to homo-crystallites disappeared, and the diffraction peaks at 12° , 21° and 24° ascribed to stereocomplex crystallites (Lee *et al.*, 2018) were the only peaks observed. As PDLA ratio increased, the intensity of these diffraction peaks tended to increase. The results indicate that only stereocomplex crystallites formed in the blend films. This can be explained by external compression-forces induced stereocomplexation of the blend films (Cui *et al.*, 2016).

The chain-extended PLLA-PEG-PLLA film in Fig. 34 (below, a) was completely amorphous. This film did not have any diffraction peaks. Only diffraction peaks of stereocomplex crystallites were detected for all the chain-extended blend films [Fig. 34 (below, b-e)]. These diffraction peaks of stereocomplex crystallites more obvious as the PDLA ratio increased.



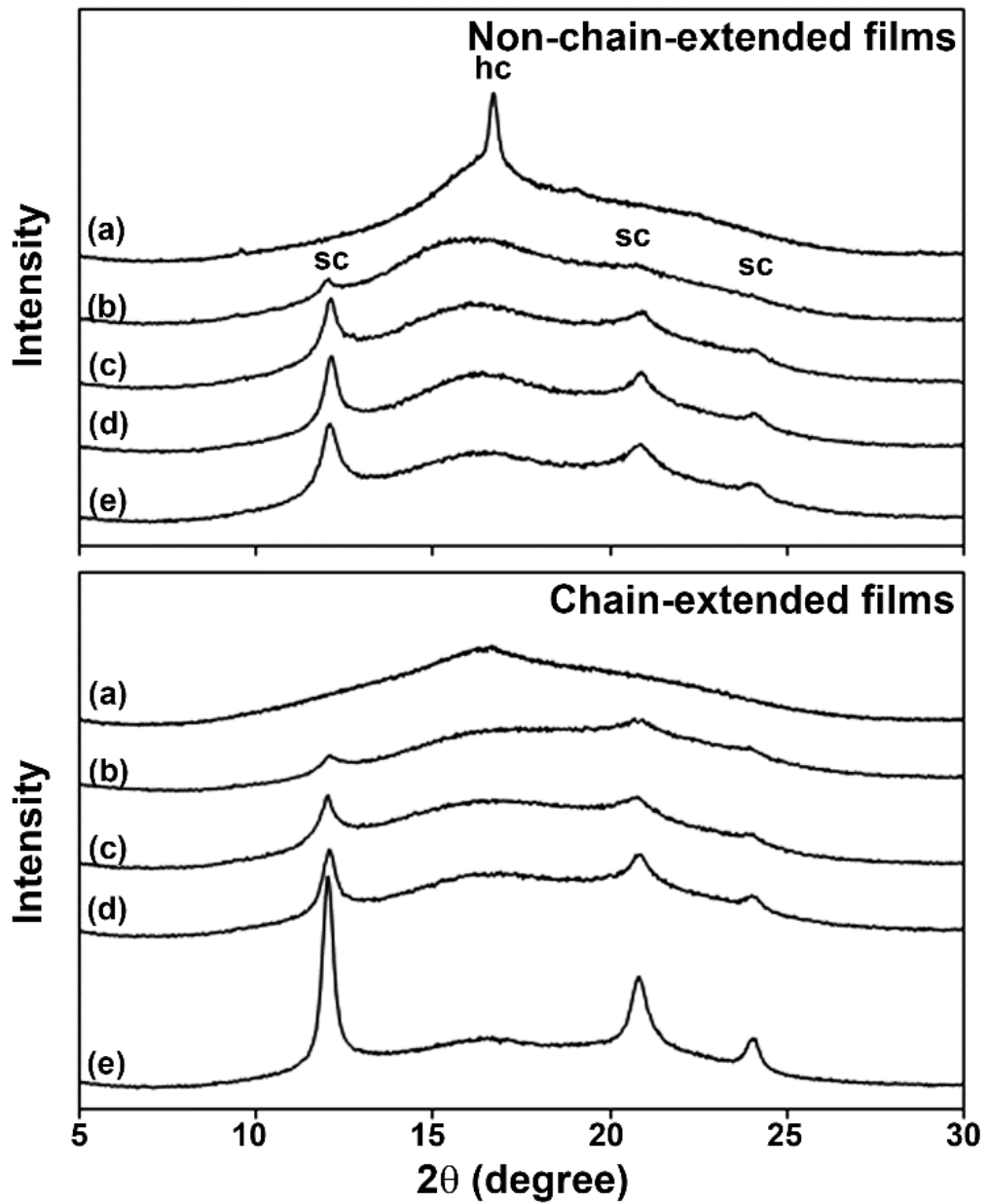


Fig. 34. XRD patterns of (above) non-chain-extended and (below) chain-extended blend films with PLLA-PEG-PLLA/PDLA ratios of (a) 100/0, (b) 90/10, (c) 80/20, (d) 70/30 and (e) 60/40 (w/w).

The XRD- $X_{c,hc}$ and XRD- $X_{c,sc}$ of the film samples without and with chain extension were compared in table. 17. The pure PLLA-PEG-PLLA film without chain extension had only a homo-crystallite peak (XRD- $X_{c,hc} = 7.5\%$) while all the blend films had only stereocomplex crystallite peaks. The PLLA-PEG-PLLA film with chain extension was completely amorphous. From table. 17, it can be seen that the XRD- $X_{c,sc}$ of the blend films increased as the PDLA ratio increased. The larger XRD- $X_{c,sc}$ values were observed for the blend films with chain extension. This is due to the blends with chain extension experiencing faster stereocomplex crystallization than without chain extension according to the T_c results in Fig. 33.

Table 17. XRD results of PLLA-PEG-PLLA/PDLA blend films.

PLLA-PEG-PLLA/PDLA (w/w)	XRD- $X_{c,hc}$ (%)	XRD- $X_{c,sc}$ (%)
Non-chain-extended		
100/0	7.5	-
90/10	-	3.41
80/20	-	11.56
70/30	-	12.63
60/40	-	15.44
Chain-extended		
100/0	-	-
90/10	-	9.5
80/20	-	12.57
70/30	-	13.56
60/40	-	31.2

4.3.3. Tensile properties

Fig. 35 shows selected tensile curves of the film samples, except the 60/40 (w/w) PLLA-PEG-PLLA/PDLA blend film without chain extension because it was highly brittle. The inset tensile-curves are also presented for clarity. The averaged tensile results are compared in Fig. 36. The blend films exhibited a yield point except the chain-extended 60/40 blend film indicating more flexibility of the blend films. For the blend films without chain extension, the stress at break of the films increased until the PDLA ratio was 20 wt% or higher. The stereocomplex crystallites linked between the PLLA-PEG-PLLA chains acted as cross-linkers to improve stress at break of the blend films (Tsuji *et al.*, 1991; Tsuji & Ikada, 1991). However the stress at break of the blend films dramatically dropped when the 30 wt% PDLA ratio was blended. The latter films became brittle because they contained a larger fraction of low M.W. PDLA (30 wt%).

The strain at break of PLLA-PEG-PLLA film without chain extension increased from 33% to 148% as the 10 wt% PDLA was blended due to plasticizing effect of PEG middle-blocks for the film with low crystallinity ($DSC-X_{c,sc} = 3.4\%$). However, the strain at break largely decreased to 10% when the 20 wt% PDLA was blended. This is due to increasing the $XRD-X_{c,sc}$.

The strain at break of the PLLA-PEG-PLLA film was largely improved with chain extension. This is due to the long-chain branching structures suppressed the homo-crystallization of the PLLA end-blocks and enhanced plasticizing effect of the PEG middle-blocks (Baimark *et al.*, 2018). The blend films with chain extension showed better stress and strain at break than the blend films without chain extension for the same blend ratio. The results may be due to the longer chains of chain-extended blend films increased tie-chain density between stereocomplex crystallites (Tsuji & Ikada, 1991).

The stress and strain at break of the blend films with chain extension decreased as increasing PDLA ratio. The larger low M.W. PDLA fraction made film brittleness. The larger PDLA ratio induced higher $sc-X_{c,XRD}$ that decreased the plasticizing effect of flexible PEG middle-blocks. The Young's moduli of blend films with and without chain extension were in ranges 705–846 MPa and 490–714 MPa, respectively.

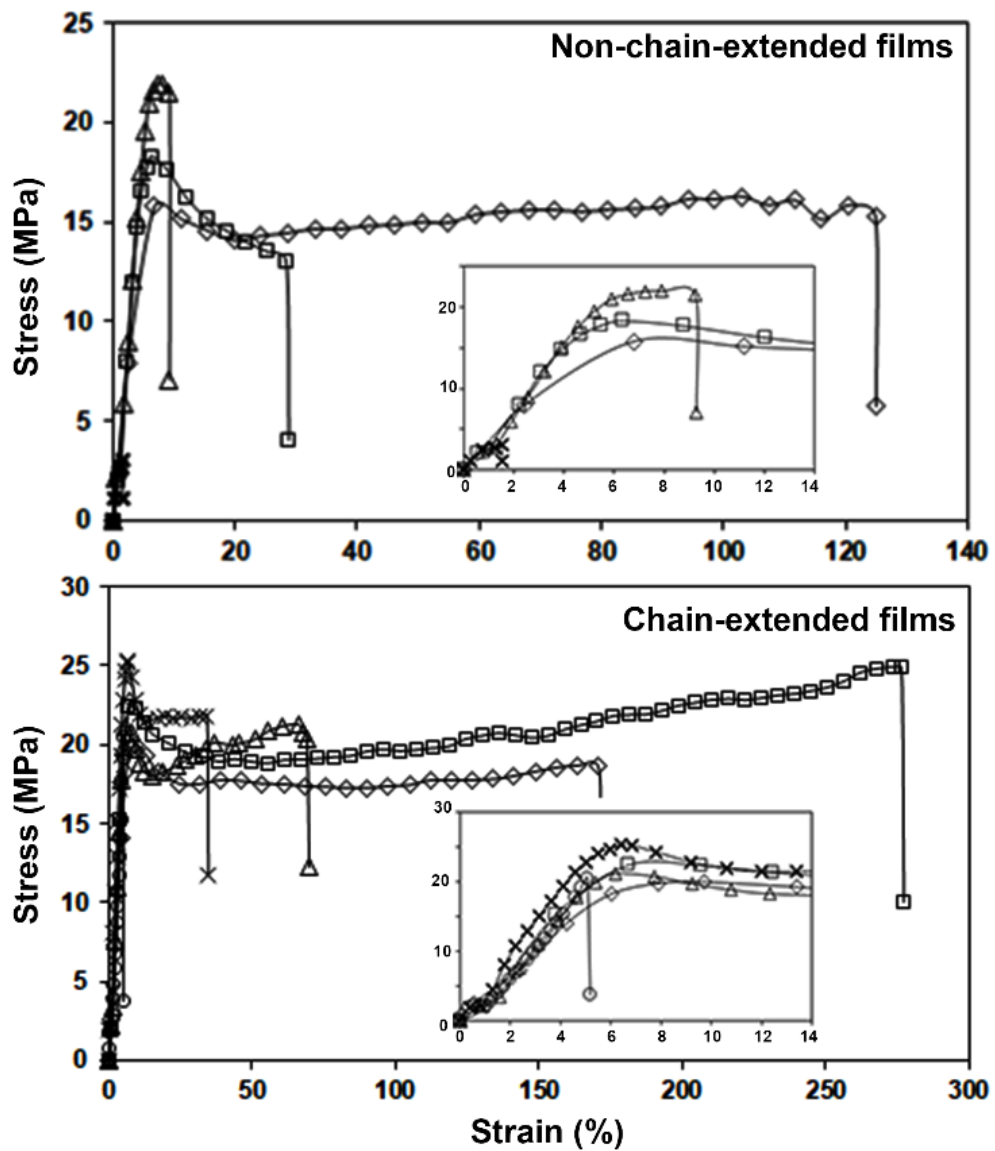


Fig. 35. Tensile curves of (above) non-chain-extended and (below) chain-extended blend films with PLLA-PEG-PLLA/PDLA ratios of (□) 100/0, (◇) 90/10, (△) 80/20, (×) 70/30 and (○) 60/40 (w/w).

พหุ ประถมศึกษา

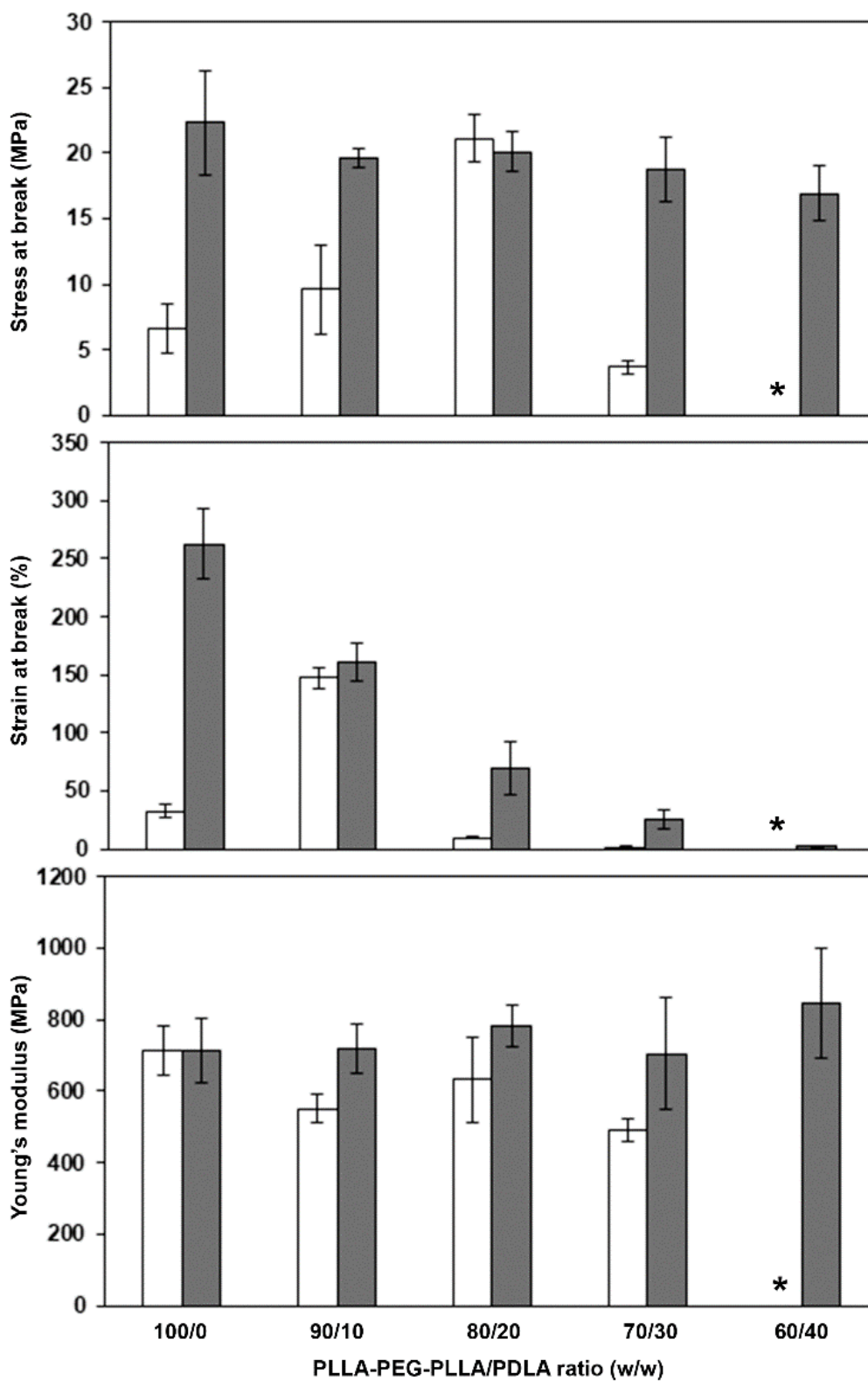
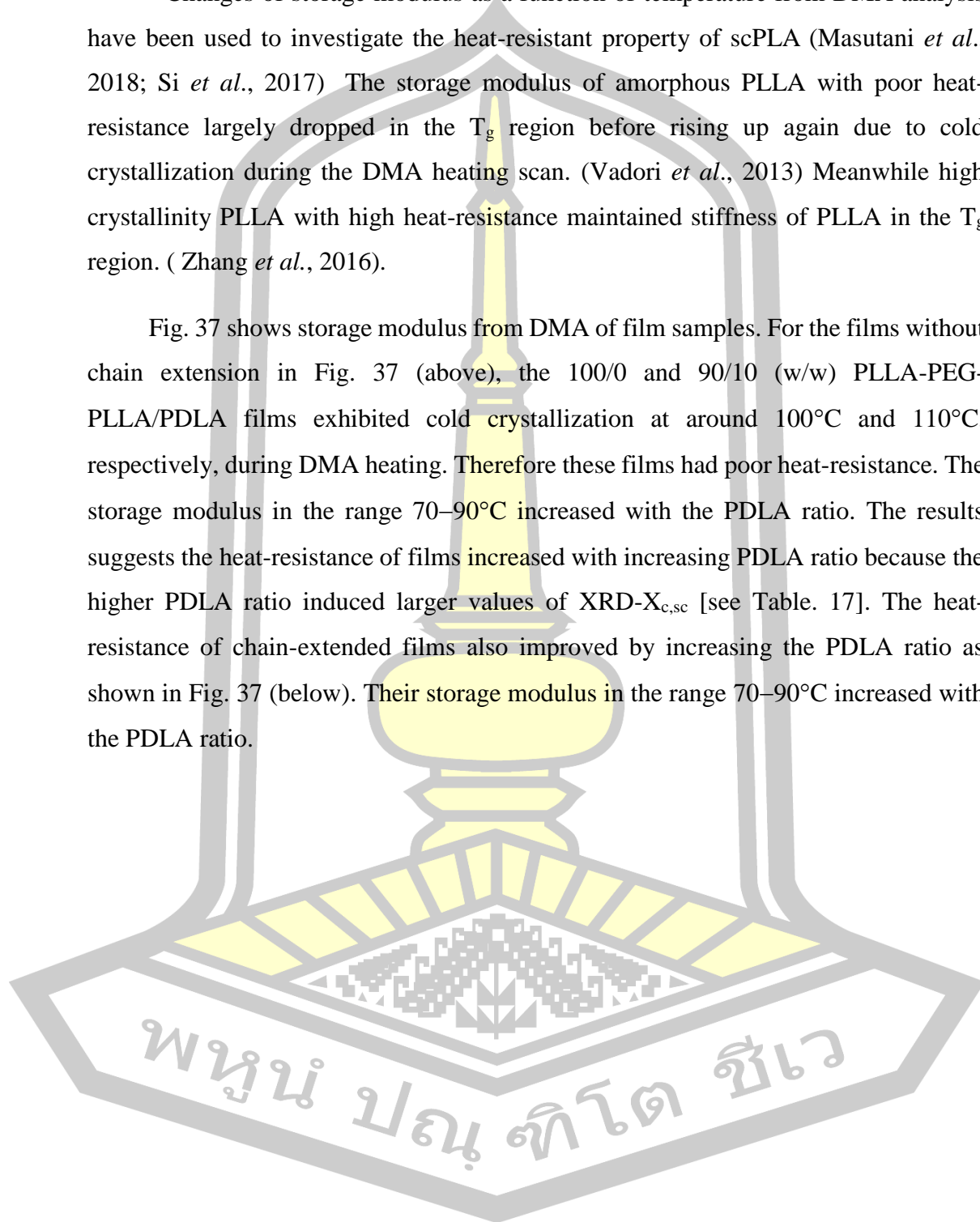


Fig. 36. Tensile properties of (□) non-chain-extended and (■) chain-extended blend films with various PLLA-PEG-PLLA/PDLA ratios (* = could not determine).

4.3.4 Thermo-mechanical properties

Changes of storage modulus as a function of temperature from DMA analysis have been used to investigate the heat-resistant property of scPLA (Masutani *et al.*, 2018; Si *et al.*, 2017). The storage modulus of amorphous PLLA with poor heat-resistance largely dropped in the T_g region before rising up again due to cold crystallization during the DMA heating scan. (Vadori *et al.*, 2013). Meanwhile high crystallinity PLLA with high heat-resistance maintained stiffness of PLLA in the T_g region. (Zhang *et al.*, 2016).

Fig. 37 shows storage modulus from DMA of film samples. For the films without chain extension in Fig. 37 (above), the 100/0 and 90/10 (w/w) PLLA-PEG-PLLA/PDLA films exhibited cold crystallization at around 100°C and 110°C, respectively, during DMA heating. Therefore these films had poor heat-resistance. The storage modulus in the range 70–90°C increased with the PDLA ratio. The results suggest the heat-resistance of films increased with increasing PDLA ratio because the higher PDLA ratio induced larger values of XRD- $X_{c,sc}$ [see Table. 17]. The heat-resistance of chain-extended films also improved by increasing the PDLA ratio as shown in Fig. 37 (below). Their storage modulus in the range 70–90°C increased with the PDLA ratio.



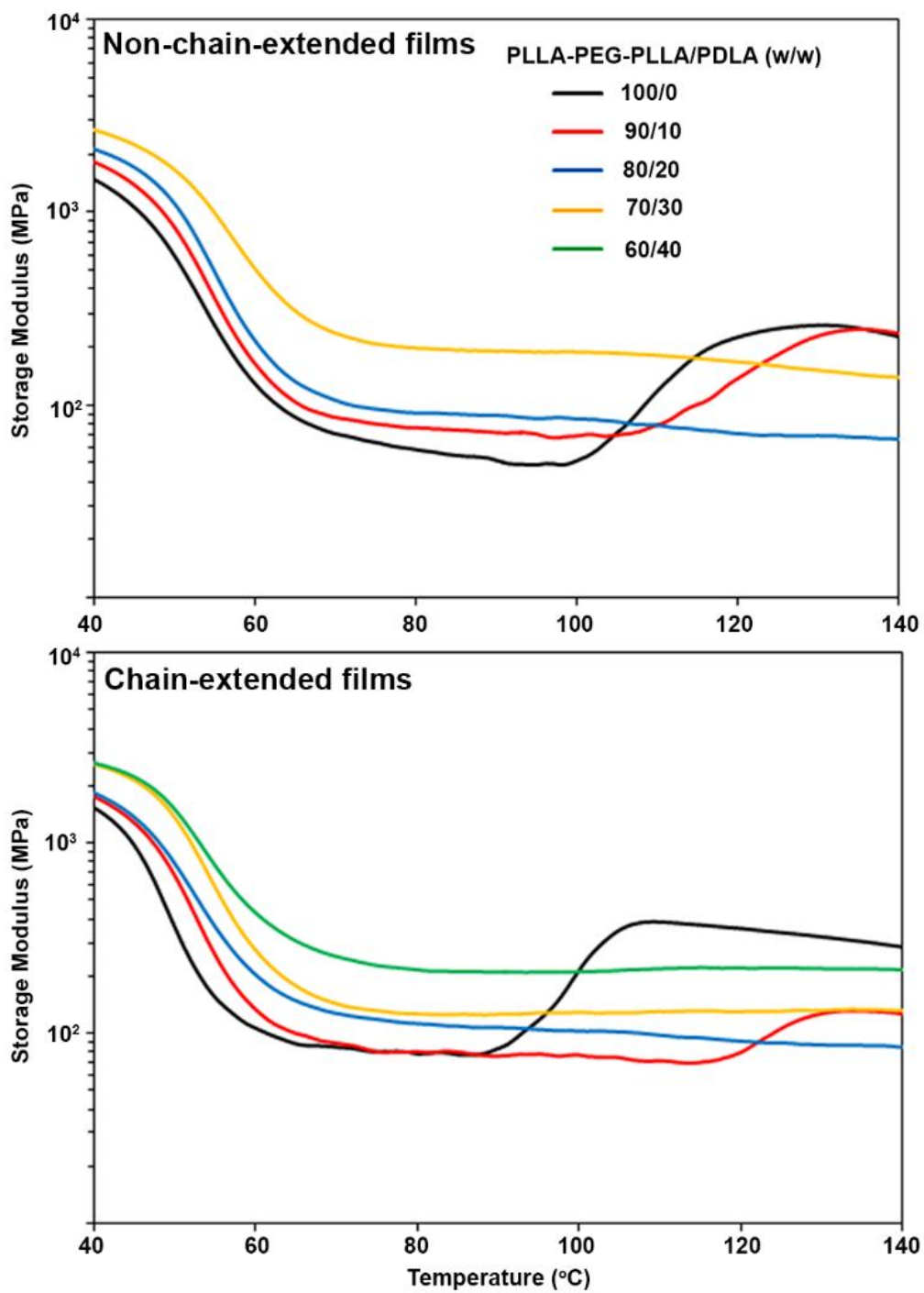


Fig. 37. Storage modulus from DMA of (above) non-chain-extended and (below) chain-extended films with various PLLA-PEG-PLLA/PDLA ratios.

4.3.5 Dimensional stability to heat

The film samples before and after testing of dimensional stability to heat are shown in Fig. 38. The 60/40 PLLA-PEG-PLLA/PDLA blend film was not determined due to its high brittleness. Both the PLLA-PEG-PLLA films with and without chain extension exhibited the largest film-extension [Fig. 38(above)] indicating they had poor heat-resistance. All the blend films after testing exhibited shorter film-extension than the PLLA-PEG-PLLA film. The results suggested that the blend films had better heat-resistance because they contained stereocomplex crystallites. The film extension significantly decreased as the PDLA ratio was increased from 10 to 20 wt% This is due to increasing the XRD- $X_{c,sc}$ of the blend films.

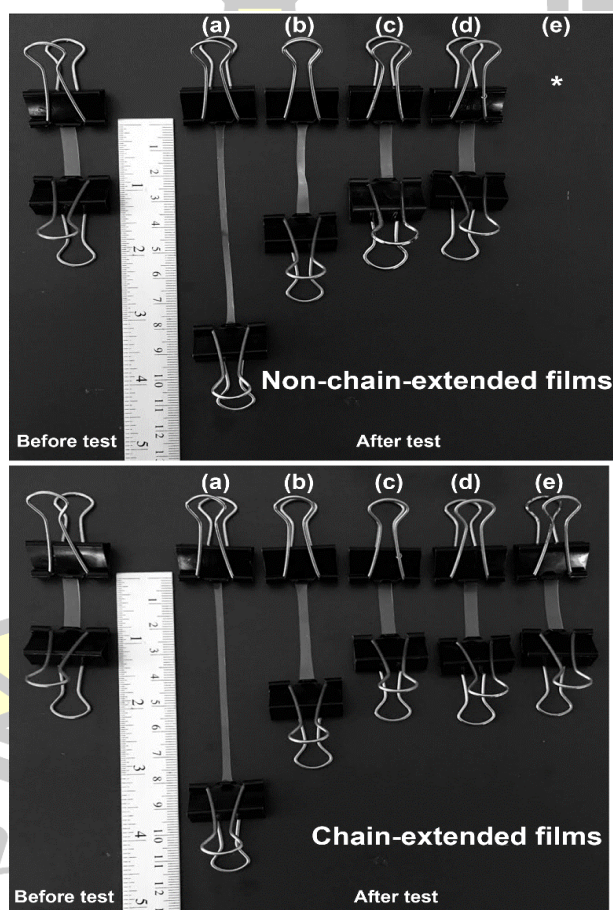


Fig. 38. Photographs of dimensional stability to heat at 80°C of (above) non-chain-extended and (below) chain-extended blend films with PLLA-PEG-PLLA/PDLA ratios of (a) 100/0, (b) 90/10, (c) 80/20, (d) 70/30 and (e) 60/40 (w/w) (* = could not determine).

The heat resistance of the film samples was clearly compared with the dimensional stability to heat. Fig. 39 shows the results of dimensional stability to heat. The dimensional stability to heat of PLLA-PEG-PLLA films were 26% and 31% for with and without chain extension, respectively. These values increased up to 56% and 53% when the 10 wt% PDLA was blended. The results of dimensional stability to heat of blend films were in the range 83–91% for the PDLA ratios of 20–40 wt%. Thus, the heat resistances of the blend films were better than the PLLA-PEG-PLLA films for both the blend films with and without chain extension. The PLA stereocomplexation with the PDLA can improve heat resistance of the PLLA-PEG-PLLA films.

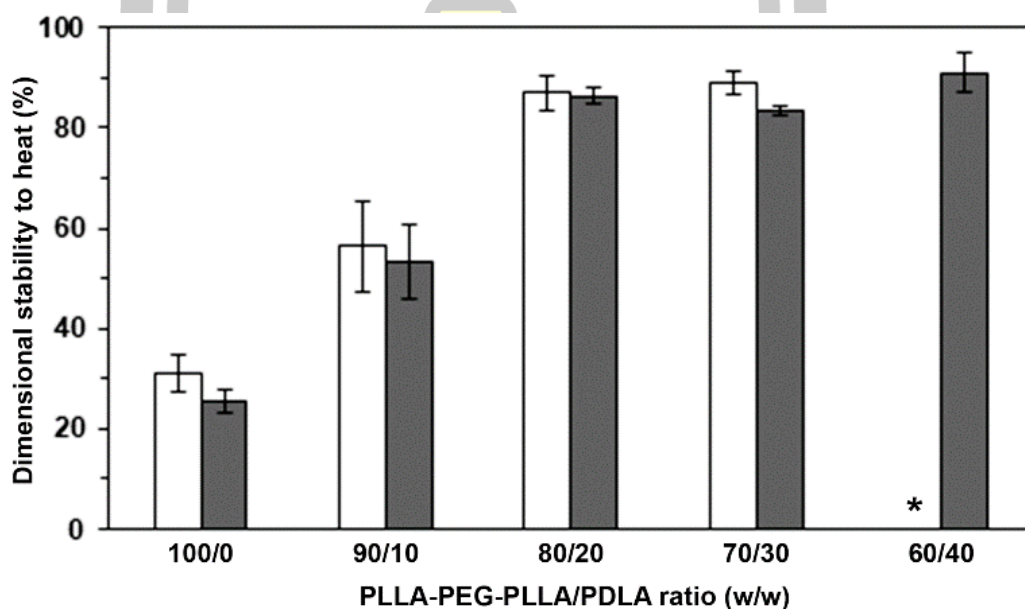


Fig. 39. Dimensional stability to heat of (□) non-chain-extended and (■) chain-extended blend films with various PLLA-PEG-PLLA/PDLA ratios (* = could not determine).

4.4. Characterization of PLLA-PEG-PLLA/PDLA-PEG-PDLA blends

4.4.1. Thermal transition properties

The stereocomplexation between PLLA and PDLA end-blocks of the blends was investigated from DSC heating thermograms as shown in Fig. 40. The DSC results are summarized in Table 18. The T_g of the non-chain-extended and chain-extended blends were in ranges 27–29°C and 34–38°C, respectively. The stereocomplexation of PLLA and PDLA end-blocks did not affect glass-transition behaviours of the blends. The long-chain branching structures of chain-extended blends inhibited chain mobility to increase the T_g .

The PLLA-PEG-PLLA had only a $T_{m,hc}$ at 169°C, while the blends had both $T_{m,hc}$ and $T_{m,sc}$ in the ranges 161–168°C and 216–218°C, respectively. There were no peaks of cold crystallization suggested that crystallization completed during the quenching process in the DSC method. As shown in Table 18, a large decrease in $DSC-X_{c,hc}$ and considerable increase in $DSC-X_{c,sc}$ steadily with increasing PDLA-PEG-PDLA ratio from 0 to 40 wt% were observed. The higher PDLA-PEG-PDLA ratio gave larger PDLA fraction for stereocomplex formation with the PLLA end-blocks of PLLA-PEG-PLLA.

All the chain-extended blends exhibited T_{cc} peaks indicated the crystallization did not complete during quenching in DSC method. The $DSC-X_{c,hc}$ and $DSC-X_{c,sc}$ could not calculate because of T_{cc} peaks of homo- and stereocomplex crystallites could not separate (see Fig. 40 (below)). However, the $\Delta H_{m,hc}$ of the blends significantly decreased and the $\Delta H_{m,sc}$ steadily increased as increasing the PDLA-PEG-PDLA ratio. This suggests the stereocomplexation increased with the PDLA-PEG-PDLA ratio.

พหุ ประถมศึกษา

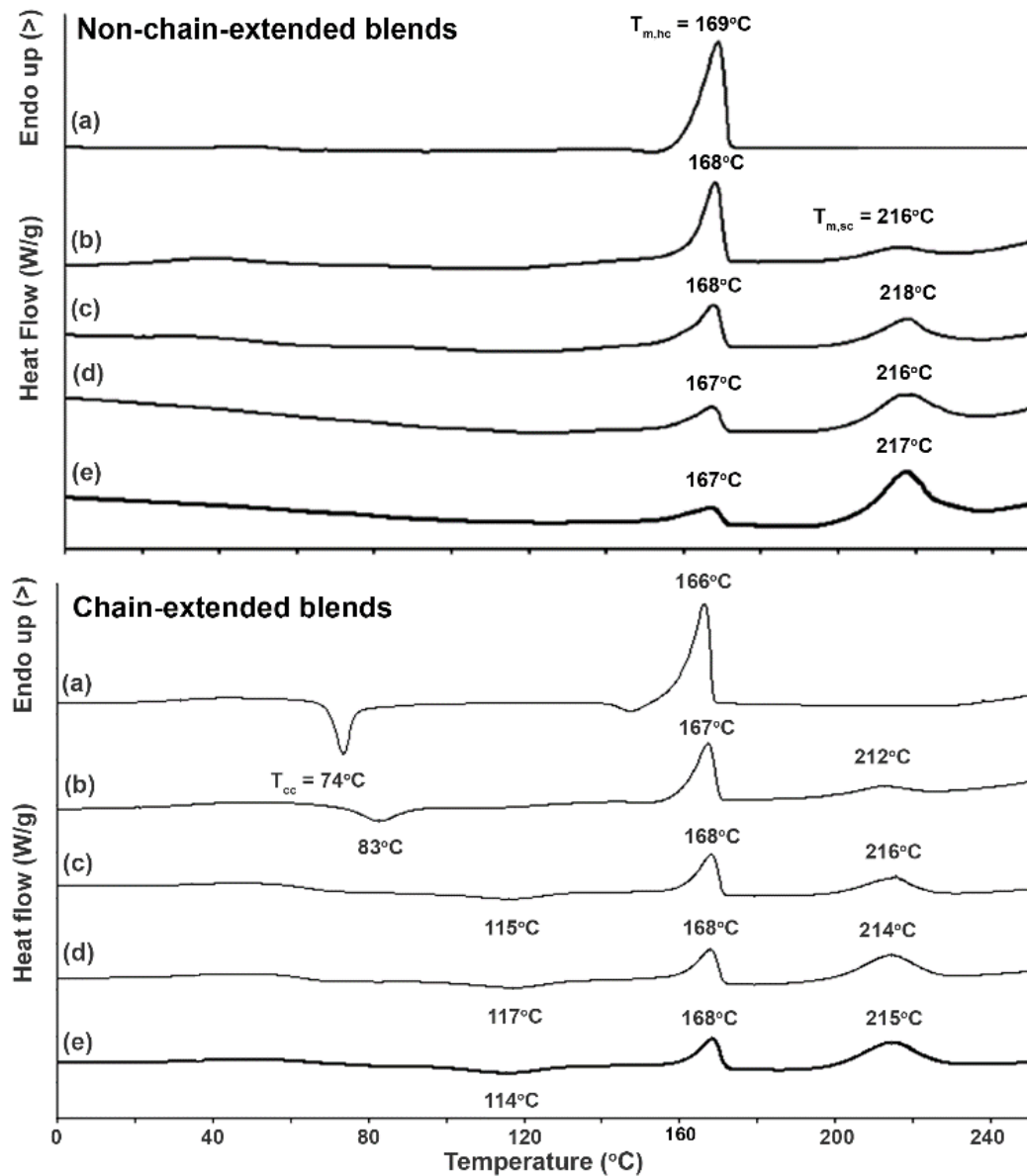


Fig. 40. DSC second heating thermograms of (above) non-chain-extended and (below) chain-extended blends with PLLA-PEG-PLLA/PDLA-PEG-PDLA ratios of (a) 100/0, (b) 90/10, (c) 80/20, (d) 70/30 and (e) 60/40 (w/w).

Table 18. Thermal transition properties of PLLA-PEG-PLLA/PDLA-PEG-PDLA blends.

PLLA-PEG- PLLA/PDLA-PEG- PDLA ratio (w/w)	T _g (°C)	ΔH _{cc} (J/g)	ΔH _{m,hc} (J/g)	ΔH _{m,sc} (J/g)	DSC-X _{c,hc} (%)	DSC-X _{c,sc} (%)
Non-chain-extended						
100/0	29	-	44.9	-	58.1	-
90/10	28	-	30.7	7.6	39.8	6.5
80/20	27	-	21.0	20.0	27.2	17.0
70/30	28	-	12.6	27.4	16.3	23.2
60/40	28	-	10.5	40.3	13.6	34.2
Chain-extended						
100/0	34	19.6	41.0	-	26.9	-
90/10	37	11.6	24.1	6.8	- ^a	- ^a
80/20	36	7.9	18.9	15.9	- ^a	- ^a
70/30	38	7.7	18.1	25.9	- ^a	- ^a
60/40	38	7.5	14.5	26.7	- ^a	- ^a

^a could not calculate.

Fig. 41 shows DSC cooling thermograms of the PLLA-PEG-PLLA and blends, after being melted at 250°C. The non-chain-extended PLLA-PEG-PLLA had T_c at 105°C with a ΔH_c of 27.4 J/g. The flexible PEG middle-blocks enhanced plasticizing effect for homo-crystallization of PLLA end-blocks during DSC cooling scan. The 90/10 blend exhibited T_c at 84°C that is lower than the pure PLLA-PEG-PLLA. However, the T_c and ΔH_c values of the blends significantly increased with increasing of the PDLA-PEG-PDLA ratio. This suggests the crystallization of the blends was accelerated during the DSC cooling scan by increasing the PDLA-PEG-PDLA ratio. The results could be explained by the crystallization of stereocomplex crystallites of PLA being faster than that of the homo-crystallites (Shi *et al.*, 2018).

For chain-extended blends, the PLLA-PEG-PLLA and 90/10 blend had similar the T_c (91 and 89°C, respectively). When the PDLA-PEG-PDLA ratios of chain-extended blends were higher than 10 wt%, the T_c shifted to higher temperature. This suggests faster crystallization was obtained for the higher PDLA-PEG-PDLA ratio. In addition, the T_c of 80/20, 70/30 and 60/40 blends with chain extension were higher temperature than the non-chain extended blends for the same blend ratio. The results confirmed that the chain-extension reaction improved stereocomplex crystallization of PLLA-PEG-PLLA/PDLA-PEG-PDLA blends similar to the PLLA-PEG-PLLA/PDLA blends as previous described above.

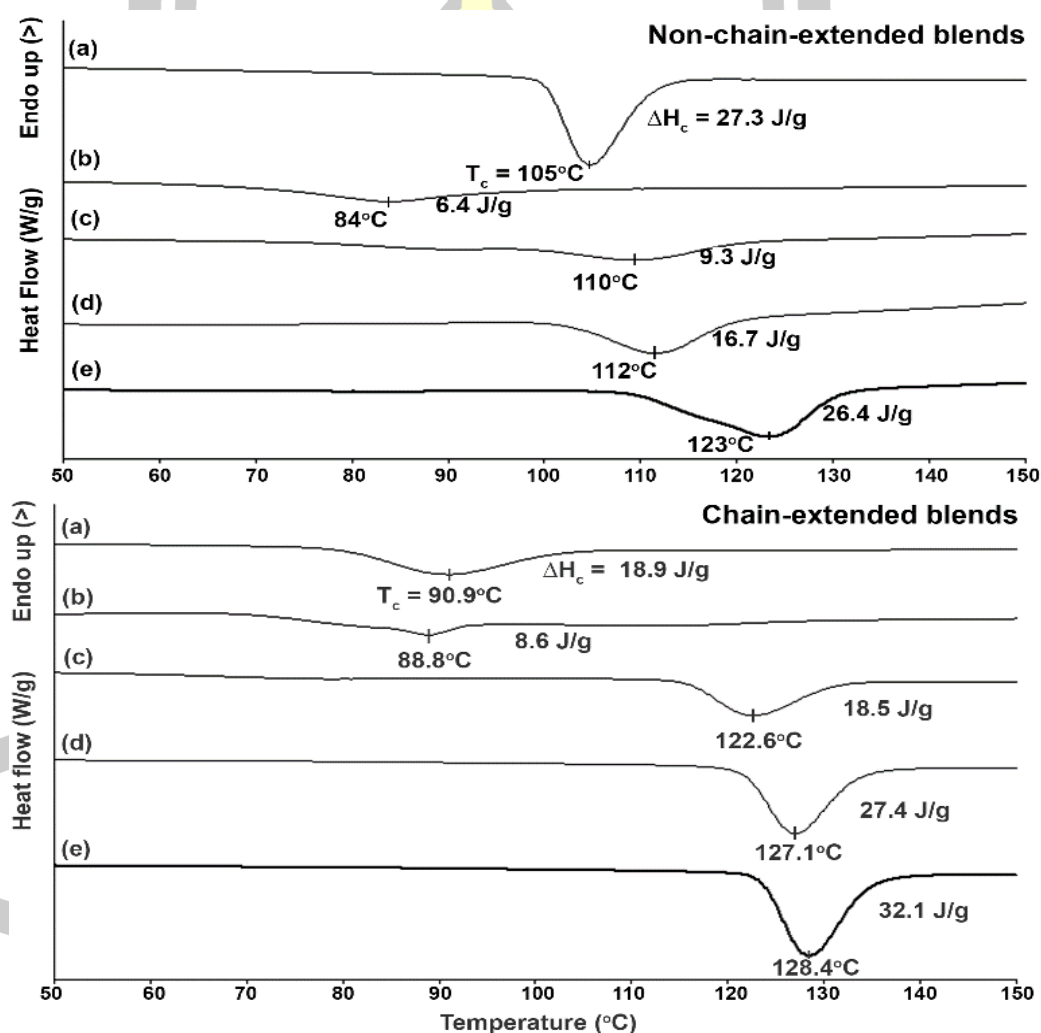


Fig. 41. DSC cooling thermograms of (above) non-chain-extended and (below) chain-extended blends with PLLA-PEG-PLLA/PDLA-PEG-PDLA ratios of (a) 100/0, (b) 90/10, (c) 80/20, (d) 70/30 and (d) 60/40 (w/w) (T_c peak and ΔH_c as shown).

4.4.2. Crystalline structures

The crystalline structures of the PLLA-PEG-PLLA and blend films were determined from XRD patterns as presented in Fig. 42. For non-chain-extended films in Fig. 42(above), the PLLA-PEG-PLLA film exhibited a diffraction peak at 17° attributed to homo-crystalline structure of polylactide matrix (Baimark *et al.*, 2018). While all the blend films showed weak diffraction-peaks at 12° , 21° and 24° ascribed to stereocomplex-crystalline structure (Cui *et al.*, 2016; Han *et al.*, 2016). This suggests the compression molding enhanced stereocomplexation of chain-extended blend films. The XRD- $X_{c,hc}$ of PLLA-PEG-PLLA film and XRD- $X_{c,sc}$ of blend films are summarized in Table 19. The XRD- $X_{c,sc}$ of blend films increased with the PDLA-PEG-PDLA ratio. The XRD- $X_{c,hc}$ and XRD- $X_{c,sc}$ values in Table 19 were lower than the DSC- $X_{c,hc}$ and DSC- $X_{c,sc}$ values in Table 18. This may be related to the easier mobility of the copolymer chains, having occurred during the quenching process, without compression forces in the DSC method to enhance more crystallisation of PLA end-blocks. In addition, some disagreements among the quantitative results of the crystallinity by different measurement methods are frequently encountered.

For the chain-extended blend films in Fig. 42(below), the PLLA-PEG-PLLA film did not show any XRD peaks attributable to completely amorphous states. The long-chain branching structures of chain-extended PLLA-PEG-PLLA inhibited crystallization of PLLA end-blocks (Baimark *et al.*, 2018). All the blend films exhibited only stereocomplex-crystalline structure with XRD peaks at 12° , 21° and 24° (Baimark & Kittipoom, 2018). The XRD- $X_{c,sc}$ of chain-extended blend films increased with the PDLA-PEG-PDLA ratio. It should be noted that the chain-extended blend films had higher XRD- $X_{c,sc}$ than the non-chain-extended blend films. This indicates the branching structures of chain-extended blend films enhanced stereocomplexation between PLLA and PDLA end-blocks. More free-volume of branching structures may enhance chain mobility for stereocomplex crystallization.

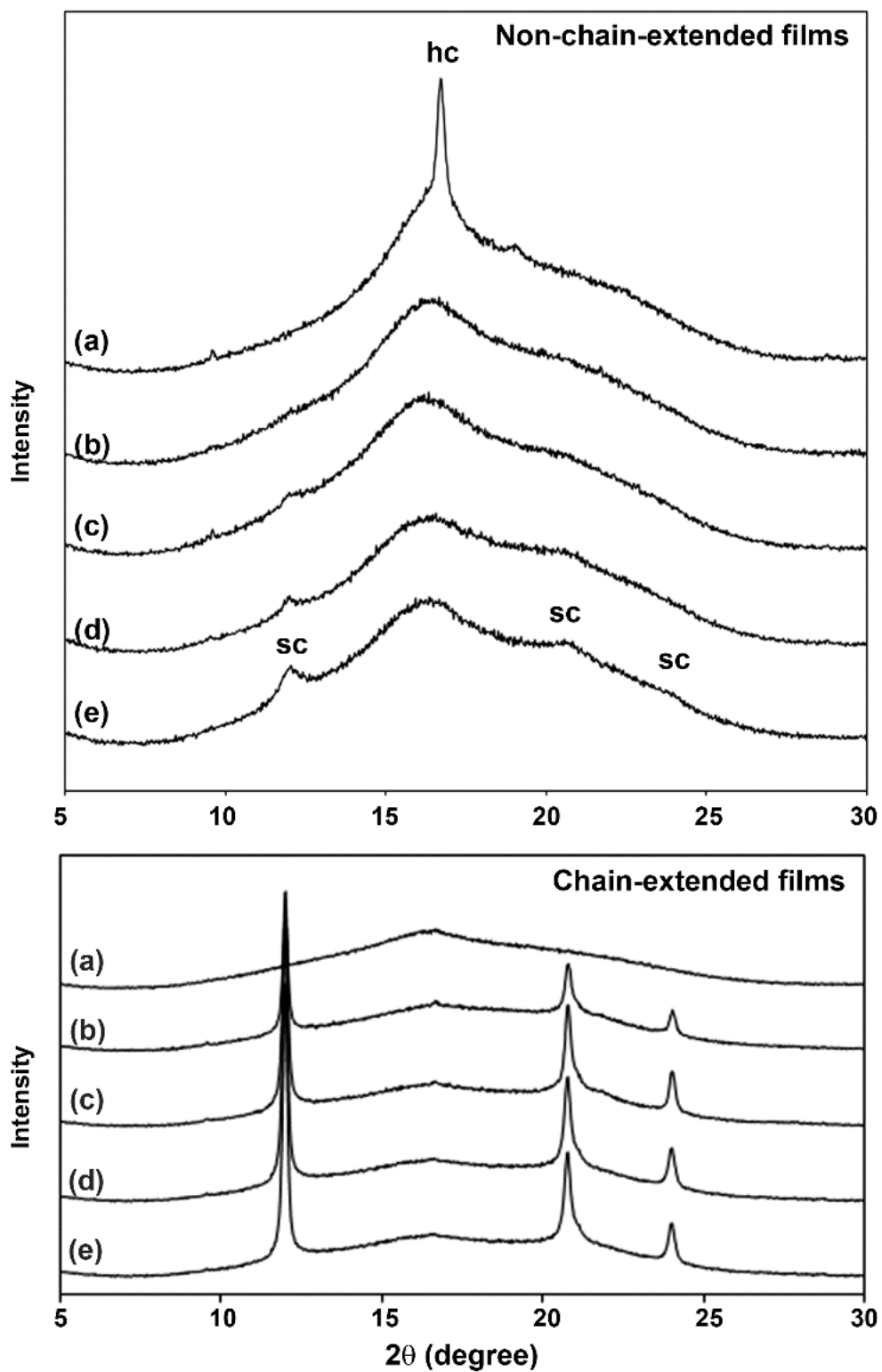


Fig. 42. XRD patterns of (above) non-chain-extended and (below) chain-extended blend films with PLLA-PEG-PLLA/PDLA-PEG-PDLA ratios of (a) 100/0, (b) 90/10, (c) 80/20, (d) 70/30 and (e) 60/40 (w/w).

Table 19. XRD results of PLLA-PEG-PLLA/PDLA-PEG-PDLA blend films.

PLLA-PEG-PLLA/PDLA-PEG-PDLA (w/w)	XRD- $X_{c,hc}$ (%)	XRD- $X_{c,sc}$ (%)
Non-chain-extended		
100/0	7.84	-
90/10	-	1.94
80/20	-	2.76
70/30	-	3.81
60/40	-	4.72
Chain-extended		
100/0	-	-
90/10	-	15.1
80/20	-	26.5
70/30	-	27.2
60/40	-	28.5

4.4.3. Tensile properties

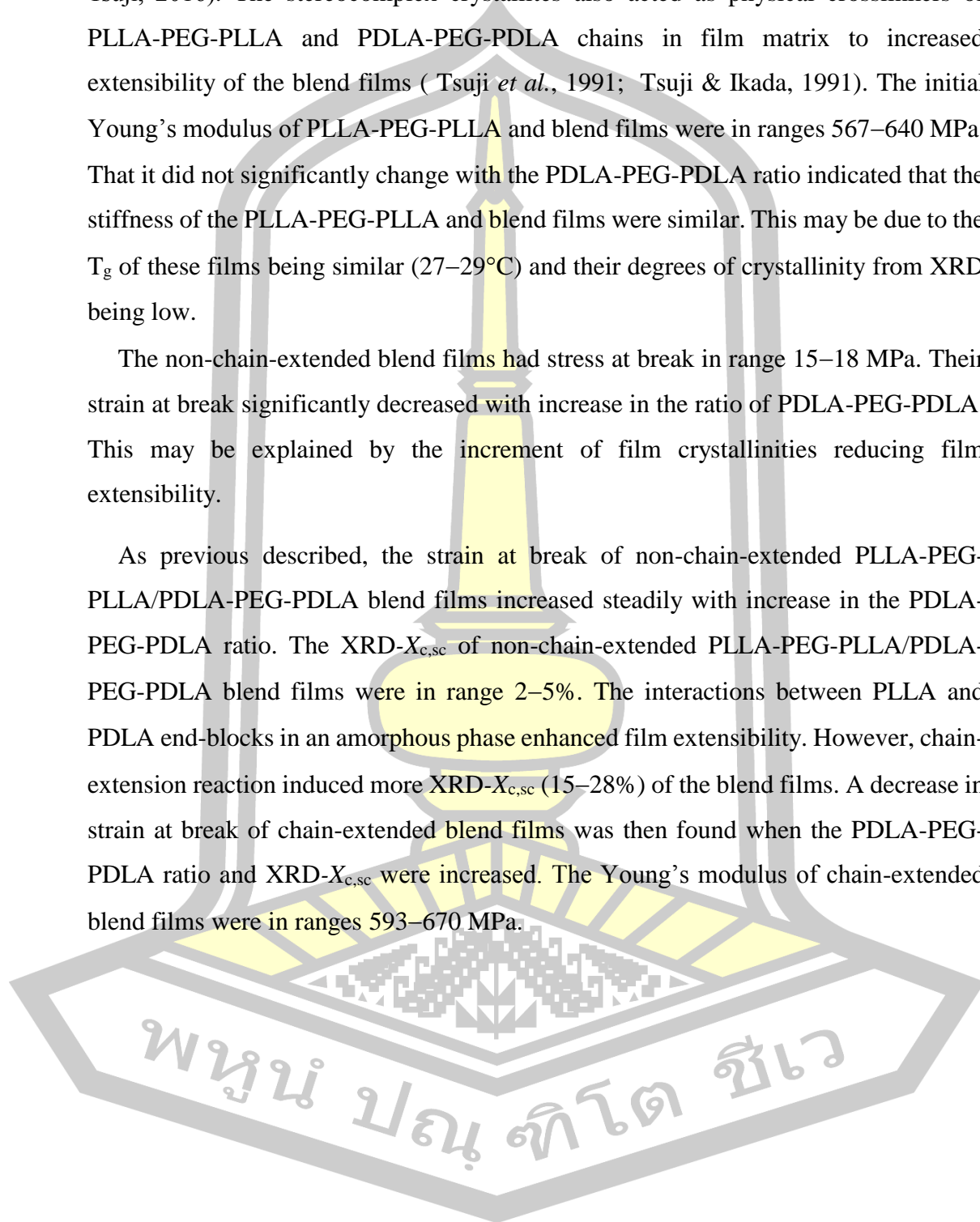
Fig. 43 shows selected tensile curves of PLLA-PEG-PLLA and blend films. All the films had a yield point indicating the films were flexible. The flexible PEG middle-blocks enhanced the plasticizing effect of the polylactide end-blocks (Baimark *et al.*, 2018; Yun *et al.*, 2018). The stress at yield of films increased with the PDLA-PEG-PDLA ratio. The averaged tensile properties including stress and strain at break as well as Young's modulus are clearly compared in Fig. 44.

For non-chain-extended films, the blend films showed higher stress and strain at break than the PLLA-PEG-PLLA film. The stress and strain at break of the blend films increased as the PDLA-PEG-PDLA ratio increased. The results suggested that stereocomplexation between PLLA-PEG-PLLA and PDLA-PEG-PDLA of the blend films improved their tensile properties. The stereocomplex crystallites of PLLA/PDLA end-blocks had better tensile strength than the homo-crystallites of PLLA and PDLA

end-blocks due to stronger intermolecular forces in the stereocomplex crystallites (Tsuji, 2016). The stereocomplex crystallites also acted as physical crosslinkers of PLLA-PEG-PLLA and PDLA-PEG-PDLA chains in film matrix to increased extensibility of the blend films (Tsuji *et al.*, 1991; Tsuji & Ikada, 1991). The initial Young's modulus of PLLA-PEG-PLLA and blend films were in ranges 567–640 MPa. That it did not significantly change with the PDLA-PEG-PDLA ratio indicated that the stiffness of the PLLA-PEG-PLLA and blend films were similar. This may be due to the T_g of these films being similar (27–29°C) and their degrees of crystallinity from XRD being low.

The non-chain-extended blend films had stress at break in range 15–18 MPa. Their strain at break significantly decreased with increase in the ratio of PDLA-PEG-PDLA. This may be explained by the increment of film crystallinities reducing film extensibility.

As previous described, the strain at break of non-chain-extended PLLA-PEG-PLLA/PDLA-PEG-PDLA blend films increased steadily with increase in the PDLA-PEG-PDLA ratio. The XRD- $X_{c,sc}$ of non-chain-extended PLLA-PEG-PLLA/PDLA-PEG-PDLA blend films were in range 2–5%. The interactions between PLLA and PDLA end-blocks in an amorphous phase enhanced film extensibility. However, chain-extension reaction induced more XRD- $X_{c,sc}$ (15–28%) of the blend films. A decrease in strain at break of chain-extended blend films was then found when the PDLA-PEG-PDLA ratio and XRD- $X_{c,sc}$ were increased. The Young's modulus of chain-extended blend films were in ranges 593–670 MPa.



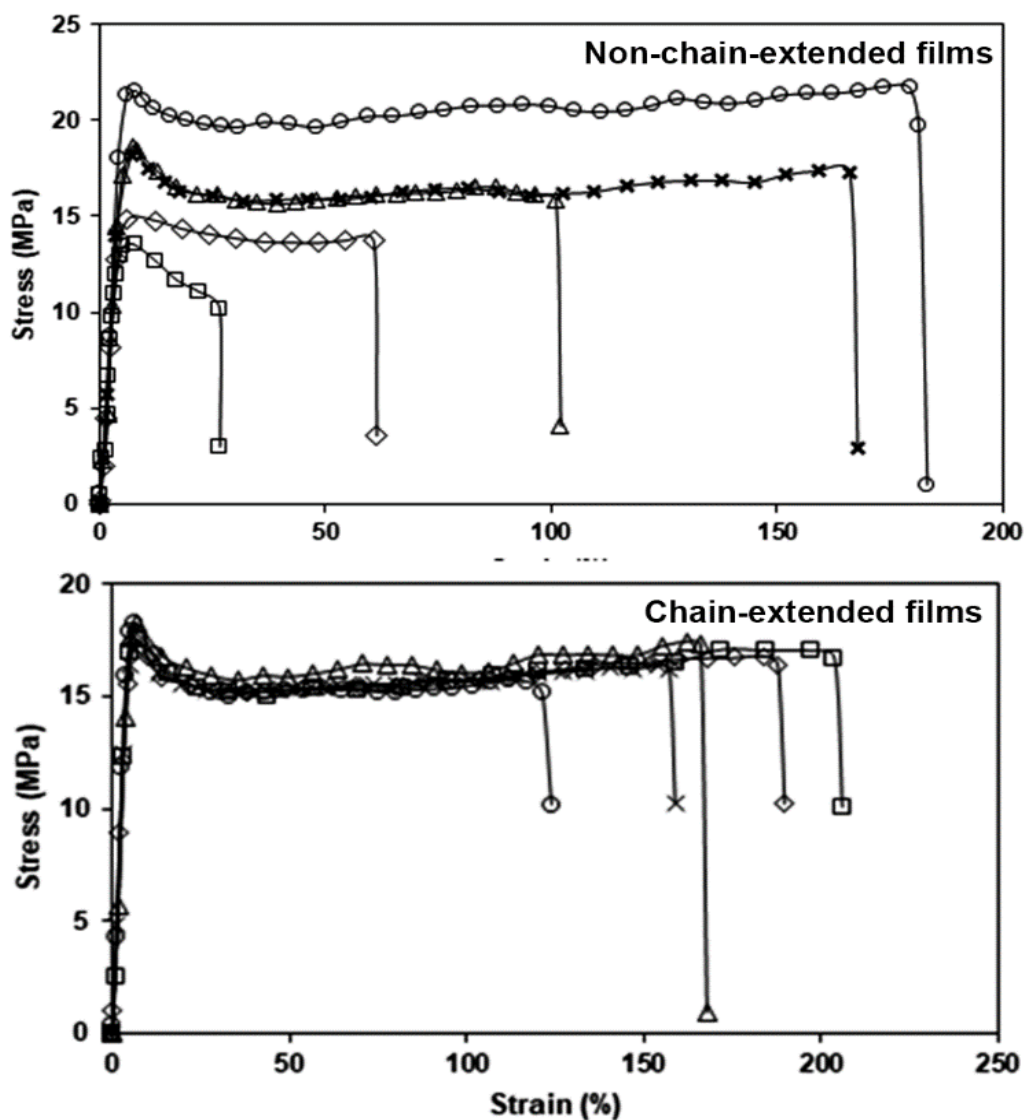


Fig. 43. Tensile curves of (above) non-chain-extended and (below) chain-extended blend films with PLLA-PEG-PLLA/PDLA-PEG-PDLA ratios of (□) 100/0, (◇) 90/10, (△) 80/20, (×) 70/30 and (○) 60/40 (w/w).

พหุ ประถมศึกษา

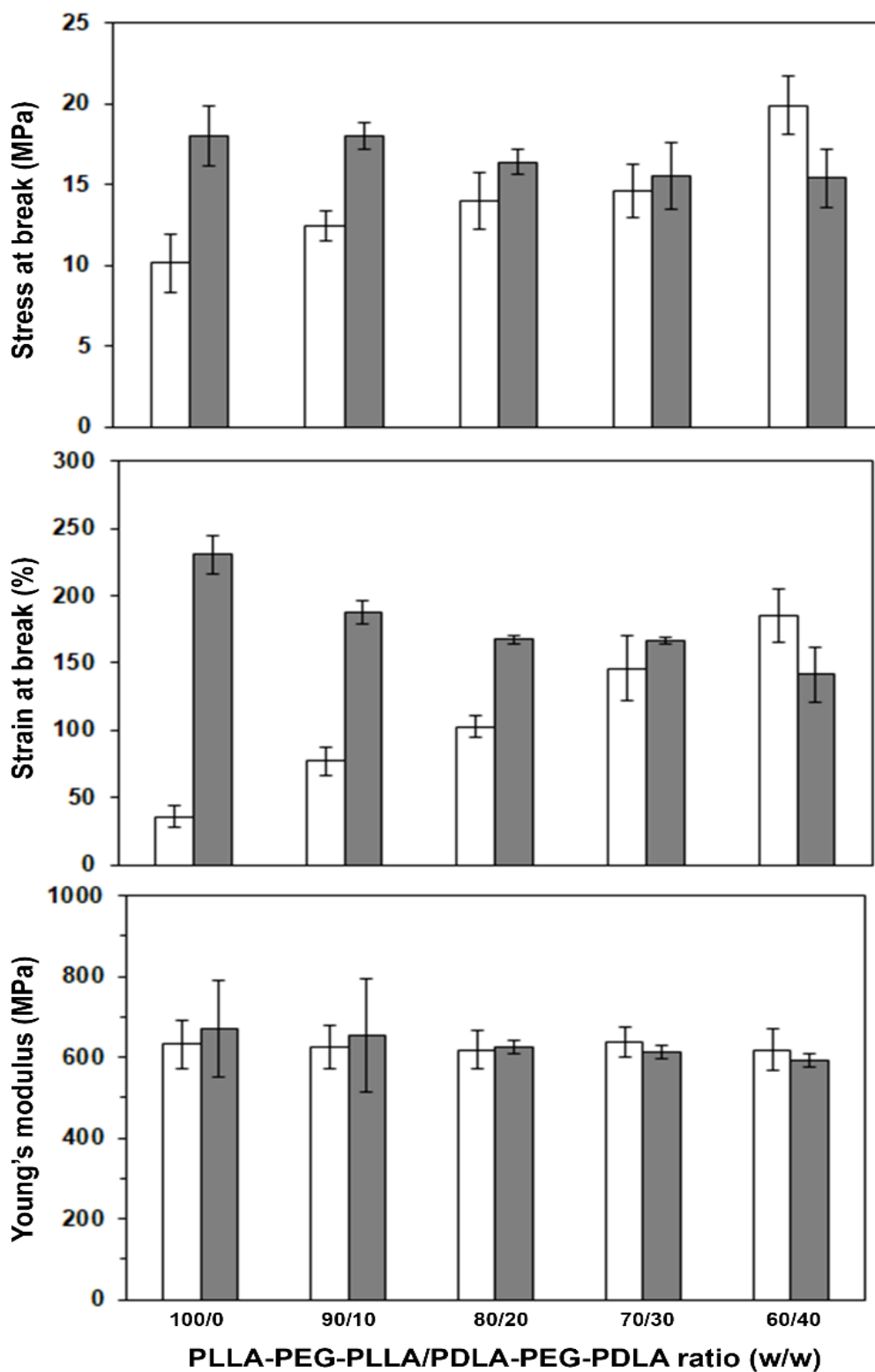


Fig. 44. Tensile properties of (□) non-chain-extended and (■) chain-extended blend films with various PLLA-PEG-PLLA/PDLA-PEG-PDLA ratios.

4.4.4. Thermo-mechanical properties

Fig. 45 shows storage modulus of film samples from DMA analysis. The storage modulus of PLLA-PEG-PLLA and blend films dramatically dropped with increasing temperature in the range 30–60°C due to rubber-like character and low crystallinity of all the films. This indicates these films were low heat-resistance. All the films were then extended for the test of dimensional stability to heat. The storage modulus increased again in the range 90–130°C due to cold crystallization of PLA end-blocks. This suggests that the crystallisation of compressed films did not complete. This may be due to the compression forces reducing the chain mobility for crystallisation of PLA end-blocks during the film cooling. However, the cold-crystallization regions of the blend films from DMA analysis were detected at higher temperature than the PLLA-PEG-PLLA film and shifted to higher temperatures as the PDLA-PEG-PDLA ratio increased. This could be explained by the chain mobility of copolymers during cold crystallization in DMA heating scan being restricted by the stronger intermolecular interactions between PLLA and PDLA end-blocks.

In addition, the PLLA-PEG-PLLA film exhibited the largest rising up of storage modulus during cold crystallization (see black line in Fig. 45). This curve type indicates poor heat-resistance of the PLLA-PEG-PLLA film because film stiffness to heat was the lowest (Vadori *et al.*, 2013). The increases of storage modulus during cold crystallization of the blend films were lower than the PLLA-PEG-PLLA film and steadily decreased as the PDLA-PEG-PDLA ratio increased. The DMA results suggested that the interactions between PLLA and PDLA end-blocks in the amorphous phases of the blend films enhanced its stiffness and heat resistance. The changes of storage modulus of blend films without and with chain extension were similar for the same blend ratio.

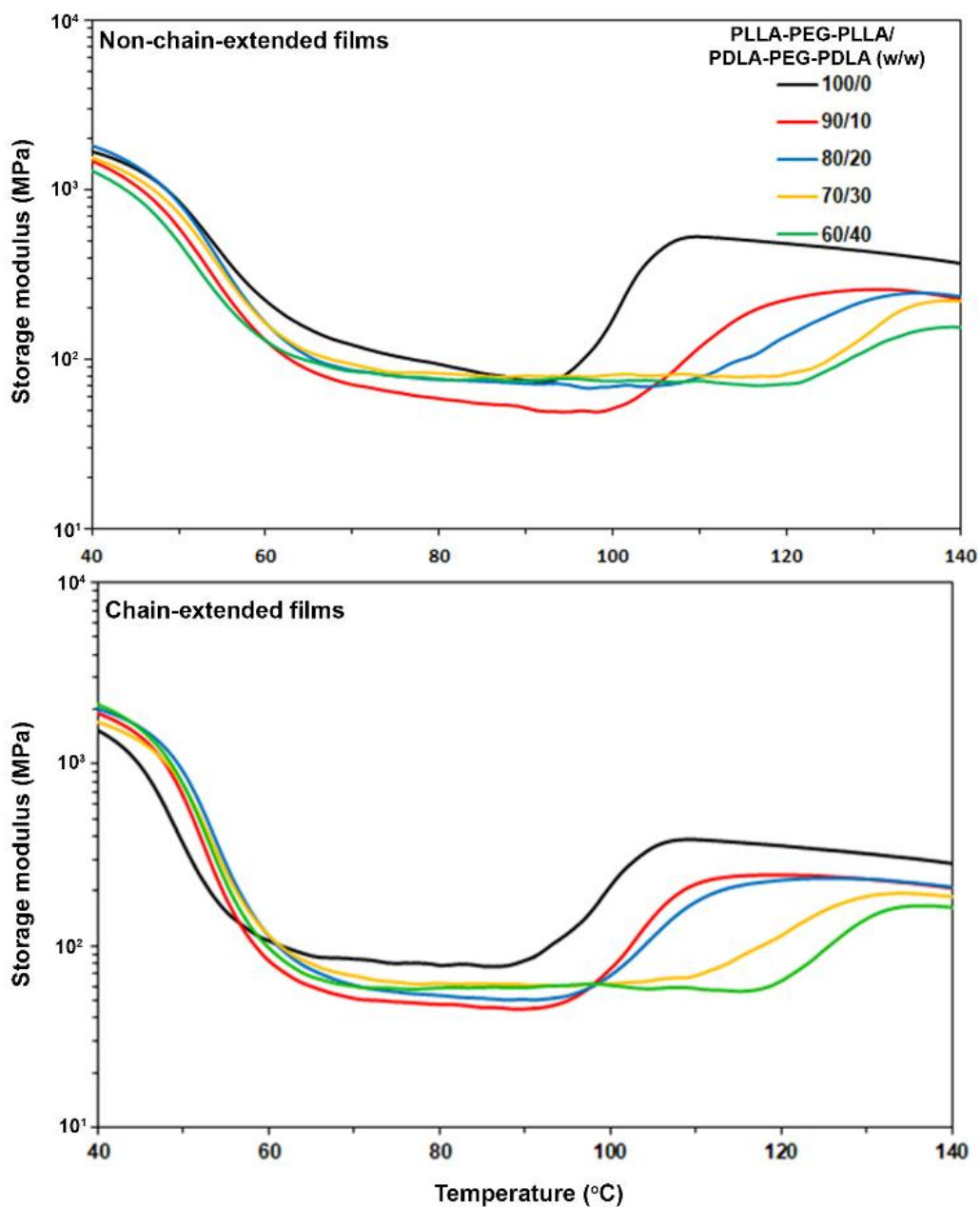


Fig. 45. Storage modulus from DMA of (above) non-chain-extended and (below) chain-extended films with various PLLA-PEG-PLLA/PDLA-PEG-PDLA ratios.

4.4.5. Dimensional stability to heat

The film samples before and after testing of dimensional stability to heat are shown in Fig. 46. Both the PLLA-PEG-PLLA films with and without chain extension exhibited the largest film-extension indicating they had poor heat-resistance according to DMA results. All the blend films after testing exhibited shorter film-extension than the PLLA-PEG-PLLA film. The results suggested that the blend films had better heat-resistance because they contained stereocomplex crystallites.

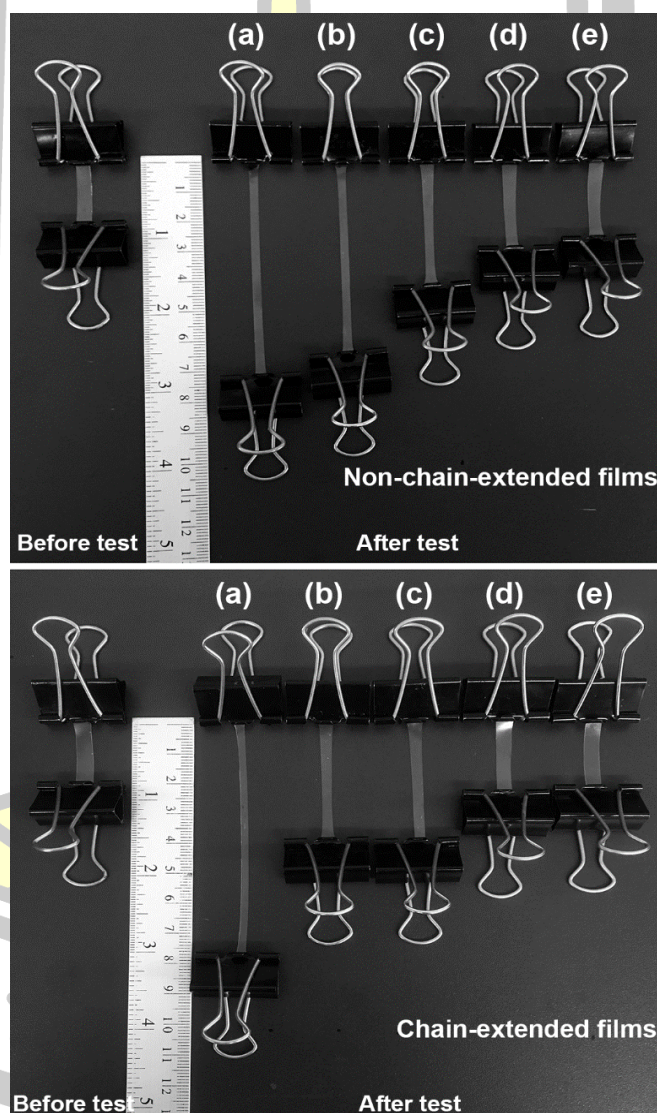


Fig. 46. Photographs of dimensional stability to heat at 80°C of (above) non-chain-extended and (below) chain-extended blend films with PLLA-PEG-PLLA/PDLA-PEG-PDLA ratios of (a) 100/0, (b) 90/10, (c) 80/20, (d) 70/30 and (e) 60/40 (w/w).

The heat resistance of the film samples was clearly compared with the dimensional stability to heat. Fig. 47 shows the calculated results of dimensional stability to heat. The dimensional stability to heat of PLLA-PEG-PLLA films were 27% and 26% for without and with chain extension, respectively. The dimensional stability to heat of the blend films increased with the PDLA-PEG-PDLA ratio for both the film series. Thus, the heat resistances of the blend films were better than the PLLA-PEG-PLLA films for both the blend films with and without chain extension. The PLA stereocomplexation with the PDLA can improve heat resistance of the PLLA-PEG-PLLA films. In addition, the chain-extended blend films exhibited better heat resistance than the non-chain-extended blend films. This is due to the higher $XRD-X_{c,sc}$ of the chain-extended blend films.

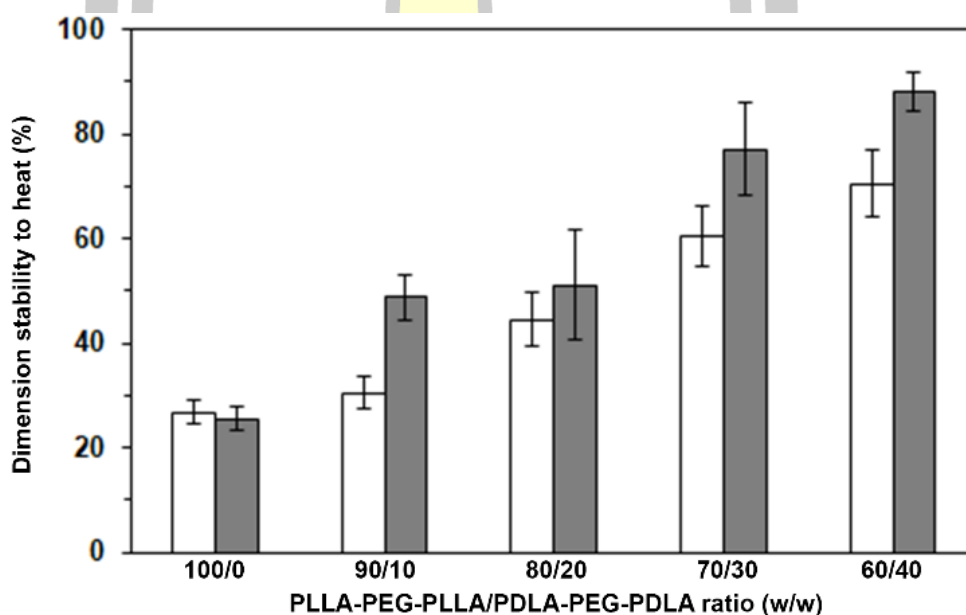


Fig. 47. Dimensional stability to heat of (□) non-chain-extended and (■) chain-extended blend films with various PLLA-PEG-PLLA/PDLA-PEG-PDLA ratios.

CHAPTER V

CONCLUSIONS

Most of the results presented in the preceding Chapter 4 have already been discussed in detail. This final Chapter 5 of this thesis now aims to bring together the main conclusions and correlate them as far as possible. These conclusions can be divided up under the following main headings:

- Synthesis and characterization of polymers
- Preparation and characterization of polymer blends

5.1 Synthesis and characterization of polymers

The PLLA-PEG-PLLA, PDLA and PDLA-PEG-PDLA were synthesized via ring-opening polymerisation in bulk of the lactide monomer under nitrogen atmosphere at 165°C for 6.0 and 2.5 h for the triblock copolymers and PDLA, respectively. Stannous octoate catalyst was 0.01 and 0.075 mol% for the triblock copolymers and PDLA, respectively. Some un-reacted lactide was removed by dried at 110°C for 2 h under vacuum. The residue lactide was less than 5 wt% as demonstrated by TGA.

Polymer characterisation in this work was carried out by a combination of analytical techniques, namely: molecular weight measurements (dilute-solution viscometry, GPC), spectroscopic analysis (¹H-NMR) and thermal analysis (DSC, TG). The main conclusions arising from the results obtained (Chapter 4) can be summarized as follows:

- (1) From molecular weight characterization, the M_v of PDLA from dilute-solution viscometry (5,200 g/mol) are nearly value with the M_n from GPC (5,700 g/mol). The M_n of both the triblock copolymers (90,000 and 85,000 g/mol) were less than the theoretical M_n (120,000 g/mol). Some thermal decomposition may occur during polymerization of high M.W. polymer.
- (2) From GPC curves, the unimodal distribution curves were obtained for the triblock copolymers. This confirms that the PEG acted as macro-initiators to polymerize the added lactide monomer at its chain-end.
- (3) From TGA, the PDLA exhibited a single-step of thermal decomposition in the range 150–400°C. While the triblock copolymers showed two-step of thermal

decompositions in the ranges 200–350°C and 350–450°C for the polylactide end-blocks and PEG middle-blocks, respectively.

- (4) From DSC, the triblock copolymers exhibited lower T_g (33–34°C) than the PDLA (47°C). This due to the plasticizing effect of the flexible PEG middle-blocks. However the T_m of the triblock copolymers (170°C) were higher than the PDLA (161°C). This could be explained by the longer polylactide blocks of triblock copolymers enhanced the larger crystallites.
- (5) From $^1\text{H-NMR}$, the chemical functional groups of triblock copolymers and PDLA were indicated. Moreover chemical bonding between the PEG middle-blocks and polylactide end-blocks was confirmed.

5.2 Preparation and characterization of polymer blends

In this work, polymer blends of PLLA-PEG-PLLA/PDLA and PLLA-PEG-PLLA/PDLA-PEG-PDLA without and with chain extension were prepared by melt blending at 200°C for 4.0 min with rotor speed of 100 rpm using an internal mixer. The PLLA-PEG-PLLA and blend films were produced by compression molding at 240°C without any compression force for 1.0 min followed with 5.0 tons compression force for 1.0 min before cooling to room temperature for 1.0 min under 5.0 tons compression force.

The polymer blends were characterized by a combination of analytical techniques: thermal analysis method (DSC), spectroscopic method (XRD), mechanical property method (tensile testing) and heat resistant method (DMA and dimensional stability to heat). The main conclusions arising from the results obtained (Chapter 4) can be summarized as below:

- (1) The T_c from DSC cooling curves of both the PLLA-PEG-PLLA/PDLA and PLLA-PEG-PLLA/PDLA-PEG-PDLA blend films shifted to higher temperature while the $\Delta H_{m,sc}$ and $X_{c,sc}$ increased steadily with the PDLA and PDLA-PEG-PDLA ratio, respectively, as demonstrated by XRD results. The chain-extension reaction improved degrees of crystallinity of the both blend film series.

- (2) The tensile properties of the PLLA-PEG-PLLA/PDLA blends strongly depended upon $X_{c,sc}$ and PDLA content. The higher PDLA content enhanced stereocomplexation but induced film brittleness. This is due to the PDLA was low M.W. (5,000 g/mol). The stronger intermolecular forces between PLLA end-blocks and PDLA chains as well as chain-extension reaction enhanced tensile properties.
- (3) For PLLA-PEG-PLLA/PDLA-PEG-PDLA blend films, the non-chain-extended blend films contained low $X_{c,sc}$. Therefore the tensile properties depended on intermolecular forces between PLLA and PDLA end-blocks in the amorphous phases of the blends. Both the stress and strain at break increased with the PDLA-PEG-PDLA ratio. However, the chain-extended blend films had higher $X_{c,sc}$ than the non-chain-extended blend films for the same blend ratio. Therefore the strain at break of the chain-extended blend films decreased as the PDLA-PEG-PDLA ratio increased.
- (4) Heat resistance of the both blend-film series were better than the PLLA-PEG-PLLA film and increased with the PDLA and PDLA-PEG-PDLA ratio. The PLLA-PEG-PLLA/PDLA blend films exhibited better heat-resistance than the PLLA-PEG-PLLA/PDLA-PEG-PDLA blend films for the same blend ratio. The chain-extension reaction improved the heat resistance of the PLLA-PEG-PLLA/PDLA-PEG-PDLA blend films but did not the PLLA-PEG-PLLA/PDLA blend films.

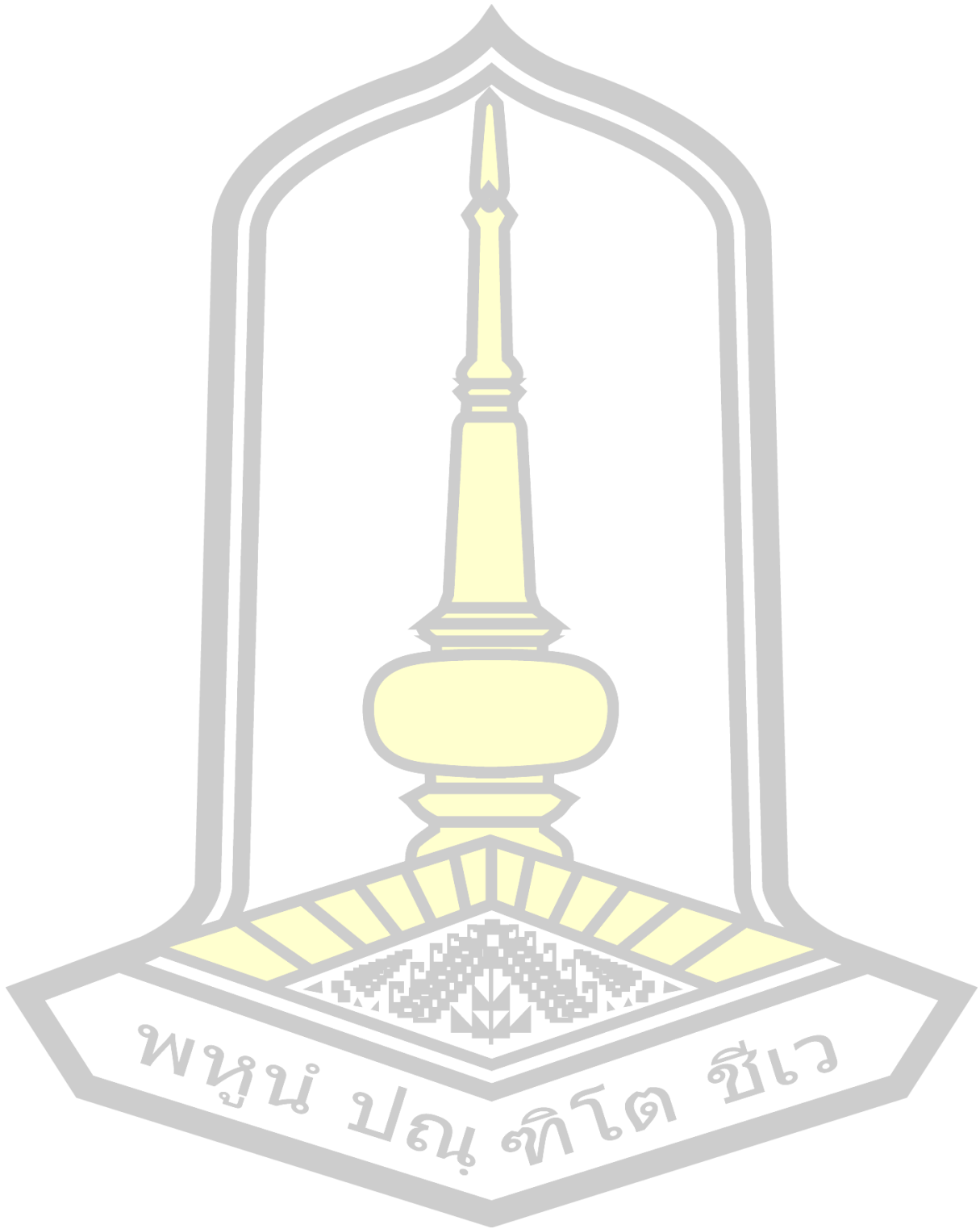
In summary, the PLLA-PEG-PLLA/PDLA blend films exhibited better heat resistant properties obtained from DMA and dimensional stability to heat tests but lower flexibility obtained from tensile test than the PLLA-PEG-PLLA/PDLA-PEG-PDLA blend films for the same blend ratio. The chain extender improved film flexibility of both the PLLA-PEG-PLLA/PDLA and PLLA-PEG-PLLA/PDLA-PEG-PDLA blend films. The blend films produced in this work show potential for use as flexible and good heat resistant bioplastic films. The selection of each formulation depended on each packaging application.

SUGGESTIONS FOR FURTHER WORK

This work has been concerned mainly with the preparation and characterization of the stereocomplex PLLA-PEG-PLLA/PDLA and PLLA-PEG-PLLA/PDLA-PEG-PDLA films. Actual biodegradability testing has not been within the scope of this work. As a logical extension, *in vitro* hydrolysability testing should be studied towards establishing their likely timescale for biodegradation. In addition, gas permeation testing is also important for packaging applications.



REFERENCES



REFERENCES

- Avérous, L., & Pollet, E. (2012). Environmental Silicate Nano-Biocomposites. *Green Energy and Technology*, 50.
<https://doi.org/10.1007/978-1-4471-4108-2>
- Baimark, Y., & Kittipoom, S. (2018). Influence of Chain-Extension Reaction on Stereocomplexation, Mechanical Properties and Heat Resistance of Compressed Stereocomplex-Polylactide. *Polymer*, 15–17.
<https://doi.org/10.3390/polym10111218>
- Baimark, Y., Rungseesantivanon, W., & Prakymoramas, N. (2018). Improvement in melt flow property and flexibility of poly(L -lactide) - b - poly(ethylene glycol) - b - poly (L -lactide) by chain extension reaction for potential use as flexible bioplastics. *Materials & Design*, 154, 73–80.
<https://doi.org/10.1016/j.matdes.2018.05.028>
- Brizzolara, D., Cantow, H. J., Diederichs, K., Keller, E., & Domb, A. J. (1996). Mechanism of the stereocomplex formation between enantiomeric poly(lactide)s. *Macromolecules*, 29(1), 191–197.
<https://doi.org/10.1021/ma951144e>
- Celli, A., & Scandola, M. (1992). Thermal properties and physical ageing of poly(l-lactic acid). *Polymer*, 33(13), 2699–2703.
[https://doi.org/10.1016/0032-3861\(92\)90440-8](https://doi.org/10.1016/0032-3861(92)90440-8)
- Chang, R., Shan, G., Bao, Y., & Pan, P. (2015). Enhancement of crystallizability and control of mechanical and shape-memory properties for amorphous enantiopure supramolecular copolymers via stereocomplexation. *Macromolecules*, 48(21), 7872–7881.
<https://doi.org/10.1021/acs.macromol.5b01986>

- Cui, L. I., Wang, Y., Guo, Y. I., Liu, Y. U. N., Zhao, J., Zhang, C., & Zhu, P. (2016). Effects of Temperature and External Force on the Stereocomplex Crystallization in Poly(lactic acid) Blends. *Advances in Polymer Technology*, 0(0), 1–6.
<https://doi.org/10.1002/adv.21743>
- Danner, H., & Braun, R. (1999). Biotechnology for the production of commodity chemicals from biomass. *Chemical Society Reviews*, 28(6), 395–405.
<https://doi.org/10.1039/a806968i>
- Discher, D. E., & Ahmed, F. (2006). Polymersomes. *Annual Review of Biomedical Engineering*, 8(1), 323–341.
<https://doi.org/10.1146/annurev.bioeng.8.061505.095838>
- Fan, Y., Nishida, H., Shirai, Y., Tokiwa, Y., & Endo, T. (2004). Thermal degradation behaviour of poly(lactic acid) stereocomplex. *Polymer Degradation and Stability*, 86(2), 197–208. <https://doi.org/10.1016/j.polymdegradstab.2004.03.001>
- Feng, L., Bian, X., Chen, Z., Li, G., & Chen, X. (2013). Mechanical, aging , optical and rheological properties of toughening polylactide by melt blending with poly (ethylene glycol) based copolymers. *Polymer Degradation and Stability*, 98(9), 1591–1600.
<https://doi.org/10.1016/j.polymdegradstab.2013.06.025>
- Feng, L., Sun, B., Bian, X., Chen, Z., & Chen, X. (2010). Determination of D-lactate content in poly(lactic acid) using polarimetry. *Polymer Testing*, 29, 771–776.
<https://doi.org/10.1016/j.polymertesting.2010.06.005>
- Fortunati, E., Armentano, I., Iannoni, A., & Kenny, J. M. (2010). Development and thermal behaviour of ternary PLA matrix composites. *Polymer Degradation and Stability*, 95(11), 2200–2206.
<https://doi.org/10.1016/j.polymdegradstab.2010.02.034>
- Garlotta, D. (2002). A Literature Review of Poly(Lactic Acid). *Journal of Polymers and the Environment*, 9(2), 63-84.
<https://doi.org/10.1023/A:1020200822435>

- Garric, X., Guillaume, O., Dabboue, H., Vert, M., & Molès, J. P. (2012). Potential of a PLA-PEO-PLA-based scaffold for skin tissue engineering: In vitro evaluation. *Journal of Biomaterials Science, Polymer Edition*, 23(13), 1687–1700.
<https://doi.org/10.1163/092050611X590912>
- Giita Silverajah, V. S., Ibrahim, N. A., Md Zin Wan Yunus, W., Hassan, H. A., & Woei, C. B. (2012). A comparative study on the mechanical, thermal and morphological characterization of poly(lactic acid)/epoxidized palm oil blend. *International Journal of Molecular Sciences*, 13(5), 5878–5898.
<https://doi.org/10.3390/ijms13055878>
- Gross, R. A., & Kalra, B. (2002). Biodegradable polymers for the environment. *Science*, 297(5582), 803–807.
<https://doi.org/10.1126/science.297.5582.803>
- Han, L., Yu, C., Zhou, J., Shan, G., Bao, Y., Yun, X., & Pan, P. (2016). Enantiomeric blends of high-molecular-weight poly(lactic acid)/poly(ethylene glycol) triblock copolymers: Enhanced stereocomplexation and thermomechanical properties. *Polymer*, 103, 376–386.
<https://doi.org/10.1016/j.polymer.2016.09.073>
- He, H., Yu, J., Cao, J., E, L., Wang, D., Zhang, H., & Liu, H. (2011). Biocompatibility and osteogenic capacity of periodontal ligament stem cells on nHAC/PLA and HA/TCP scaffolds. *Journal of Biomaterials Science, Polymer Edition*, 22(1–3), 179–194.
<https://doi.org/10.1163/092050609X12587018007767>
- He, Y., Xu, Y., Wei, J., Fan, Z., & Li, S. (2008). Unique crystallization behavior of poly(l-lactide)/poly(d-lactide) stereocomplex depending on initial melt states. *Polymer*, 49(26), 5670–5675.
<https://doi.org/10.1016/j.polymer.2008.10.028>

- Hu, Y., Rogunova, M., Topolkaev, V., Hiltner, A., & Baer, E. (2003). Aging of poly(lactide)/poly(ethylene glycol) blends. Part 1. Poly(lactide) with low stereoregularity. *Polymer*, *44*(19), 5701–5710.
[https://doi.org/10.1016/S0032-3861\(03\)00614-1](https://doi.org/10.1016/S0032-3861(03)00614-1)
- Huang, Y., Chang, R., Han, L., Shan, G., Bao, Y., & Pan, P. (2016). ABA-Type Thermoplastic Elastomers Composed of Poly(ϵ -caprolactone-co- δ -valerolactone) Soft Midblock and Polymorphic Poly(lactic acid) Hard End blocks. *ACS Sustainable Chemistry and Engineering*, *4*(1), 121–128.
<https://doi.org/10.1021/acssuschemeng.5b00855>
- Huang, Y., Pan, P., Shan, G., & Bao, Y. (2014). Polylactide-b-poly(ethylene-co-butylene)-b-poly(lactide) thermoplastic elastomers: Role of polylactide crystallization and stereocomplexation on microphase separation, mechanical and shape memory properties. *RSC Advances*, *4*(89), 47965–47976.
<https://doi.org/10.1039/c4ra08612k>
- Ikada, Y., & Tsuji, H. (2000). Biodegradable polyesters for medical and ecological applications. *Macromolecular Rapid Communications*, *21*(3), 117–132.
[https://doi.org/10.1002/\(SICI\)1521-3927\(20000201\)21:3<117::AID-MARC117>3.3.CO;2-O](https://doi.org/10.1002/(SICI)1521-3927(20000201)21:3<117::AID-MARC117>3.3.CO;2-O)
- Ikeda, N., Saito, E., Kondo, N., Inoue, M., Ikeda, S., Satoh, T., & Shibuya, K. (2011). What has made the population of Japan healthy? *The Lancet*, *378*(9796), 1094–1105.
[https://doi.org/10.1016/S0140-6736\(11\)61055-6](https://doi.org/10.1016/S0140-6736(11)61055-6)
- Kakuta, M., Hirata, M., & Kimura, Y. (2009). Stereoblock polylactides as high-performance bio-based polymers. *Polymer Reviews*, *49*(2), 107–140.
<https://doi.org/10.1080/15583720902834825>
- Kulinski, Z., & Piorkowska, E. (2005). Crystallization, structure and properties of plasticized poly(L-lactide). *Polymer*, *46*(23), 10290–10300.
<https://doi.org/10.1016/j.polymer.2005.07.101>

- Kumar, S., Bhatnagar, N., & Ghosh, A. K. (2016). Effect of enantiomeric monomeric unit ratio on thermal and mechanical properties of poly (lactide). *Polymer Bulletin*, 73(8), 2087–2104.
<https://doi.org/10.1007/s00289-015-1595-x>
- Lai, W. C., Liau, W. Bin, & Lin, T. T. (2004). The effect of end groups of PEG on the crystallization behaviors of binary crystalline polymer blends PEG/PLLA. *Polymer*, 45(9), 3073–3080.
<https://doi.org/10.1016/j.polymer.2004.03.003>
- Lee, S. H., Zhang, Z., & Feng, S. S. (2007). Nanoparticles of poly(lactide)-tocopheryl polyethylene glycol succinate (PLA-TPGS) copolymers for protein drug delivery. *Biomaterials*, 28(11), 2041–2050.
<https://doi.org/10.1016/j.biomaterials.2007.01.003>
- Lee, S., Kimoto, M., Tanaka, M., Tsuji, H., & Nishino, T. (2018). Crystal modulus of poly(lactic acid)s, and their stereocomplex. *Polymer*, 138, 124–131.
<https://doi.org/10.1016/j.polymer.2018.01.051>
- Li, Y., & Shimizu, H. (2009). Improvement in toughness of poly(l-lactide) (PLLA) through reactive blending with acrylonitrile-butadiene-styrene copolymer (ABS): Morphology and properties. *European Polymer Journal*, 45(3), 738–746.
<https://doi.org/10.1016/j.eurpolymj.2008.12.010>
- Liu, Y., Shao, J., Sun, J., Bian, X., Feng, L., Xiang, S., & Chen, X. (2014). Improved mechanical and thermal properties of PLLA by solvent blending with PDLA-b-PEG-b-PDLA. *Polymer Degradation and Stability*, 101(1), 10–17.
<https://doi.org/10.1016/j.polymdegradstab.2014.01.023>
- Martin, O., & Averous, L. (2001). Poly(Lactic Acid): Plasticization and properties of biodegradable multiphase systems. *Polymer*, 42, 6209–6219.
[https://doi.org/10.1016/S0032-3861\(01\)00086-6](https://doi.org/10.1016/S0032-3861(01)00086-6)

Martínez-Abad, A., Lagarón, J. M., & Ocio, M. J. (2014). Characterization of transparent silver loaded poly(l-lactide) films produced by melt-compounding for the sustained release of antimicrobial silver ions in food applications. *Food Control*, 43, 238–244.

<https://doi.org/10.1016/j.foodcont.2014.03.011>

Masutani, K., Kobayashi, K., Kimura, Y., Lee, C. W., & Lee, C. W. (2018). Properties of stereo multi-block polylactides obtained by chain-extension of stereo tri-block polylactides consisting of poly (L-lactide) and poly (D-lactide). *Journal of Polymer Research*, 25, 74.

<https://doi.org/10.1007/s10965-018-1444-3>

Moon, S. Il, Lee, C. W., Miyamoto, M., & Kimura, Y. (2000). Melt polycondensation of L-lactic acid with Sn(II) catalysts activated by various proton acids: A direct manufacturing route to high molecular weight poly(L-lactic acid). *Journal of Polymer Science, Part A: Polymer Chemistry*, 38(9), 1673–1679.

[https://doi.org/10.1002/\(SICI\)1099-0518\(20000501\)38:9<1673::AID-POLA33>3.0.CO;2-T](https://doi.org/10.1002/(SICI)1099-0518(20000501)38:9<1673::AID-POLA33>3.0.CO;2-T)

Nijenhuis, A. J., Colstee, E., Grijpma, D. W., & Pennings, A. J. (1996). High molecular weight poly(L-lactide) and poly(ethylene oxide) blends: Thermal characterization and physical properties. *Polymer*, 37(26), 5849–5857.

[https://doi.org/10.1016/S0032-3861\(96\)00455-7](https://doi.org/10.1016/S0032-3861(96)00455-7)

Okihara, T., Tsuji, M., Kawaguchi, A., Katayama, K. I., Tsuji, H., Hyon, S. H., & Ikada, Y. (1991). Crystal Structure of Stereocomplex of Poly(L-lactide) and Poly(D-lactide). *Journal of Macromolecular Science, Part B*, 30(1–2), 119–140.

<https://doi.org/10.1080/00222349108245788>

Pan, G. (2018). Polylactide fibers with enhanced hydrolytic and thermal stability via complete stereo-complexation of poly (L - lactide) with high molecular weight of 600000 and lower-molecular-weight poly (D -lactide). *Journal of Materials Science*, 53(7), 5490–5500.

<https://doi.org/10.1007/s10853-017-1944-2>

- Pan, P., Yang, J., Shan, G., Bao, Y., Weng, Z., Cao, A., & Inoue, Y. (2011). Temperature-Variable FTIR and Solid-State ^{13}C NMR Investigations on Crystalline Structure and Molecular Dynamics of Polymorphic Poly(L-lactide) and Poly(L-lactide)/Poly(D-lactide) Stereocomplex. *Macromolecules*, 45, 189–197
<https://doi.org/10.1021/ma201906a>
- Perego, G., Cella, G. D., & Bastloll, C. (n.d.). Effect of Molecular Weight and Crystallinity on Poly(lactic acid) Mechanical Properties. *Journal of Applied Polymer Science*, Vol. 59, 37–43 (1996), 37–43.
[https://doi.org/10.1002/0021-8995\(199603\)59:1<37::AID-POLA37>3.0.CO;2-1](https://doi.org/10.1002/0021-8995(199603)59:1<37::AID-POLA37>3.0.CO;2-1)
- Piorkowska, E., Kulinski, Z., Galeski, A., & Masirek, R. (2006). Plasticization of semicrystalline poly(l-lactide) with poly(propylene glycol). *Polymer*, 47(20), 7178–7188.
<https://doi.org/10.1016/j.polymer.2006.03.115>
- Plackett, D. V., Holm, V. K., Johansen, P., Ndoni, S., Nielsen, P. V., Sipilainen-Malm, T. & Verstichel, S. (2006). Characterization of L-poly lactide and L-poly lactide-polycaprolactone co-polymer films for use in cheese-packaging applications. *Packaging Technology and Science*, 19(1), 1–24.
<https://doi.org/10.1002/pts.704>
- Prabaharan, M., Grailer, J. J., Pilla, S., Steeber, D. A., & Gong, S. (2009). Folate-conjugated amphiphilic hyperbranched block copolymers based on Boltorn® H40, poly(l-lactide) and poly(ethylene glycol) for tumor-targeted drug delivery. *Biomaterials*, 30(16), 3009–3019.
<https://doi.org/10.1016/j.biomaterials.2009.02.011>
- Quynh, T. M., Mitomo, H., Nagasawa, N., Wada, Y., Yoshii, F., & Tamada, M. (2007). Properties of crosslinked polylactides (PLLA & PDLA) by radiation and its biodegradability. *European Polymer Journal*, 43(5), 1779–1785.
<https://doi.org/10.1016/j.eurpolymj.2007.03.007>

- Ren, J., Hong, H., Song, J., & Ren, T. (2005). Particle size and distribution of biodegradable poly-D,L-lactide-co- poly(ethylene glycol) block polymer nanoparticles prepared by nanoprecipitation. *Journal of Applied Polymer Science*, 98(5), 1884–1890. H
<https://doi.org/10.1002/app.22070>
- Saeidlou, S., Huneault, M. A., Li, H., Sammut, P., & Park, C. B. (2012). Evidence of a dual network/spherulitic crystalline morphology in PLA stereocomplexes. *Polymer*, 53(25), 5816–5824.
<https://doi.org/10.1016/j.polymer.2012.10.030>
- Sears, D. W., Grossman, J. N., & Melcher, C. L. (1982). Chemical and physical studies of type 3 chondrites-I: Metamorphism related studies of Antarctic and other type 3 ordinary chondrites. *Geochimica et Cosmochimica Acta*, 46(12), 2471–2481.
[https://doi.org/10.1016/0016-7037\(82\)90370-2](https://doi.org/10.1016/0016-7037(82)90370-2)
- Shao, J., Sun, J., Bian, X., Cui, Y., Li, G., & Xuesi, C. (2012). Investigation of poly(lactide) stereocomplexes: 3-Armed poly(L-lactide) blended with linear and 3-armed enantiomers. *Journal of Physical Chemistry B*, 116(33), 9983–9991.
<https://doi.org/10.1021/jp303402j>
- Shao, J., Xiang, S., Bian, X., Sun, J., Li, G., & Chen, X. (2015). Remarkable Melting Behavior of PLA Stereocomplex in Linear PLLA / PDLA Blends. *Industrial & Engineering Chemistry Research*, 54 (7), 2246–2253.
<https://doi.org/10.1021/ie504484b>
- Shi, X., Jing, Z., & Zhang, G. (2018). Influence of PLA stereocomplex crystals and thermal treatment temperature on the rheology and crystallization behavior of asymmetric poly(L-Lactide)/ poly(D-lactide) blends. *Journal of Polymer Research*, 25, 71
<https://doi.org/10.1007/s10965-018-1467-9>

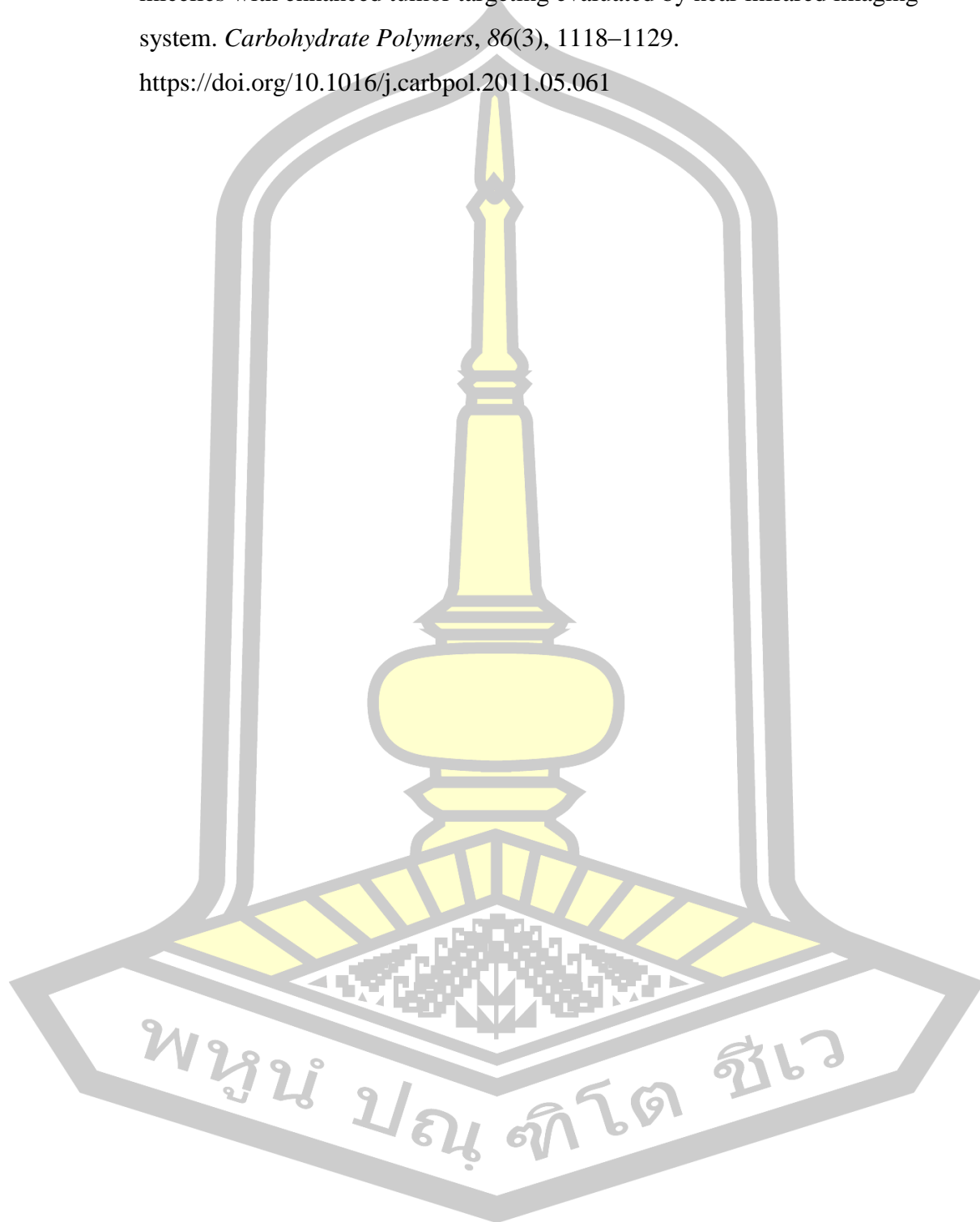
- Si, W., An, X., Zeng, J., Chen, Y., & Wang, Y. (2017). Fully bio-based, high toughened and heat-resistant poly(L-lactide) ternary blends via dynamic vulcanization. *SCIENCE CHINA Materials*, 60(10), 1008–1022.
<https://doi.org/10.1007/s40843-017-9111-1>
- Slager, J., & Domb, A. J. (2003). Stereocomplexes based on poly(lactic acid) and insulin: formulation and release studies. *Biopolymer*, 55(4), 549–583.
[https://doi.org/10.1016/S0169-409X\(03\)00042-5](https://doi.org/10.1016/S0169-409X(03)00042-5)
- Song, Y., Wang, D., Jiang, N., & Gan, Z. (2015). Role of PEG Segment in Stereocomplex Crystallization for PLLA/PDLA-*b*-PEG-*b*-PDLA Blends. *ACS Sustainable Chemistry and Engineering*, 3(7), 1492–1500.
<https://doi.org/10.1021/acssuschemeng.5b00214>
- Srisuwan, Y., & Baimark, Y. (2018). Controlling stereocomplexation, heat resistance and mechanical properties of stereocomplex polylactide films by using mixtures of low and high molecular weight poly(D-lactide)s. *e-Polymers*, 18(6), 485–490.
<https://doi.org/10.1515/epoly-2018-0115>
- Stefani, M., Coudane, J., & Vert, M. (2006). In vitro ageing and degradation of PEG-PLA diblock copolymer-based nanoparticles. *Polymer Degradation and Stability*, 91(11), 2554–2559.
<https://doi.org/10.1016/j.polymdegradstab.2006.05.009>
- Sun, J., Yu, H., Zhuang, X., Chen, X., & Jing, X. (2011). Crystallization behavior of asymmetric PLLA/PDLA blends. *Journal of Physical Chemistry B*, 115(12), 2864–2869.
<https://doi.org/10.1021/jp111894m>
- Tacha, S., Saelee, T., Khotasen, W., Punyodom, W., Molloy, R., Worajittiphon, P. & Manokruang, K. (2015). Stereocomplexation of PLL/PDL-PEG-PDL blends: Effects of blend morphology on film toughness. *European Polymer Journal*, 69, 308–318.
<https://doi.org/10.1016/j.eurpolymj.2015.06.015>

- Tessmar, J. K., & Göpferich, A. M. (2007). Customized PEG-derived copolymers for tissue-engineering applications. *Macromolecular Bioscience*, 7(1), 23–39.
<https://doi.org/10.1002/mabi.200600096>
- Tsuji, H. (2016). Poly(lactic acid) stereocomplexes : A decade of progress ☆.
Advanced Drug Delivery Reviews, 107, 97–135.
<https://doi.org/10.1016/j.addr.2016.04.017>
- Tsuji, H., & Fukui, I. (2003). Enhanced thermal stability of poly(lactide)s in the melt by enantiomeric polymer blending. *Polymer*, 44(10), 2891–2896.
[https://doi.org/10.1016/S0032-3861\(03\)00175-7](https://doi.org/10.1016/S0032-3861(03)00175-7)
- Tsuji, H., Horii, F., Hyon, S. H., & Ikada, Y. (1991). Stereocomplex Formation between Enantiomeric Poly(lactic acid)s. 2. Stereocomplex Formation in Concentrated Solutions. *Macromolecules*, 24(10), 2719–2724.
<https://doi.org/10.1021/ma00010a013>
- Tsuji, H., & Ikada, Y. (1991). Stereocomplex Formation between Enantiomeric Poly(lactic acid)s. 3. Calorimetric Studies on Blend Films Cast from Dilute Solution, *Macromolecules*, 24 (20), 5651–5656.
<http://doi.org/10.1021/ma00020a026>
- Tsuji, H., & Ikada, Y. (1993). Stereocomplex Formation between Enantiomeric Poly(lactic acid)s. 9. Stereocomplexation from the Melt. *Macromolecules*, 26(25), 6918–6926.
<https://doi.org/10.1021/ma00077a032>
- Tsuji, H., & Ikada, Y. (1999). Stereocomplex formation between enantiomeric poly(lactic acid)s. XI. Mechanical properties and morphology of solution-cast films. *Polymer*, 40(24), 6699–6708.
[https://doi.org/10.1016/S0032-3861\(99\)00004-X](https://doi.org/10.1016/S0032-3861(99)00004-X)
- Vadori, R., Mohanty, A. K., & Misra, M. (2013). The Effect of Mold Temperature on the Performance of Injection Molded Poly (lactic acid) -Based Bioplastic. *Macromolecular materials and Engineering*, 298, 981–990.
<https://doi.org/10.1002/mame.201200274>

- Velde, K. Van De, & Kiekens, P. (2001). Ein Jahrhundert Bahnelektroindustrie. *Eb - Elektrische Bahnen*, 99(12), 483.
[https://doi.org/10.1016/S0142-9418\(01\)00107-6](https://doi.org/10.1016/S0142-9418(01)00107-6)
- Wee, Y., Kim, J., & Ryu, H. (2006). Biotechnological Production of Lactic Acid and Its Recent Applications. *Food Technology and Biotechnology*, 44 (2) 163–172.
<https://doi.org/citeulike-article-id:7853424>
- Wei, X. F., Bao, R. Y., Cao, Z. Q., Zhang, L. Q., Liu, Z. Y., Yang, W., & Yang, M. B. (2014). Greatly accelerated crystallization of poly(lactic acid): Cooperative effect of stereocomplex crystallites and polyethylene glycol. *Colloid and Polymer Science*, 292(1), 163–172.
<https://doi.org/10.1007/s00396-013-3067-x>
- Xiao, P., Yao, W., & Römken, M. J. M. (2011). Effects of grass and shrub cover on the critical unit stream power in overland flow. *International Journal of Sediment Research*, 26(3), 387–394.
[https://doi.org/10.1016/S1001-6279\(11\)60102-9](https://doi.org/10.1016/S1001-6279(11)60102-9)
- Xie, Y., Lan, X., Bao, R., Lei, Y., Cao, Z., & Yang, M. (2018). Materials Science & Engineering C High-performance porous polylactide stereocomplex crystallite scaffolds prepared by solution blending and salt leaching. *Materials Science & Engineering*, 90, 602–609.
<https://doi.org/10.1016/j.msec.2018.05.023>
- Yamane, H., Sasai, K., Takano, M., & Takahashi, M. (2004). Poly(D-lactic acid) as a rheological modifier of poly(L-lactic acid): Shear and biaxial extensional flow behavior. *Journal of Rheology*, 48(3), 599–609.
<https://doi.org/10.1122/1.1687736>
- Yang, J., Liang, Y., & Han, C. C. (2015). Effect of crystallization temperature on the interactive crystallization behavior of poly(l-lactide)-block-poly(ethylene glycol) copolymer. *Polymer*, 79, 56–64.
<https://doi.org/10.1016/j.polymer.2015.09.067>

- Yang, J., Liang, Y., Luo, J., Zhao, C., & Han, C. C. (2012). Multilength Scale Studies of the Confined Crystallization in Poly(L- lactide)-block-Poly(ethylene glycol) Copolymer. *Macromolecules*, 45, 4254–4261.
<https://doi.org/10.1021/ma202505f>
- Yu, L., Dean, K., & Li, L. (2006). Polymer blends and composites from renewable resources. *Progress in Polymer Science (Oxford)*, 31(6), 576–602.
<https://doi.org/10.1016/j.progpolymsci.2006.03.002>
- Yun, X., Li, X., Jin, Y., Sun, W., & Dong, T. (2018). Fast Crystallization and Toughening of Poly (L -lactic acid) by Incorporating with Poly (ethylene glycol) as a Middle Block Chain , *Polymer Science, Series A*, 60(2), 141–155.
<https://doi.org/10.1134/S0965545X18020141>
- Zhang, H., Ruan, J., Zhou, Z., & Li, Y.,(2005) Preparation of monomer of degradable biomaterial poly(L-lactide). *Journal of Central South University of Technology*, 12(3), 246–250.
Article ID. 1005 - 9784(2005)03 - 0246 - 05
- Zhang, H., Wang, G., & Yang, H. (2011). Drug delivery systems for differential release in combination therapy. *Expert Opinion on Drug Delivery*, 8(2), 171–190.
<https://doi.org/10.1517/17425247.2011.547470>
- Zhang, X., Meng, L., Li, G., Liang, N., Zhang, J., Zhu, Z., & Wang, R. (2016). Effect of nucleating agents on the crystallization behavior and heat resistance of poly (L -lactide). *Applied polymer science*, 42999, 1–7.
<https://doi.org/10.1002/app.42999>
- Zhou, D., Shao, J., Li, G., Sun, J., Bian, X., & Chen, X. (2015). Crystallization behavior of PEG/PLLA block copolymers: Effect of the different architectures and molecular weights. *Polymer*, 62, 70–76.
<https://doi.org/10.1016/j.polymer.2015.02.019>

Zhu, H., Liu, F., Guo, J., Xue, J., Qian, Z., & Gu, Y. (2011). Folate-modified chitosan micelles with enhanced tumor targeting evaluated by near infrared imaging system. *Carbohydrate Polymers*, 86(3), 1118–1129.
<https://doi.org/10.1016/j.carbpol.2011.05.061>



BIOGRAPHY

NAME	Supasin Pasee
DATE OF BIRTH	24 March 1991
PLACE OF BIRTH	Sisaket Province of Thailand
ADDRESS	46 Moo. 9, Bankram, Tambom Pri, Amphoe Khunhan, Sisaket Province, 33150.
EDUCATION	2006 Junior School, Bankram School 2009 Senior High School, Praitumkhunvitya school 2013 Bachelor of Science degree in Chemistry (B.Sc.), Mahasakham University 2015 Master of Science degree in Chemistry (M.Sc.), Mahasakham University 2019 Doctor of Philosophy degree in Chemistry (Ph.D.), Mahasakham University
Research grants & awards	Science Achievement Scholarship of Thailand (SAST)
Research output	Pasee, S. Cheerarot, O. & Baimark, Y. (2015) Preparation of stereocomplex polylactide bioplastics from star-shaped/linear polylactide blending, Oriental Journal of Chemistry, 31(3),1551-1558. http://dx.doi.org/10.13005/ojc/310333 Pasee, S. & Baimark, Y. (2019) Improvement in Mechanical Properties and Heat Resistance of PLLA-b-PEG-b-PLLA by Melt Blending with PDLA-b-PEG-b-PDLA for Potential Use as High-Performance Bioplastics, Advances in Polymer Technology,2019, Article ID 8690650, 9 pages. https://doi.org/10.1155/2019/8690650

พหุบัณฑิต ชีวะ